

**OREGON HEALTH & SCIENCE UNIVERSITY  
SCHOOL OF MEDICINE**

**APPLICATION OF MOLECULAR BIOLOGICAL TOOLS TO THE STUDY OF  
BIOREMEDIATION IN CONTAMINATED SEDIMENTS**

By

Christina N. Brow

A DISSERTATION

Presented to the Division of Environmental & Biomolecular Systems  
and the Oregon Health & Science University  
School of Medicine  
in partial fulfillment of  
the requirements for the degree of

Doctor of Philosophy

April 2011

DIVISION OF ENVIRONMENTAL AND BIOMOLECULAR SYSTEMS  
INSTITUTE OF ENVIRONMENTAL HEALTH  
OREGON HEALTH & SCIENCE UNIVERSITY

---

CERTIFICATE OF APPROVAL

---

This is to certify that the Ph.D. dissertation of

Christina N. Brow

has been approved

---

Dr. Holly M. Simon, Assistant Professor  
Research Co-Advisor

---

Dr. Richard L. Johnson, Professor  
Research Co-Advisor

---

Dr. Paul G. Tratnyek, Professor

---

Dr. Lewis Semprini, Oregon State University  
External Examiner

# Table of Contents

TABLE OF CONTENTS.....	I
ACKNOWLEDGEMENTS.....	III
ABSTRACT.....	IV
<b>1. INTRODUCTION .....</b>	<b>1</b>
1.1. BIODEGRADATION.....	1
1.2. METHODS OF ASSESSING BIODEGRADATION.....	1
1.2.1. <i>Hydrogeochemical methods</i> .....	2
1.2.2. <i>Microbial and molecular methods</i> .....	3
1.3. SAMPLING APPROACHES FOR MBT ANALYSIS.....	5
1.4. TOLUENE AS A MODEL CONTAMINANT .....	6
1.4.1 <i>BTEX</i> .....	6
1.4.2. <i>Biodegradation of toluene</i> .....	7
1.5. AIM OF THIS THESIS.....	7
1.6. ORGANIZATION OF THIS THESIS.....	8
<b>2. GENERAL METHODS .....</b>	<b>11</b>
2.1. CHEMICAL ANALYSIS OF MODEL AQUIFER PORE WATER.....	11
2.2. <i>BSSA</i> AND <i>TMOA</i> QPCR PRIMER DESIGN.....	11
2.3. CONSTRUCTION OF PLASMID STANDARDS FOR QPCR.....	12
2.4. CLONE LIBRARY ANALYSIS OF ARCHAEAL ENRICHMENT CULTURE .....	13
<b>3. BENCH SCALE EVALUATION OF CRYOGENIC PRESERVATION AND STORAGE FOR THE MOLECULAR CHARACTERIZATION OF MICROORGANISMS IN SEDIMENT .....</b>	<b>20</b>
3.1. ABSTRACT .....	20
3.2. INTRODUCTION .....	21
3.3. METHODS.....	23
3.3.1. <i>Laboratory-generated samples</i> .....	23
3.3.2. <i>DNA and RNA extraction</i> .....	24
3.3.3. <i>Effects of freezing on quantification of genes and gene transcripts</i> .....	25
3.3.4. <i>Effects of storage on quantification of genes and gene transcripts</i> .....	26
3.3.5. <i>Effects of freezing and storage on relative phylotype abundance</i> .....	26
3.4. RESULTS AND DISCUSSION.....	28
3.4.1 <i>Effects of freezing and storage on quantification of genes and gene transcripts</i> .....	28
3.4.2 <i>Effects of freezing and storage on the relative abundance of bacterial phylotypes</i> .....	30
3.5. CONCLUSION.....	31
<b>4. MESOCOSM SCALE EVALUATION OF CRYOGENIC PRESERVATION AND STORAGE, AND HIGH-RESOLUTION CRYOGENIC CORE SAMPLING FOR THE MOLECULAR CHARACTERIZATION OF MICROORGANISMS IN SEDIMENT .....</b>	<b>49</b>
4.1. ABSTRACT .....	49
4.2. INTRODUCTION .....	50

4.3.	METHODS.....	52
4.3.1.	<i>Model aquifer</i> .....	52
4.3.2.	<i>Sample collection for MBT analysis</i> .....	52
4.3.3.	<i>Nucleic acid extraction and qPCR</i> .....	53
4.3.4.	<i>Quantitative PCR</i> .....	54
4.3.5.	<i>Microbial community analysis</i> .....	54
4.4.	RESULTS AND DISCUSSION.....	55
4.4.1.	<i>Chemical analysis of pore water</i> .....	55
4.4.2.	<i>Cryogenic sample preservation and storage</i> .....	56
4.4.3.	<i>Cryogenic core sampling</i> .....	57
4.5.	CONCLUSIONS.....	59
<b>5.</b>	<b>EFFECTS OF SAMPLING BIAS REVEALED BY HIGH-RESOLUTION MOLECULAR BIOLOGICAL ANALYSIS OF PAIRED SEDIMENT AND WATER SAMPLES FROM A MODEL AQUIFER .....</b>	<b>73</b>
5.1.	ABSTRACT .....	73
5.2.	INTRODUCTION .....	74
5.3.	METHODS.....	75
5.3.1.	<i>Model Aquifer</i> .....	75
5.3.2.	<i>Sample collection for MBT analysis</i> .....	75
5.3.3.	<i>DNA extraction and quantitative PCR</i> .....	75
5.3.4.	<i>Microbial community analysis</i> .....	76
5.4.	RESULTS AND DISCUSSION .....	77
5.4.1.	<i>Toluene plume</i> .....	77
5.4.2.	<i>DNA yields</i> .....	78
5.4.3.	<i>Microbial community analysis</i> .....	78
5.4.4.	<i>Depth distribution of functional genes</i> .....	78
5.5.	CONCLUSIONS.....	81
<b>6.</b>	<b>MICROBIAL TRANSPORT HINDERS USE OF FUNCTIONAL GENE ABUNDANCE IN PORE WATER TO CHARACTERIZE ZONES OF ACTIVE BIODEGRADATION.....</b>	<b>91</b>
6.1.	ABSTRACT .....	91
6.2.	INTRODUCTION .....	92
6.3.	METHODS.....	93
6.3.1.	<i>Model aquifer</i> .....	93
6.3.2.	<i>Sample collection for MBT analysis</i> .....	94
6.3.3.	<i>Nucleic acid extraction and quantitative PCR</i> .....	94
6.3.4.	<i>Lifetime of bssA transcripts following removal of toluene</i> .....	95
6.4.	RESULTS AND DISCUSSION.....	95
6.4.1.	<i>Phase 1</i> .....	95
6.4.2.	<i>Phase 2</i> .....	96
6.4.3.	<i>Phase 3</i> .....	97
6.4.4.	<i>Lifetime of bssA transcripts following removal of toluene</i> .....	99
6.4.5.	<i>Phase 4</i> .....	100
6.5.	CONCLUSIONS.....	102
<b>7.</b>	<b>SUMMARY .....</b>	<b>112</b>
<b>8.</b>	<b>REFERENCES .....</b>	<b>115</b>

## Acknowledgements

This work was supported by a grant from the Strategic Environmental Research and Development Program (SERDP) as part of project ER-1559.

I would like to thank my advisors Dr. Holly Simon, and Dr. Richard Johnson for their invaluable support, encouragement, and mentorship, throughout this process. I would also like to thank the other members of my examination committee, Dr. Paul Tratnyek, and Dr. Lewis Semprini.

Dr. Semprini and Dr. Simon are acknowledged for provided cells from a *Dehalococcoides* enrichment culture, and an archaeal enrichment culture, respectively, which were used in experiments described in chapter 3. Drs. Mitchiko Nakano, and Daniel Arp are also acknowledged for providing cell material, and starter culture material, respectively. Dr. Johnson is acknowledged for designing and building the cryogenic core sampler described in chapter 4, as well as performing the measurements of internal core temperature during freezing.

Reid O'Brien Johnson is acknowledged for performing all of the groundwater analyses described in this work. Mouzhong Xu is acknowledged for performing the characterization of the archaeal enrichment culture described in chapter 3. Thanks are also extended to Dr. Mariya Smit for sharing her expertise in working with RNA.

Finally, I extend my heartfelt thanks to my parents, friends, and fiancé, for picking me up, dusting me off, and walking with me down this path. Your continual support and encouragement has made this journey possible for me, and I am forever grateful.

## Abstract

Laboratory-generated samples, and samples from a toluene-“contaminated” model aquifer were used to systematically evaluate the efficacy of cryogenic preservation and storage for the molecular characterization of microorganisms in sediment. Using qPCR, RT-qPCR, and PCR-SSCP, no significant differences were observed between frozen and unfrozen sediment. Furthermore, it was demonstrated the cryogenic coring, i.e. freezing the core *in-situ* prior to extraction to the surface, was a viable way to accurately characterize subsurface microbial populations.

Using functional genes as biomarkers, significant differences were observed between sediment-attached and suspended toluene-degrading microbial communities from paired high-resolution sediment and water samples from a model aquifer. Results from sediment were in better agreement with groundwater chemistry suggesting that functional genes detected in groundwater may not be highly expressed, and may have been artifacts of transport. This was later confirmed by functional gene expression analysis.

One implication of this work is that functional gene abundance may not be an appropriate biomarker for active biodegradation, particularly when recovered from groundwater. It turns out, however, that functional gene transcripts are also not ideal, as they can be transcribed at basal levels even in the absence of biodegradation. It is therefore proposed that an integrated approach be used to gauge the activity of degrading populations. The ratio of functional gene transcripts to gene copies provides a measure of the metabolic activity of microbial populations. Experimentally determined “activity

thresholds” would have to be determined for different systems, but could possibly provide the best measure of *in-situ* metabolic activity.

# **1. Introduction**

## **1.1. Biodegradation**

As a result of human activity, organic pollutants have become ubiquitous contaminants in soil and groundwater systems across the globe, threatening both environmental and human health. Conventional treatment technologies of the “pump-and-treat” variety are time-consuming, costly, and often not capable of completely remediating a site. As a result, there has been increasing interest in methodologies which employ biodegradation, which is seen as a more environmentally sustainable technology by comparison (1).

The term “biodegradation” refers to the power of microorganisms to break down, or transform pollutants to nontoxic, or less toxic compounds. When used as a treatment strategy, the biodegradation process is generally classified as either natural attenuation (NA), or enhanced bioremediation. NA is a strategy which employs the natural metabolic capabilities of indigenous microorganisms with no additional intervention aside from monitoring (often called monitored natural attenuation, or MNA). Enhanced bioremediation, on the other hand, typically employs some form of active intervention to either enhance, or stimulate biodegradation. This can include the addition of limiting nutrients (biostimulation), or the addition of specific microorganisms capable of degrading the contaminant of interest (bioaugmentation) (2).

## **1.2. Methods of assessing biodegradation**

One of the challenges associated with both MNA and enhanced bioremediation lies in demonstrating that the *in-situ* reductions in contaminant concentrations do result

from biodegradation as opposed to some other physical process (1-4). Methods used to assess the effectiveness of MNA and bioremediation fall into one of two categories, hydrogeochemical, or microbial/molecular.

### **1.2.1. Hydrogeochemical methods**

Hydrogeochemical methods can be employed to monitor and quantify microbial transformation processes. When an organic pollutant enters an aquifer, the geochemistry of the impacted groundwater changes rapidly in response to the consumption of naturally occurring electron acceptors by microorganisms. Geochemical methods documenting the depletion of electron acceptors and the accumulation of their reduced redox species can provide information about the predominant redox conditions in the subsurface. It has been demonstrated that microorganisms will preferentially use electron acceptors in an order based on the energy which they can derive from the reaction (5). As a result, organic-contaminated aquifers are often anoxic since oxygen is the first electron acceptor utilized. Alternative electron acceptors include nitrate, ferric iron, sulfate, and carbon dioxide. The use of these electron acceptors is often segregated into zones, i.e. methanogenic nearest the contaminant source, followed by sulfate reducing, iron reducing, and nitrate reducing, in that order (1,6).

In order to distinguish between biodegradation, and reductions in contaminant concentration resulting from physical processes such as dispersion, tracer tests are often performed. This typically involves the injection and monitoring of a conserved tracer in the aquifer (1). Additionally, it is possible to monitor the production of intermediate metabolites that are produced and excreted during biodegradation of the contaminant. In order for this technique to be useful, the signature metabolite must be highly specific to a

particular biodegradation pathway, and not be produced by any abiotic means (1,2). Several such metabolites have been reported in the literature. For example, benzylsuccinate (7), ethylbenzylsuccinate (8), and methylbenzylsuccinate (9) are preeminent metabolites used as metabolic biomarkers of toluene, ethylbenzene, and xylene biodegradation, respectively.

Finally, compound-specific isotope analysis (CISA) can be used to prove, and quantify *in-situ* contaminant degradation. CISA is based on the fact that microorganisms will preferentially degrade isotopically lighter molecules. In CISA, changes in the isotopic ratios of contaminants within the aquifer are quantified. Such changes have been shown to result almost entirely from microbial activity, and thus can be used to prove the occurrence of biodegradation (10).

### **1.2.2. Microbial and molecular methods**

Often times, cultivation-based methods such as laboratory microcosms are used to demonstrate the biodegradation potential of *in-situ* microbial communities. Microcosms are constructed using either aquifer sediment or groundwater as the inoculum. Decreasing contaminant concentrations within the microcosms provide evidence that the site contains populations capable of degrading the contaminant or contaminants of interest. Sterilized microcosms can also be used to distinguish between biotic and abiotic degradation.

Laboratory microcosms are attractive because of the relative ease with which they can be set up. However, there are drawbacks associated with such cultivation methods. The inocula used in microcosms may not be representative of the entire aquifer, and

laboratory conditions may not accurately reflect those in the field. There is also the additional constraint that <1% of bacteria are thought to be cultivatable in the lab (1).

An alternative approach is to employ *in-situ* microcosms which consist of granular substrates within a porous housing. The microcosms can be loaded with an isotopically-labeled version of the contaminant of interest. Microorganisms colonizing the microcosm degrade the labeled contaminant, incorporating the label (most often  $^{13}\text{C}$ ) into cellular components such as DNA, and RNA which can then be probed via stable isotope probing (SIP) (1,3). Detection of the label within those biomarkers is used to prove that microbial biodegradation is taking place, and often times identify the species responsible for the degradation.

Although the cultivation approach can demonstrate that degrading populations exist within a contaminated aquifer, they are time consuming, and it can often be difficult to translate that information into estimations of *in-situ* biodegradation rates. For this reason, functional genes have received much attention for their potential use as biomarkers of biodegradation. Functional genes are those which encode enzymes specific to certain biodegradation pathways. They can be enumerated using molecular biological tools (MBTs) such as quantitative polymerase chain reaction (qPCR). Because the number of functional genes is related to the abundance of contaminant degrading organisms, it would follow that *in-situ* functional gene concentrations could be used to make assessments of biodegradation rates.

However, the abundance of functional genes is not always proportional to the degradation rate. This is likely because genes may be present, but not expressed, depending on environmental conditions. Therefore, mRNA transcripts of functional

genes may be a more appropriate biomarker of *in-situ* degradation activity (1,6), and can be quantified using reverse transcriptase qPCR (RT-qPCR). It is the latter two MBT methods, the detection of functional genes, and gene transcripts, that are used in this thesis.

### **1.3. Sampling approaches for MBT analysis**

Most molecular studies of microbial communities in aquifers, including aquifers impacted by organic pollution, are based on analyses of groundwater (11). This is due to the relative ease with which samples can be collected from monitoring wells, filtered on site, and stored in buffers (i.e. RNeasy®) to preserve biomolecules such as DNA and RNA. However, it has long been known that on a volume per volume basis, sediment-attached microorganisms are numerically dominant in the subsurface, often by several orders of magnitude (12-16). This has prompted some to suggest that sediment samples are thus more representative of subsurface microbial communities. It has also been repeatedly shown that sediment-attached and suspend populations differ in microbial community structure (11,14,17,18), and function (12,19-22). To date, however, the lack of data from paired, high-resolution sediment and groundwater samples from polluted aquifers has made it difficult to assess how these differences could affect assessments of biodegradation.

Apart from potentially imparting sampling bias, groundwater sampling also suffers from a lack of vertical resolution in comparison to sediment core sampling. This is an important consideration since biodegradation hotspots may exist on spatial scales too small to be adequately captured by conventional groundwater sampling (23,24). It is likely that degradation processes in the subsurface occur largely in narrow interfaces

where overlapping countergradients of electron donors and acceptors exist. “Plume fringe theory,” as this is sometimes called, has been repeatedly validated in both laboratory (25) and field studies (23,24,26), and highlights the importance of sediment sampling for the characterization of subsurface microbial communities during NA and bioremediation.

Despite its advantages, sediment sampling for MBT analysis is not without its difficulties. Whereas water samples can be filtered and preserved on site, it is difficult to separate cells from soil in the field, and placing entire sediment cores into buffers is not practical. As a result, the preservation of DNA and RNA within intact sediment cores is an important issue.

## **1.4. Toluene as a model contaminant**

### **1.4.1 BTEX**

Much of the work described in this thesis was performed using samples taken from a model aquifer in which toluene was added to simulate a contaminant plume. Toluene is the most readily biodegradable of the BTEX family of pollutants which includes benzene, toluene, ethylbenzene, and xylene (2). BTEX are the most soluble and thereby mobile component of gasoline, and enter the groundwater primarily through leaking underground storage tanks (LUSTs) (27). Due to their toxicity, and mobility in the environment, cleanup standards for BTEX are more stringent than for other petroleum components (28). According to the US environmental Protection Agency, there are more than 93,000 active LUST sites in the US (29), making BTEX pollution a significant issue.

### 1.4.2. Biodegradation of toluene

Toluene is readily biodegradable under aerobic conditions. Degradation is initiated by either direct oxidation of the aromatic ring via a monooxygenase enzyme (toluene-2,3, or 4 monooxygenase), a dioxygenase enzyme, or oxidation of the alkyl side chain (**Figure 1**) (3). Under anaerobic conditions, the degradation of toluene is initiated by the addition of a fumarate by benzylsuccinate synthase to the methyl group to form benzylsuccinate (**Figure 2**) (30). In this work, MBTs were designed to examine the toluene-4-monooxygenase pathway, and the benzylsuccinate synthase pathway by targeting the genes encoding these key enzymes. The toluene-4-monooxygenase pathway is encoded by *tmoA*, and *tmoA*-like genes, while the benzylsuccinate synthase pathway is encoded by the *bssA* gene.

### 1.5. Aim of this thesis

The aim of this thesis is to use MBTs to examine the differences between sediment-attached and suspended microbial communities within a model aquifer. Particular emphasis is placed on understanding the nature and causes of those differences, and how they can affect our understanding of subsurface biodegradation. In the process, I also examine the efficacy of cryogenic storage and cryogenic core sampling for the preservation of DNA and RNA within sediments. Some of the questions tackled in this thesis include:

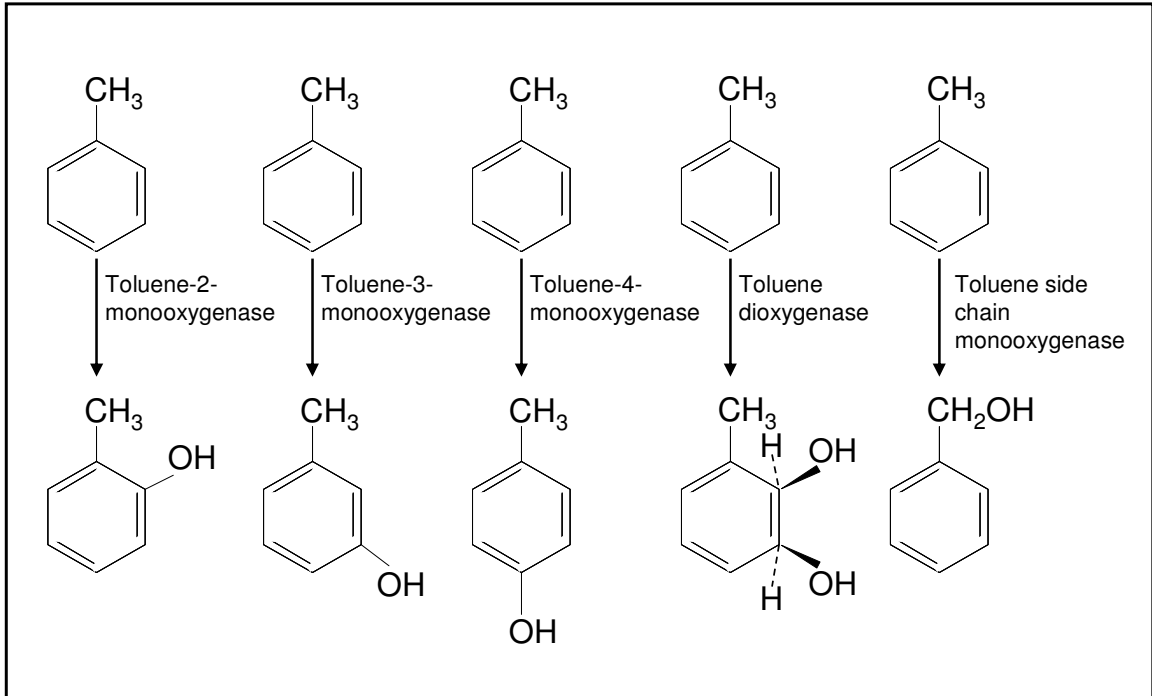
- How does whole-sample freezing or freeze/thaw affect DNA and RNA quantity, and quality?
- Does freezing or freeze/thaw disproportionately affect some phylotypes?

- Can cryogenic coring be used to preserve, and accurately characterize subsurface microbial communities?
- What, if any, differences can be observed between sediment-attached and suspended microbial communities?
- Can those differences be attributed to any particular physical or biological processes?
- Based on the data, what type of sampling strategy, or strategies would be best suited to characterize subsurface biodegradation?
- What do the data tell us about MBT use for characterizing *in-situ* degradation?

## **1.6. Organization of this thesis**

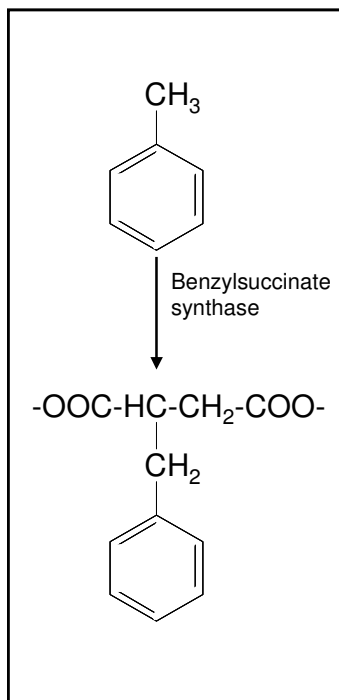
General methods common to multiple chapters of this thesis are presented in chapter 2. Methods specific to individual chapters are presented at the beginning of the relevant chapter. Chapter 3 describes bench scale investigations into the effects of freezing and cryogenic storage on the recovery, and integrity of DNA and RNA in simulated sediment samples. This work is expanded in chapter 4 to include samples from a model aquifer. Chapter 4 also describes the testing of a cryogenic core sampling technique in which a sediment core from the model aquifer was frozen *in-situ* prior to extraction to the surface. Chapter 5 presents work in which paired high-resolution sediment and water samples from the model aquifer were compared using MBTs. Differences were evaluated in relation to detailed analyses of groundwater chemistry. Finally, chapter 6 describes work designed to elucidate the cause(s) of differences observed between sediment-attached and suspended populations reported in chapter 5. This is followed by a summary chapter (chapter 7) and references (chapter 8).

**Figure 1. Initial reactions of aerobic toluene biodegradation pathways**



*Reactions of the first stage of aerobic toluene degradation, and the enzymes associated with those reactions.*

**Figure 2. Initial reaction of the anaerobic toluene degradation pathway**



*Reaction of the first stage of anaerobic toluene degradation, and the enzyme associated with that reaction.*

## **2. General methods**

This chapter describes general methods which are common to many of the subsequent chapters. Included are methods used by Mouzhong Xu to characterize the bacteria in the archaeal enrichment culture used in chapter 3, as well as those used by Reid O'Brien Johnson for the chemical analysis of water samples in chapters 4, 5, and 6. Chapter-specific methods are included within their relevant chapters.

### **2.1. Chemical analysis of model aquifer pore water**

This section describes procedures used for the chemical analysis of pore water samples in chapters 4, 5, and 6. Pore water samples ( $\approx 15$  ml) for chemical analyses were collected in airtight syringes from water sampling ports in the model aquifer. Toluene concentrations in pore water samples were measured by headspace gas chromatography (GC) (7694 headspace sampler attached to a 5890 gas chromatograph with a flame ionization detector, Agilent Technologies, Wilmington, DE). Nitrate was analyzed by ion chromatography (IC25 ion chromatograph, Dionex Corp., Sunnyvale, CA). Dissolved oxygen (DO) was measured by a flow-thru oxygen electrode (Model 8-730, Microelectrodes, Inc., Bedford, NH), and fluorescein was measured by a flow-through fluorometer (Model 121, Gilson Inc., Middleton, WI). The GC method had a detection limit of 0.05 mg/L and an associated error of  $\pm 5\%$  ( $n=15$ ). The ion chromatography method had a detection limit of 0.01 mg/L. The DO electrode had a detection limit of 1% of saturation, and the fluorometer had a detection limit of 50 ppb fluorescence.

### **2.2. *bssA* and *tmoA* qPCR primer design**

This section describes the procedures used to design the *bssA* and *tmoA* primers used in qPCR in chapters 4, 5, and 6. The CLC Genomics Workbench (CLC Bio, Cambridge, MA) was used to design qPCR primers (**Table 1**) based on conserved sequences within alignments of benzylsuccinate synthase (*bssA*) genes from denitrifying toluene-degrading organisms, and toluene-4-monooxygenase (*tmoA*) gene sequences. Accession numbers for the sequences used to construct the alignments can be found in **Table 2**. Primer specificity was confirmed with the Basic Local Alignment Search Tool (31). qPCR using the primers produced single bands of the expected size when electrophoresized in an agarose gel, and produced singular sharp peaks by qPCR melt curve analysis (**Figure 1**).

### **2.3. Construction of plasmid standards for qPCR**

This section describes the procedures used in the construction of plasmid standards for qPCR in chapters 4, 5, and 6. Genomic DNA from the model aquifer was extracted, and *bssA* and *tmoA* gene sequences were PCR-amplified. PCR products were purified using the Wizard SV gel and PCR clean-up system (Promega Corp., Madison, WI) and cloned into *E. coli* with the pCR®2.1 vector system using a TOPO TA cloning kit (Invitrogen Corp., Carlsbad, CA) according to the manufacturers' instructions. Randomly-selected clones were analyzed by PCR and gel electrophoresis to ensure the presence of the insert. Sequences of purified plasmids were confirmed with an ABI 3130XL Genetic Analyzer (ABI, Foster City, CA) at the OHSU DNA Services Core Center.

Plasmids with insert sequences most similar to those of *bssA* and *tmoA* genes from *Magnetospirillum* TS-6, and *Pseudomonas mendocina* KR1 (identity = 98% for

both) were linearized by digestion with restriction exonuclease *Xba* I (New England Biolabs, Ipswich, MA). Concentrations of linearized plasmids were determined fluorometrically using PicoGreen (Invitogen Corp., Carlsbad, CA) and a NanoDrop fluorometer (Thermo Scientific, Wilmington, DE), and were used to determine gene copy number based on the molecular weight of the plasmid. Dilutions of linearized plasmids, each tested in duplicate, spanning 5 orders of magnitude were used as standard curves for the determination of gene copy numbers. Representative standard curves (**Figure 2**) were linear ( $R^2 > 0.998$ ) and amplification efficiencies averaged 88 and 96% for *bssA* and *tmoA*, respectively.

#### **2.4. Clone library analysis of archaeal enrichment culture**

This section describes the procedures used to characterize the archaeal enrichment culture used in chapter 3. The culture was characterized by Mouzhong Xu of Oregon Health & Science University. In brief, DNA from the archaeal enrichment culture was extracted and purified. Bacterial 16S rRNA gene sequences were amplified by PCR using primers 27F (bacteria biased, 5'-AGA-GTT-TGA-TCM-TGG-CTC-AG - 3') and 1492R (universal, 5' - GGY-TAC-CTT-GTT-ACG-ACT-T - 3') (32). PCR was performed in a MyiQ real-time PCR detection system (BioRad Laboratories Inc., Hercules, CA) in 25  $\mu$ L reactions containing 15  $\mu$ L iQ Supermix (BioRad Laboratories Inc., Hercules, CA), 1  $\mu$ L of template DNA, and primers at a final concentration of 800 nM. The PCR cycling conditions were as follows: 1 min initial denaturation at 94°C followed by 30 cycles of 30 s denaturation at 94°C, 1.5 min annealing at 55°C, and 2.5 min extension at 72°C, and a final extension of 5 min at 72°C. After amplification, the PCR products were purified with the Wizard SV gel and PCR clean-up system (Promega

Corp., Madison, WI) and cloned with pCR®2.1 vector system using the TOPO TA cloning kit (Invitrogen Corp., Carlsbad, CA) according to the manufactures' instructions.

Randomly-selected clones were analyzed by PCR and gel electrophoresis to ensure the presence of insert, after which sequencing was performed in an ABI 3730XL high-throughput capillary DNA Analyzer (Washington University - Genome Sequencing Center, St. Louis, MO). For complete coverage, each clone was sequenced with 4 primers; 2 targeting vector sequences (M13F 5'-GTA-AAA-CGA-CGG-CCA-G-3' and M13R, 5'-CAG-GAA-ACA-GCT-ATG-AC3-'), (33) and 2 targeting internal sequences (870F, 5' -CCT-GGG-GAG-TAC-GGT-CGC-AAG-3' (34) and U926Rmod, 5'-CCG-TCW-ATT-CCT-TTR-AGT-TT-3' (35)). Sequences were assembled and aligned using the CLC Genomics Workbench 1 (CLC Bio, Cambridge, MA) and refined manually to remove or correct regions of ambiguity. Sequences from 90 clones were analyzed using the Basic Local Alignment Search Tool (BLAST) (31) against the GenBank database to determine closest phylogenetic affiliations. Results of the clone library analysis are shown in **Table 3**.

**Table 1. Primer sequences for qPCR**

<b>Gene</b>	<b>Primer</b>	<b>Primer sequence</b>
<i>bssA</i>	<i>997F</i>	5'- CTG-CTG-TGG-CCS-TAY-TAC-AAG -3'
	<i>1230R</i>	5'- GAT-GGC-GTC-GGT-CAT-GTC-GKT -3'
<i>tmoA</i>	<i>595F</i>	5'- GGC-TTY-ACC-AAC-ATG-CAG-TTY-C -3'
	<i>882R</i>	5'- CAT-RAA-CTC-CTT-GAA-BGA-CT -3'

*Shown are sequences of primers designed for use in qPCR. Positions are given relative to the bssA and tmoA genes of Azoarcus sp. EbN1, and Pseudomonas mendocina KRI, respectively.*

**Table 2. Accession numbers for sequences used in alignments for qPCR primer design**

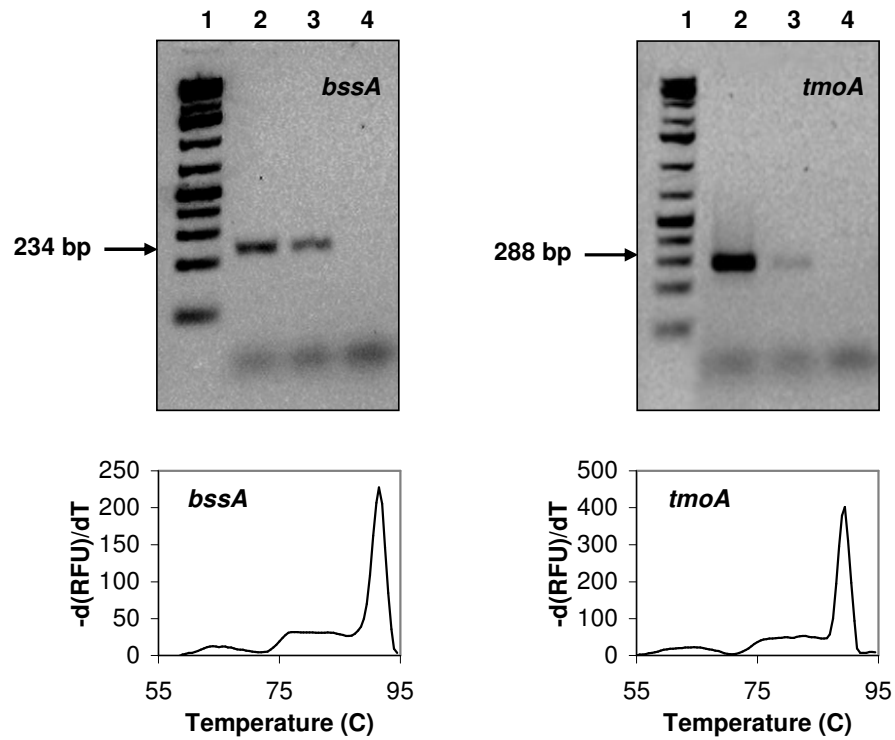
<b>Organism</b>	<b>Gene</b>	<b>Accession Number</b>
<i>Azoarcus</i> sp. DN11	bssA	AB285034
<i>Thauera</i> sp. DNT-1	bssA	AB066263
<i>Azoarcus</i> sp. T	bssA	AY032676
<i>Thauera aromatica</i>	bssA	AJ001848
<i>Magnetospirillum</i> sp. TS-6	bssA	AB167725
<i>Azoarcus aromaticum</i> EbN1	bssA	CR555306
<i>Pseudomonas mendocina</i> KR1	tmoA	M65106
<i>Burkholderia cepacia</i> strain JS150	tbc2A	AF282898
<i>Pseudomonas stutzeri</i> OX1	touA	AJ005663
<i>Ralstonia pickettii</i> PK01	tbuA1	AY541701
<i>Ralstonia metallidurans</i> CH34	tmoA	CP000352
<i>Cuprividus taiwanensis</i> strain LMG19424	tmoA	CU633751

*Shown are organisms whose sequences were used in alignments for the design of qPCR primers targeting genes for the alpha subunit of benzylsuccinate synthase (bssA) and the alpha subunit of toluene-4-monooxygenase (tmoA, tbc2A, touA, and tbuA).*

**Table 3. Bacterial clone library analysis of an archaeal enrichment culture**

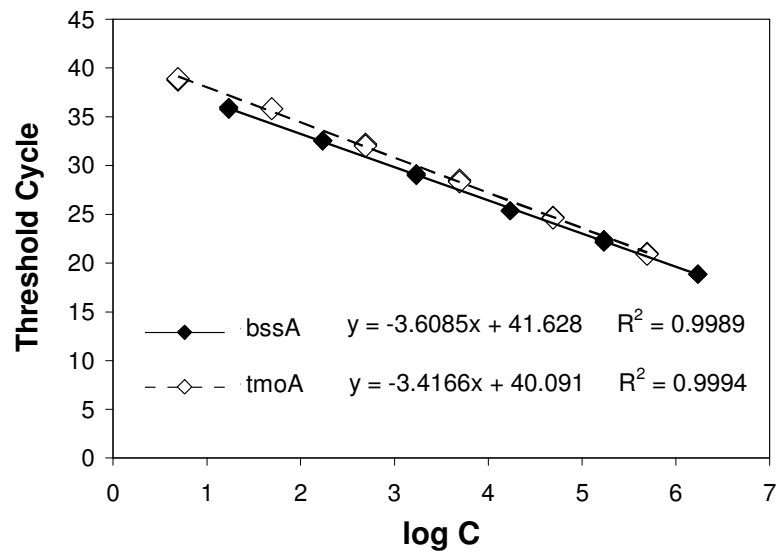
Organism (phylum/ class/ genus)	Maximum Score	Sequence Length	Expect Value (E)	Maximum Identity	Number of Clones
<b>Proteobacteria</b>					<b>44</b>
<i>α</i> - Proteobacteria					
<i>Sphingomonas</i>	2597	1431	0	99%	8
<i>Nitrobacter</i>	2416	1462	0	96%	2
<i>Rhodopseudomonas</i>	2385	1483	0	96%	2
<i>Labrys</i>	1349	759	0	98%	2
<i>β</i> - Proteobacteria					
<i>Burkholderia</i>	2726	1494	0	99%	7
<i>Ralstonia</i>	2745	1503	0	99%	7
<i>Pandorae</i>	2599	1455	0	98%	6
<i>Variovorax</i>	2697	1498	0	99%	5
<i>γ</i> - Proteobacteria					
<i>Rhodanobacter</i>	2605	1499	0	99%	5
<b>Acidobacteria</b>					<b>22</b>
<i>Acidobacteria</i>					
Unclassified <i>acidobacteriaceae</i>	2591	1459	0	98%	22
<b>Uncultured Bacteria division OP11</b>	1905	1346	0	92%	<b>11</b>
<b>Planctomycetes</b>					<b>7</b>
<i>Planctomycetacia</i>					
Environmental samples	1186	896	0	91%	7
<b>Bacteroidetes</b>					<b>4</b>
<i>Sphingobacteria</i>					
<i>Chitinophaga</i>	1247	752	0	96%	2
<i>Pedobacter</i>	1277	862	0	93%	1
<i>Sphingobacterium</i>	1428	856	0	96%	1
<b>Gemmatimonadetes</b>					
Environmental samples	1399	838	0	96%	1

**Figure 1. Evaluation of *bssA* and *tmoA* primers**



Agarose gel images (top), and melt curve analyses (bottom) of PCR products produced using *bssA* (left) and *tmoA* (right) primers designed for this study. In gel images; lane 1: ladder, lanes 2 & 3: positive signal, lane 4: negative control.

**Figure 2. Representative qPCR standard curves**



*Shown are representative standard curves generated using linearized plasmids containing bssA (closed symbols) and tmoA (open symbols) gene fragments.*

### **3. Bench scale evaluation of cryogenic preservation and storage for the molecular characterization of microorganisms in sediment**

#### **3.1. Abstract**

Laboratory-generated sediment samples were used to systematically assess the effects of whole-sample cryogenic preservation and storage on the integrity of biomolecules relevant to bioremediation. Impacts of freezing on DNA and RNA were assessed using quantitative PCR (qPCR) as well as the community fingerprinting method, PCR single-strand conformation polymorphism (PCR-SSCP). No degradation was observed for a suite of genes and gene transcripts, including short-lived mRNA transcripts, from *P. putida* F1 or from *B. subtilis* JH642 in single-species samples, or from either archaea, or *Dehalococcoides* species in enrichment culture samples. Similarly, freezing did not change the relative abundance of dominant phlotypes in enrichment culture samples as measured by PCR-SSCP of bacterial 16S rDNA. Of even greater significance is that freezing and storage did not affect the relative abundance of 16S rRNA phlotypes, since *in-vivo* rRNA content is often correlated with cellular growth rate. It is thus concluded that cryogenic preservation and storage of intact sediment samples can be used for accurate molecular characterization of microbial populations, and may facilitate high-resolution capture of biogeochemical interfaces important to biodegradation.

### **3.2. Introduction**

Subsurface bioremediation strategies should be based on knowledge of indigenous microbial organisms, including their metabolic capabilities and the ways in which they respond to changing environmental conditions (6,36). Because most microorganisms are not easily cultured in the laboratory, the use of molecular biological tools (MBTs) for gene detection and quantification, community fingerprinting, and gene expression has tremendous potential to improve the design, monitoring, and field performance of subsurface remediation.

Many studies suggest that 90% to 99% of bacterial populations, including those that degrade a variety of contaminants, are attached to solid phase materials in both laboratory-scale column experiments and in the field (19-22,12). There are additionally a number of reports documenting the enhancement, by particle-attached bacteria, of the rates of dechlorination of chlorinated hydrocarbons (19), biodegradation of aromatic hydrocarbons (21) and other cellular activities (20,22,12), compared to rates observed for unattached bacteria. Collection of intact core samples is, therefore, an optimal approach for accurately characterizing subsurface microbial populations.

Furthermore, a mounting body of evidence suggests that biodegradation “hotspots” in the subsurface may exist on spatial scales too fine to be adequately captured by conventional groundwater sampling (24,23). For example, the degradation process may largely be confined to the fringes of contaminant plumes, where overlapping “counter-gradients” of electron donors and acceptors exist. This “plume fringe theory” has been repeatedly validated in both laboratory (25,37) and field studies (23,24,26,38),

further demonstrating the need for fine-resolution sampling such as that provided by sediment coring.

However, the collection and storage of core samples for molecular analyses can be problematic. Whereas water samples can be filtered on site and stored in extraction buffer or preservation media (RNAlater®, etc.) to prevent the degradation of nucleic acids, it is difficult to separate cells from soil in the field. For this reason, soil samples for molecular analyses are often stored in buffers as well, but doing so with core samples is not practical. Disturbing or destroying the core would obscure biogeochemical interfaces that may be relevant to biodegradation. Consequently, the preservation of biomolecules such as DNA and RNA within intact core samples is an important issue. This is particularly true due to the relatively recent, and rapidly increasing use of MBTs by the bioremediation community, and is of heightened concern for the study of gene expression (messenger RNA, mRNA). Gene expression, rather than gene presence, is a better indicator of physiological activity because mRNA molecules are relatively short-lived compared to DNA molecules. For example, reported *in-vivo* mRNA half-lives for the *Dehalococcoides* reductive dehalogenase genes *vcrA* and *tceA* are 4.8 and 6.1 hours, respectively (39), underscoring the importance of sample preservation.

Cryogenic preservation is commonly used for environmental samples, but the effects of whole-core freezing on the integrity of biomolecules such as DNA and RNA has not been systematically examined. Additionally, cryogenic drilling (freezing the core *in-situ* prior to extraction to the surface) has been used to preserve the *in-situ* microbiological and physical characteristics of core samples for at least 30 years (40-43), though its use for molecular biological analysis has been limited.

DNA and RNA become increasingly fragmented as samples degrade. This can lead to reductions in PCR amplification efficiencies, increases in detection limits, and even amplification failure. These effects become increasingly pronounced for longer target sequences as the yield of complete target fragments is greatly reduced (44-46). Additionally, sample degradation can lead to the preferential amplification of undamaged targets (46), thus affecting assessments of microbial community structure. In the work reported here, the impacts of whole-sample freezing on the integrity of DNA and RNA are examined through the detection and quantification of a suite of genes and gene transcripts from Bacteria and Archaea.

Single-strain experiments using laboratory-generated samples were performed with both *Pseudomonas putida* F1 and *Bacillus subtilis* JH642, two bacterial strains with very different cellular properties (e.g., cell wall composition and structure) potentially resulting in different responses to the freezing and thawing processes. PCR single-strand conformation polymorphism (PCR-SSCP) was used to assess the effects of freezing on relative phylogenetic type (phylotype) abundance within more complex laboratory samples containing cells from enrichment cultures. A subset of frozen samples was also stored at  $-80^{\circ}\text{C}$  before DNA and RNA were extracted in order to determine the effects of frozen storage on intact samples.

### **3.3. Methods**

#### **3.3.1. Laboratory-generated samples**

*Pseudomonas putida* F1 and *Bacillus subtilis* JH642 strains were obtained from Dr. Dan Arp, and Dr. Michiko Nakano, respectively. Cultures of *P. putida* F1 were grown at room temperature, overnight, in 2xYT medium (47) with shaking at 120 rpm.

*B. subtilis* JH642 was grown at 37°C, overnight, in 2xYT (47) medium with shaking at 150 rpm. An archaeal enrichment culture also containing members of diverse bacterial phyla was grown as described by Simon et al. (48). Each culture was used to create a set of three samples (unfrozen, frozen, and frozen with granular media) consisting of 300 µL of the culture in 2 mL microcentrifuge tubes. One of each set of samples contained 0.5 g of sterile 0.1 mm zirconia/silica beads (Biospec Products, Inc. Bartlesville, OK) to simulate soil. This “simulated core sample” and one of the non-bead-containing samples were frozen by immersion in liquid nitrogen for 10 seconds. In addition, a set of simulated core samples (with sterile beads) was constructed with culture material from a *Dehalococcoides* (*DHC*) enrichment culture (49) provided by Dr. Lewis Semprini.

### **3.3.2. DNA and RNA extraction**

DNA from the majority of laboratory-generated samples was isolated via bead beating for 30 s at a speed of 5.5 m/s using a Bio101 FastPrep instrument (Thermo Fisher Scientific, Waltham, MA) followed by purification using the Wizard SV96 genomic DNA purification kit (Promega Corp., Madison, WI). DNA was extracted from the *DHC*-containing samples using a FastDNA Spin Kit for Soil (MP Biomedicals, Solon, OH). Total RNA (which includes rRNA and mRNA) was isolated as described in Smith et al. (50), except that each extraction was performed on 0.5 g sediment as opposed to filters. Total DNA and RNA concentrations were determined fluorometrically using PicoGreen and RiboGreen reagents, respectively (Invitrogen Corp., Carlsbad, CA) and a NanoDrop fluorometer (Thermo Scientific, Wilmington, DE). DNA from select laboratory-generated samples was electrophoresized and visualized in a 1% agarose gel. Additionally, the quality of RNA extracted from the single-species samples was

evaluated using an Agilent 2100 Bioanalyzer (Agilent Technologies, Inc., Santa Clara, CA). All nucleic acid extracts were stored at  $-80^{\circ}\text{C}$  until use.

### 3.3.3. Effects of freezing on quantification of genes and gene transcripts

The effects of freezing on the quantification of genes and gene transcripts were assessed by quantitative PCR (qPCR) of DNA and RNA recovered from the laboratory-generated samples. Equal amounts of either DNA or RNA were used from each set of extracts. Total RNA (including ribosomal RNA (rRNA) and messenger RNA (mRNA)) was converted to complementary DNA (cDNA) using SuperScript III First-Strand Synthesis Supermix (Invitrogen Corp., Carlsbad, CA). qPCR was performed in 25  $\mu\text{L}$  reactions in a MyiQ real-time qPCR detection system using iQ SYBR Green Supermix (BioRad Laboratories Inc., Hercules, CA). Several independent master mixes were prepared for each set of samples ( $n =$  either 5 or 10) and were tested in triplicate within a single microtiter plate.

Dilution series spanning five orders of magnitude were tested in duplicate for each experiment to ensure that product concentrations were within the instrument's linear dynamic range. Experiments performed with each set of extracts were replicated using primers targeting the following genes/transcripts: *todE* (51), *todC1* (52), and 16S rRNA (53) for *P. putida* F1; *thrB*, *pheA*, and *trpC* (54) for *B. subtilis* JH642; and archaeal 16S rRNA (48) and *amoA* for the archaeal enrichment culture. Primer sequences and cycling conditions can be found in **Table 1**. All primers were added at a final concentration of 200 nM, with the exception of *DHC* primers which were added at 500 nM. qPCR data were analyzed using software packages which were able to assess differences in amplification efficiencies between frozen and unfrozen samples based on the observation

of individual-sample reaction kinetics (i.e. DART-PCR software (55), and LinReg PCR software (56)). In all cases, fold differences were calculated relative to the unfrozen sample.

#### **3.3.4 Effects of storage on quantification of genes and gene transcripts**

Storage experiments were conducted using replicates of the single-strain simulated core samples described above (i.e., with granular media), as well as with the simulated cores containing *DHC* culture material. Experiments performed using *DHC* samples were replicated using primers (**Table 1**) targeting *DHC* 16S rRNA and rDNA, and a suite of reductive dehalogenase (*pceA*, *tceA*, *vcrA*, and *bvcA*) genes and gene transcripts (57). One sample was processed immediately and served as the unfrozen reference sample. Additional samples were stored at  $-80^{\circ}\text{C}$  until processing (1 week, 2 weeks, and 1 month for single-species samples, and 1 week, 2 weeks, and 2 months for *DHC* samples). At each time point, samples were removed from storage, and the DNA and RNA were extracted and purified as described previously. Purified DNA and RNA extracts from each time point were subsequently stored at  $-80^{\circ}\text{C}$  until use in qPCR experiments. After the final storage duration, equal amounts of either DNA or RNA (n=5) from all points were evaluated by qPCR on the same microtiter plate, ensuring that the results were directly comparable.

#### **3.3.5. Effects of freezing and storage on relative phylotype abundance**

PCR-SSCP was used to assess the effects of freezing on the relative abundance of bacterial 16S rDNA and rRNA phylotypes recovered from the archaeal enrichment culture samples (unfrozen, frozen, and frozen with granular media), and the *DHC* enrichment culture samples (unfrozen, and frozen for 1 week, 2 weeks, and 2 months).

RNA was converted to cDNA as described. DNA and cDNA from the enrichment culture samples were PCR-amplified using universal bacterial 16S rRNA gene primers 357F (5' - CCT ACG GGA GGC AGC AG -3') and 5'-phosphorylated 519R (5'-phosphorylation- ACC GCG GCT GCT GGC AC -3') (32). Cycling parameters consisted of 4 min initial denaturation at 95°C and 20 touchdown cycles of 30 s denaturation at 95°C, 1 min annealing starting at 66°C, and 1.5 min extension at 72°C. The annealing temperature was decreased 0.5°C with every cycle until a final annealing temperature of 56°C was reached. The touchdown step was followed by 20 cycles of 30 s denaturation at 95°C, 1 min annealing at 56°C, and 1.5 min extension at 72°C, with a final extension of 7 min at 72°C.

After amplification, PCR products were purified using the Wizard SV gel and PCR clean-up system (Promega Corp., Madison, WI). Purified phosphorylated PCR products were digested (to form single-stranded products), desalted, combined with SSCP stop solution (Lonza, Basel, Switzerland), denatured at 95°C for 3 minutes, and placed on ice as described in Sliwinski and Goodman (58). Products were run on a 0.75 mm 1×MDE polyacrylamide gel (Lonza, Basel, Switzerland) at 300 V for 25 hours at 17°C. After electrophoresis, the gel was imaged directly on a Typhoon variable mode imager (GE Healthcare Bio-Sciences Corp., Piscataway, NJ) following staining with GelRed (Biotum, Inc., Hayward, CA). Alternatively, it was subsequently found that the use of FAM-labeled 357F with nonphosphorylated 519R eliminated the need for the digestion to single-stranded DNA and staining steps, thus this approach was used in PCR-SSCP experiments with DNA and RNA from the *DHC*-containing samples.

Gel fingerprint patterns were analyzed using GelCompar II software (Applied Maths, Austin, TX), which was used to detect bands, create densitometric profile curves, and calculate the area under each peak. This information was transformed into a relative area under each peak (relative to the sum of the areas under all peaks), thus making possible the comparison of independent samples. Additionally, similarity matrices of the densitometric curves were calculated based on pair-wise Pearson's correlations.

### **3.4. Results and Discussion**

#### **3.4.1 Effects of freezing and storage on quantification of genes and gene transcripts**

Quantification of target genes and gene transcripts from laboratory-generated samples was accomplished by qPCR with equal starting amounts of either DNA, or RNA, respectively. Fold differences for the two frozen samples relative to the unfrozen sample should be equal to 1, barring any effects of DNA or RNA degradation. Experiments indicated 10% variability in replicate fluorometric DNA and RNA concentration measurements (data not shown), thus fold differences of less than 10% were not considered to be indicators of sample degradation.

All qPCR dilution series were linear ( $R^2 > 0.98$ ) and confirmed that concentrations examined were within the linear dynamic range of the instrument. Fold differences, relative to the unfrozen sample, for genes and gene transcripts from frozen single-species and archaeal enrichment culture samples are shown in **Table 2**. The results of t-tests indicated no statistically significant differences between target genes or gene transcripts from frozen and unfrozen samples ( $p > 0.05$ ,  $n = 10$  and  $5$  for DNA and RNA, respectively) when calculated to allow for a 10% uncertainty in initial concentration. It is particularly

noteworthy that freezing did not affect the recovery of mRNA molecules examined here (i.e., *todC*, *todE*, *trpC*, *thrB*, *pheA*, and *amoA* gene transcripts), which are particularly vulnerable to decay, make up only a fraction ( $\approx 3\%$ ) of the total RNA pool (59), and yet are crucial to gene expression analysis. Additionally, results obtained targeting archaeal genes and gene transcripts from enrichment culture samples are significant because the enrichment culture samples represent a more microbially complex, and, therefore environmentally-relevant system. Furthermore, individual sample reaction kinetics revealed no trends in amplification efficiency for any target DNA or RNA (e.g., better efficiencies for unfrozen vs. frozen samples). Amplification efficiencies for all targets from unfrozen and frozen samples were comparable ( $p > 0.05$ ,  $n = 10$  and  $5$  for DNA and RNA, respectively) and were greater than  $94.8\%$  and  $88.2\%$  for all DNA and RNA, respectively.

For practical reasons, field-collected cores are likely to be stored frozen until further subcore and/or processing can be carried out in a laboratory setting. Results from storage qPCR experiments with both single-strain sets of laboratory-generated cores, and the *DHC*-containing cores are shown in **Table 3**. Fold differences were calculated with respect to DNA or RNA from an unfrozen sample. T-tests were performed and indicated that no storage time for any sample was statistically different from the unfrozen sample ( $p > 0.05$ ,  $n = 5$ ) when allowing for a  $10\%$  uncertainty. Furthermore, calculated amplification efficiencies were comparable ( $p > 0.05$ ,  $n = 5$ ) among all storage durations for both strains regardless of the primers used, indicating that storage time did not affect the integrity of the DNA or RNA.

It is also important to note that freezing and storage did not result in any trends in either DNA or RNA yields (**Figure 1**) from laboratory-generated cores, nor was the quality of DNA and RNA affected, as visualized by electrophoresis in a 1% agarose gel (**Figure 2**). Moreover, measurement of RNA using an Agilent 2100 Bioanalyzer indicated that cryogenic preservation did not result in RNA degradation. Specifically, RNA Integrity Numbers, or RINs, did not change as a function of time at -80°C (**Table 4**).

### **3.4.2 Effects of freezing and storage on the relative abundance of bacterial phylotypes**

To further evaluate the effects of freezing and storage on DNA and RNA from a broad range of bacterial phyla, PCR-SSCP was used to generate profiles of the bacterial communities present in the enrichment culture samples. Bacterial 16S rDNA and rRNA from the suite of archaeal enrichment culture samples (unfrozen, frozen, and frozen with granular media) were profiled in triplicate. Additionally, triplicate bacterial 16S rDNA and rRNA profiles from an unfrozen *DHC*-containing simulated core sample were compared to profiles from replicate samples stored at -80°C for 1 week, 2 weeks, and 2 months.

rDNA PCR-SSCP gel fingerprint patterns and associated densitometric profiles (**Figure 3**) from the archaeal enrichment culture samples contained  $\approx 20$  distinct bands/peaks, each corresponding to a unique phylotype. This compared reasonably well with the number of individual groups (16 groups) identified by clone library analysis. (See chapter 2 for details). Pair-wise comparisons of the densitometric profiles were performed and the associated Pearson's correlation coefficients ( $r$ ) were calculated

(**Table 5**). DNA from frozen archaeal enrichment culture samples produced densitometric profiles as similar to those of unfrozen profiles ( $r > 0.95$ ) as to replicates from the same sample ( $r > 0.95$ ). Similarly, *DHC* samples stored at  $-80^{\circ}\text{C}$  for 1 week, 2 weeks, and 2 months also produced gel profiles and densitometric curves (**Figure 4**) nearly as similar to those from the unfrozen sample ( $r > 0.95$ ) as to intrasample replicates ( $r > 0.98$ ) (**Table 6**).

The area under each peak in the densitometric profiles was converted to a relative peak area by dividing by the area under all peaks in the profile. rDNA peaks comprising  $>5\%$  of the total peak area were plotted in **Figures 5 a and b** which also shows the corresponding positions in a representative PCR-SSCP gel lane and densitometric profile. PCR-SSCP profiles of bacterial rDNA from frozen and unfrozen archaeal and *DHC* enrichment culture samples were comparable in relative abundance of the dominant phylotypes, i.e. freezing did not disproportionately affect any individual phylotype.

Similarly, results from the rRNA PCR-SSCP analyses indicated that freezing and cryogenic storage had no effect on the relative abundance of 16S rRNA gene transcripts from the enrichment culture samples (**Figures 5c,d 6, & 7, Tables 7 & 8**). This is important because biodegradation depends upon active bacterial populations, and *in-vivo* rRNA content is often correlated with cellular growth rate (59-61).

### **3.5. Conclusion**

Molecular biological tools, especially those for gene detection and gene expression, have the potential to significantly improve the design and implementation of subsurface bioremediation. Of particular interest would be the ability to relate degradation rates in the field to some measurable molecular parameter such as species or

catabolic gene abundance and expression. For example, organisms of the species *Dehalococcoides* (*DHC*) are of particular interest with respect to bioremediation because they can reductively dechlorinate tetrachloroethene (PCE), trichloroethene (TCE), *cis*-dichloroethene (cDCE), and vinyl chloride (VC) to nontoxic ethane (62). Lu et al. have suggested that a *DHC* density of  $>1 \times 10^7$  cells per liter (determined via qPCR of *DHC* 16S rRNA genes) can be used as a criterion to identify sites for which monitored natural attenuation (MNA) would likely result in generally useful rates of dechlorination (defined as  $\geq 0.3$  per year) (62,63). However, they also identified sites at which MNA resulted in such dechlorination rates despite significantly lower aqueous *DHC* densities (on the order of  $10^5$  cells per liter). In fact, relative to cell density, these field sites outperformed even laboratory cultures of *DHC* grown under ideal conditions. The unlikelihood of this led the researchers to conclude that monitoring wells did not efficiently sample the *DHC* organisms at those site, and that if assays for *DHC* are to be used to predict rates of natural attenuation, it will be necessary to collect and analyze sediment samples (62,63). Consequently, the preservation of nucleic acids within intact sediment samples is an important issue.

Sample preservation for molecular biological analysis can be problematic. This is particularly true with respect to RNA, which is much more susceptible than DNA to degradation by nuclease activity (64). Our results indicated that neither freezing, nor storage for at  $-80^\circ\text{C}$  affected our ability to detect and quantify individual genes, including those from *DHC*. Especially noteworthy are the qPCR results which demonstrated that short-lived mRNA molecules were not degraded upon freezing, or storage. Additionally, the relative abundance of dominant bacterial 16S rDNA and rRNA phylotypes was

unaffected by freezing and storage of sediment at -80 °C. Results suggest that whole-core freezing is a viable way to preserve the molecular characteristics of microbial populations in sediment in terms of both gene abundance, and more significantly, gene expression. In fact, due to the short half-lives of mRNA molecules, immediate freezing, e.g. with cryogenic drilling, may be the only viable way to preserve the *in-situ* microbial signature of sediment.

**Table 1. qPCR Primer sequences and cycling conditions**

Gene (organism)	Primer sequence	Denaturation		Annealing		Extension		Reference
		sec	°C	sec	°C	sec	°C	
<i>todC1</i> ( <i>P.putida F1</i> )	Fwd: 5'-ATCCTGCGAGGCCACAAG-3' Rev: 5'-TTCTCGCTGTAGACGTTGTTG-3'	30	92	60	57	60	72	Kabir et al. (2003)
<i>todE</i> ( <i>P.putida F1</i> )	Fwd: 5'-GGATTTCAAACCTGGAGACCAG-3' Rev: 5'-GCCATTAGCTTGACGCATGAA-3'	60	94	60	58	120	72	Hendrickx et al. (2006)
16S rRNA ( <i>P.putida F1</i> )	Fwd: 5'-GAGTTTGATCCTGGCTCAG-3' Rev: 5'-CCTTCCTCCCAACTT-3'	30	95	60	60	60	72	Johnsen et al. (1999)
<i>trpC</i> ( <i>B.subtilis JH642</i> )	Fwd: 5'-TTCTCAGCGTAAAGCAATCCA-3' Rev: 5'-GCAAATCCTTTAGTGACCGAATACC-3'	30	95	60	60	60	72	Kanno et al. (2006)
<i>pheA</i> ( <i>B.subtilis JH642</i> )	Fwd: 5'-GCCAATGATATGGCAGCTTCTAC-3' Rev: 5'-TGCGGCAGCATGACCATTA-3'	30	95	60	60	60	72	Kanno et al. (2006)
<i>thrB</i> ( <i>B.subtilis JH642</i> )	Fwd: 5'-CCTGCATGAGGATGACGAGA-3' Rev: 5'-GGCATCGGCATATGGAAAC-3'	30	95	60	60	60	72	Kanno et al. (2006)
<i>amoA</i> (enrichment culture)	Fwd: 5'-TCGTGGTGTCTCCGTATC-3' Rev: 5'-GATTGTGGCGTAGTATGTGG-3'	60	95	60	60	60	72	This study
16S rRNA (Archaea)	Fwd: 5'-GTAGCCGGTTCTACAAGTC-3' Rev: 5'-ACTGGTGGTCTTCAATGGATC-3'	30	95	45	61	30	72	Simon et al. (2005)
16S rRNA ( <i>Dehalococcoides</i> )	Fwd: 5'-GGCGTAAAGTGAGCGTAG-3' Rev: 5'-GACAACCTAGAAAACCGC-3'	10	95	45	61.5	30	72	Behrens et al. (2008)
<i>pceA</i> ( <i>Dehalococcoides</i> )	Fwd: 5'-ACCGAAACCAGTTACGAACG-3' Rev: 5'-GACTATTGTTGCCGGCACTT-3'	10	95	45	61.5	30	72	Behrens et al. (2008)
<i>tceA</i> ( <i>Dehalococcoides</i> )	Fwd: 5'-GCCACGAATGGCTCACATA-3' Rev: 5'-TAATCGTATACCAAGGCCCG-3'	10	95	45	61.5	30	72	Behrens et al. (2008)
<i>vcrA</i> ( <i>Dehalococcoides</i> )	Fwd: 5'-CCCTCCAGATGCTCCCTTTA-3' Rev: 5'-ATCCCCTCTCCCGTGAACC-3'	10	95	45	61.5	30	72	Behrens et al. (2008)
<i>bvcA</i> ( <i>Dehalococcoides</i> )	Fwd: 5'-TGGGGACCTGTACCTGAAAA-3' Rev: 5'-CAAGACGCATTGTGGACATC-3'	10	95	45	61.5	30	72	Behrens et al. (2008)

*Primers and cycling conditions used in qPCR. All reactions included 4 min initial denaturation at 95°C, 4 minutes final extension at 72°C, and generation of a melt curve. (amoA primers were designed based on an alignment of 49 amoA sequences recovered from the archaeal enrichment culture using Beacon Designer software (Premier Biosoft, Palo Alto, CA)).*

**Table 2. Effect of freezing and thawing processes on quantification of individual genes and gene transcripts from laboratory-generated samples**

<b>a. <i>P. putida</i> F1</b>			
Target		Frozen	Frozen with granular media
DNA <sup>†</sup>	16S rDNA	0.86 ± 0.09	0.85 ± 0.18
	<i>todC</i>	0.84 ± 0.07	0.88 ± 0.11
	<i>todE</i>	0.83 ± 0.08	0.91 ± 0.06
rRNA <sup>‡</sup>	16S rRNA	0.95 ± 0.19	1.12 ± 0.22
mRNA <sup>‡</sup>	<i>todC</i>	0.95 ± 0.11	1.03 ± 0.07
	<i>todE</i>	0.96 ± 0.06	0.93 ± 0.07
<b>b. <i>B. subtilis</i> JH642</b>			
Target		Frozen	Frozen with granular media
DNA <sup>†</sup>	<i>trpC</i>	0.96 ± 0.21	0.97 ± 0.11
	<i>thrB</i>	0.96 ± 0.08	0.96 ± 0.18
	<i>pheA</i>	0.98 ± 0.11	0.90 ± 0.11
mRNA <sup>‡</sup>	<i>trpC</i>	1.03 ± 0.17	0.96 ± 0.13
	<i>thrB</i>	1.02 ± 0.15	0.92 ± 0.19
	<i>pheA</i>	1.13 ± 0.09	0.99 ± 0.14
<b>c. Mixed culture (targeting archaea)</b>			
Target		Frozen	Frozen with granular media
DNA <sup>‡</sup>	16S rDNA	0.87 ± 0.18	1.14 ± 0.15
	<i>amoA</i>	0.84 ± 0.11	1.10 ± 0.11
rRNA <sup>‡</sup>	16S rRNA	0.86 ± 0.11	1.06 ± 0.14
mRNA <sup>‡</sup>	<i>amoA</i>	0.82 ± 0.23	1.05 ± 0.18

Data presented as fold differences relative to the unfrozen control. Standard deviations calculated from n=5 (‡) and n=10 (†) independent sets of reactions.

**Table 3. Effect of cryogenic storage on quantification of individual genes and gene transcripts from laboratory-generated samples.**

<b>A. <i>P. putida</i> F1 samples</b>				
Target		1 week	2 weeks	1 month
DNA	16S rDNA	1.12 ± 0.20	1.10 ± 0.14	1.15 ± 0.12
	<i>todC</i>	1.15 ± 0.04	1.04 ± 0.07	0.95 ± 0.11
	<i>todE</i>	1.11 ± 0.07	1.09 ± 0.12	1.15 ± 0.10
rRNA	16S rRNA	1.05 ± 0.06	0.96 ± 0.09	0.94 ± 0.06
mRNA	<i>todC</i>	1.04 ± 0.16	0.89 ± 0.16	1.07 ± 0.24
	<i>todE</i>	1.06 ± 0.08	0.89 ± 0.05	0.99 ± 0.06

<b>B. <i>B. Subtilis</i> JH642 samples</b>				
Target		1 week	2 weeks	1 month
DNA	<i>trpC</i>	0.97 ± 0.07	1.04 ± 0.11	1.03 ± 0.06
	<i>thrB</i>	0.98 ± 0.10	0.93 ± 0.07	1.16 ± 0.07
	<i>pheA</i>	0.85 ± 0.14	0.91 ± 0.06	1.10 ± 0.10
mRNA	<i>trpC</i>	0.96 ± 0.04	0.95 ± 0.03	0.92 ± 0.05
	<i>thrB</i>	1.00 ± 0.06	1.04 ± 0.12	0.92 ± 0.12
	<i>pheA</i>	1.02 ± 0.20	1.00 ± 0.10	0.85 ± 0.19

<b>C. <i>Dehalococcoides</i> enrichment culture samples</b>				
Target		1 week	2 weeks	2 months
DNA	16S rRNA	0.99 ± 0.04	0.98 ± 0.03	1.10 ± 0.04
	<i>pceA</i>	1.01 ± 0.02	0.97 ± 0.06	1.12 ± 0.03
	<i>tceA</i>	1.04 ± 0.03	0.97 ± 0.03	1.10 ± 0.06
	<i>vcrA</i>	1.08 ± 0.04	0.98 ± 0.06	1.10 ± 0.07
	<i>bvcA</i>	1.01 ± 0.00	1.00 ± 0.01	0.99 ± 0.01
rRNA	16S rRNA	0.92 ± 0.12	1.01 ± 0.06	1.10 ± 0.06
mRNA	<i>pceA</i>	1.01 ± 0.01	1.00 ± 0.01	1.01 ± 0.01
	<i>tceA</i>	1.00 ± 0.02	1.01 ± 0.01	1.00 ± 0.01
	<i>vcrA</i>	1.11 ± 0.02	1.12 ± 0.04	1.12 ± 0.05
	<i>bvcA</i>	1.02 ± 0.04	1.00 ± 0.02	1.00 ± 0.03

Data presented as fold differences relative to the unfrozen control. Standard deviations calculated from 5 independent sets of reactions. (n= 5).

**Table 4. RNA integrity numbers**

Sample	Effects of Freezing			Effects of Storage				
	Unfrozen	Frozen	Frozen with granular media	t = 0	1 week	2 weeks	3 months	6 months
<i>P. putida F1</i>	10.0	10.0	10.0	10.0	9.7	NA	9.9	10.0
<i>B. subtilis JH642</i>	7.3	8.4	7.8	7.8	8.6	8.8	8.7	7.5

*RNA integrity numbers (RINs) determined by analysis with an Agilent 2100 Bioanalyzer for RNA extracted from single-species samples. Due to a limited amount of RNA, data are not available (NA) for P. putida F1 at a storage time of 2 weeks, or for either sample at 1 month. Data are, however, available for samples stored for both 3 and 6 months.*

**Table 5. Pearson's correlation coefficients: Archaeal enrichment culture samples rDNA PCR-SSCP**

	unfrozen 1	unfrozen 2	unfrozen 3	frozen 1	frozen 2	frozen 3	frozen with granular media 1	frozen with granular media 2	frozen with granular media 3
unfrozen 1	1.00								
unfrozen 2	0.97	1.00							
unfrozen 3	0.96	0.96	1.00						
frozen 1	0.97	0.97	0.95	1.00					
frozen 2	0.97	0.97	0.97	0.97	1.00				
frozen 3	0.96	0.97	0.98	0.96	0.97	1.00			
frozen with granular media 1	0.96	0.97	0.96	0.96	0.97	0.96	1.00		
frozen with granular media 2	0.95	0.97	0.97	0.96	0.95	0.97	0.96	1.00	
frozen with granular media 3	0.97	0.96	0.98	0.95	0.96	0.98	0.95	0.95	1.00

*Matrix of pair-wise Pearson's correlation coefficients of densitometric profiles generated from PCR-SSCP of bacterial 16S rDNA in archaeal enrichment culture samples.*

**Table 6. Pearson's correlation coefficients: DHC enrichment culture samples rDNA PCR-SSCP**

	unfrozen 1	unfrozen 2	unfrozen 3	1 week 1	1 week 2	1 week 3	2 weeks 1	2 weeks 2	2 weeks 3	2 months 1	2 months 2	2 months 3
unfrozen 1	1.00											
unfrozen 2	0.98	1.00										
unfrozen 3	0.98	0.98	1.00									
1 week 1	0.97	0.98	0.98	1.00								
1 week 2	0.97	0.99	0.98	0.98	1.00							
1 week 3	0.96	0.99	0.98	0.98	1.00	1.00						
2 weeks 1	0.98	0.98	0.99	0.99	0.98	0.99	1.00					
2 weeks 2	0.97	0.99	0.98	0.99	0.99	0.99	0.99	1.00				
2 weeks 3	0.97	0.98	0.98	0.99	0.98	0.99	0.99	0.99	1.00			
2 months 1	0.95	0.97	0.97	0.98	0.99	0.99	0.98	0.99	0.97	1.00		
2 months 2	0.98	0.99	0.98	0.98	0.99	0.99	0.99	0.99	0.99	0.98	1.00	
2 months 3	0.98	0.99	0.98	0.98	0.99	0.99	0.99	0.99	0.99	0.98	1.00	1.00

*Matrix of pair wise Pearson's correlation coefficients of densitometric profiles generated from PCR-SSCP of bacterial 16S rDNA in DHC enrichment culture samples.*

**Table 7. Pearson's correlation coefficients: Archaeal enrichment culture samples rRNA PCR-SSCP**

	unfrozen 1	unfrozen 2	unfrozen 3	frozen 1	frozen 2	frozen 3	frozen with granular media 1	frozen with granular media 2	frozen with granular media 3
unfrozen 1	1.00								
unfrozen 2	0.97	1.00							
unfrozen 3	0.96	0.97	1.00						
frozen 1	0.98	0.97	0.96	1.00					
frozen 2	0.96	0.96	0.97	0.97	1.00				
frozen 3	0.95	0.95	0.96	0.96	0.98	1.00			
frozen with granular media 1	0.98	0.97	0.97	0.97	0.97	0.96	1.00		
frozen with granular media 2	0.97	0.96	0.96	0.96	0.98	0.96	0.87	1.00	
frozen with granular media 3	0.96	0.96	0.96	0.95	0.95	0.94	0.96	0.96	1.00

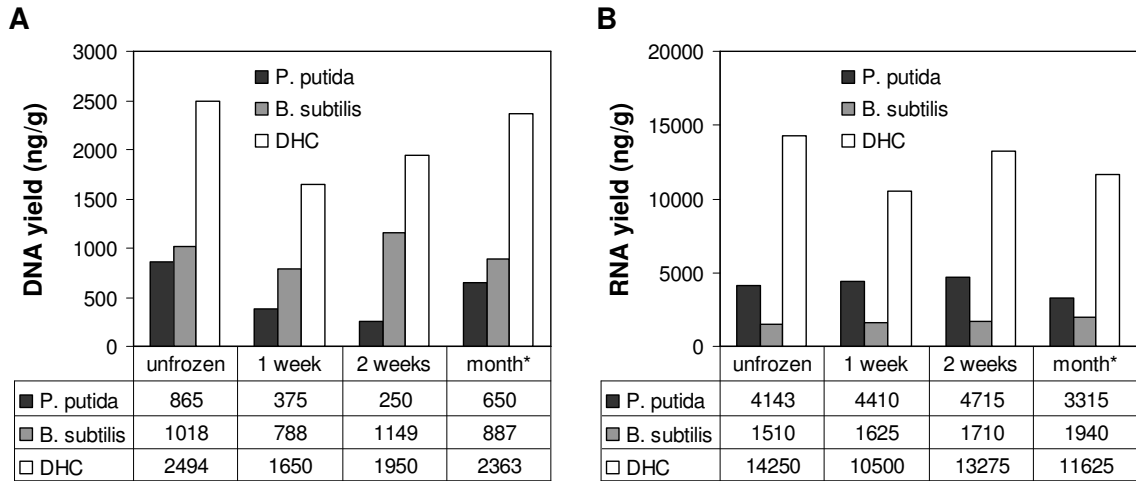
*Matrix of pair wise Pearson's correlation coefficients of densitometric profiles generated from PCR-SSCP of bacterial 16S rRNA in archaeal enrichment culture samples.*

**Table 8. Pearson's correlation coefficients: DHC enrichment culture samples rRNA PCR-SSCP**

	unfrozen 1	unfrozen 2	unfrozen 3	1 week 1	1 week 2	1 week 3	2 weeks 1	2 weeks 2	2 weeks 3	2 months 1	2 months 2	2 months 3
unfrozen 1	1.00											
unfrozen 2	0.97	1.00										
unfrozen 3	0.96	0.98	1.00									
1 week 1	0.97	0.99	0.98	1.00								
1 week 2	0.97	0.98	0.98	0.99	1.00							
1 week 3	0.93	0.96	0.96	0.96	0.98	1.00						
2 weeks 1	0.97	0.96	0.95	0.96	0.96	0.93	1.00					
2 weeks 2	0.97	0.98	0.96	0.97	0.97	0.93	0.98	1.00				
2 weeks 3	0.96	0.96	0.95	0.97	0.97	0.94	0.97	0.96	1.00			
2 months 1	0.96	0.96	0.95	0.97	0.97	0.94	0.97	0.96	1.00	1.00		
2 months 2	0.96	0.98	0.97	0.99	0.98	0.95	0.97	0.98	0.97	0.97	1.00	
2 months 3	0.94	0.96	0.96	0.96	0.96	0.97	0.94	0.94	0.94	0.94	0.96	1.00

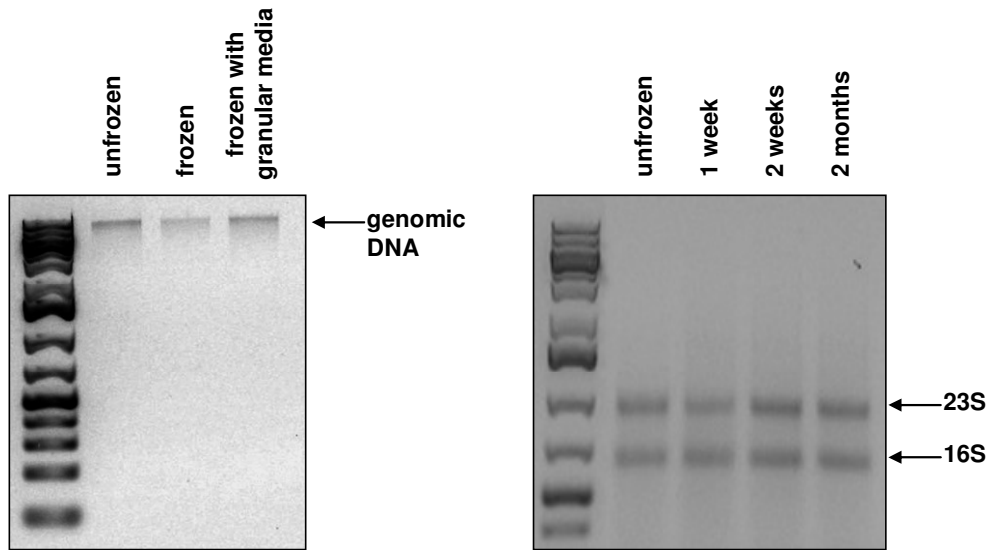
*Matrix of pair wise Pearson's correlation coefficients of densitometric profiles generated from PCR-SSCP of bacterial 16S rRNA in DHC enrichment culture samples.*

**Figure 1. DNA and RNA yields from laboratory-generated core samples**



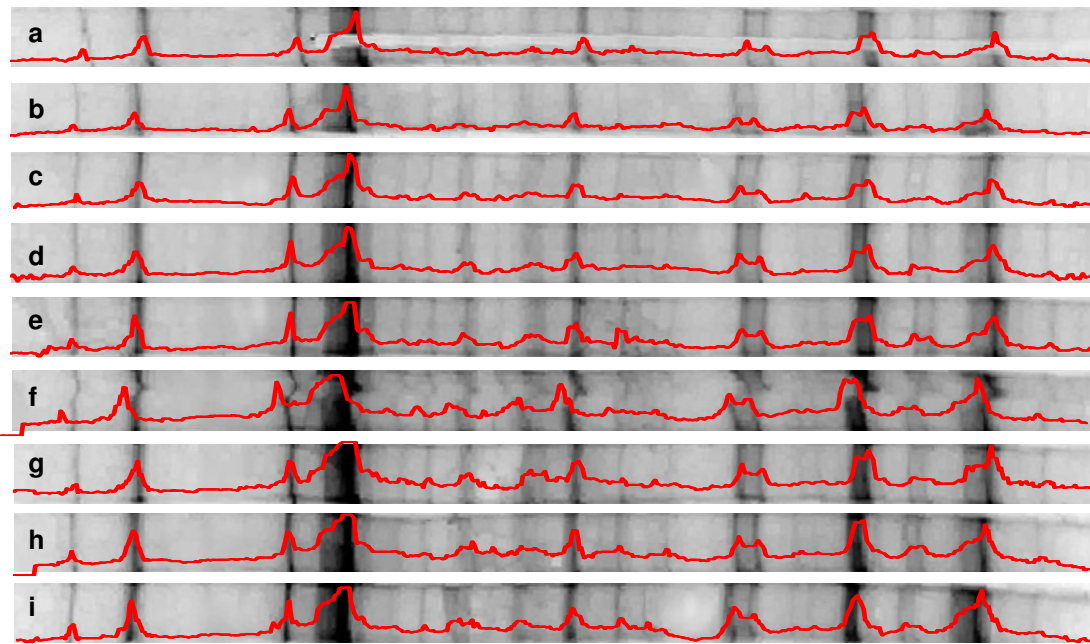
*DNA (A) and RNA (B) yields from single-species and DHC enrichment culture simulated core samples (containing zirconia/silica beads). Data shown for unfrozen samples, and intact samples stored at -80°C. The “\*” denotes that the P. putida and B. subtilis samples were stored for 1 month, while the DHC sample was stored for 2 months.*

**Figure 2. Agarose gel images of DNA and RNA extracted from laboratory-generated samples**



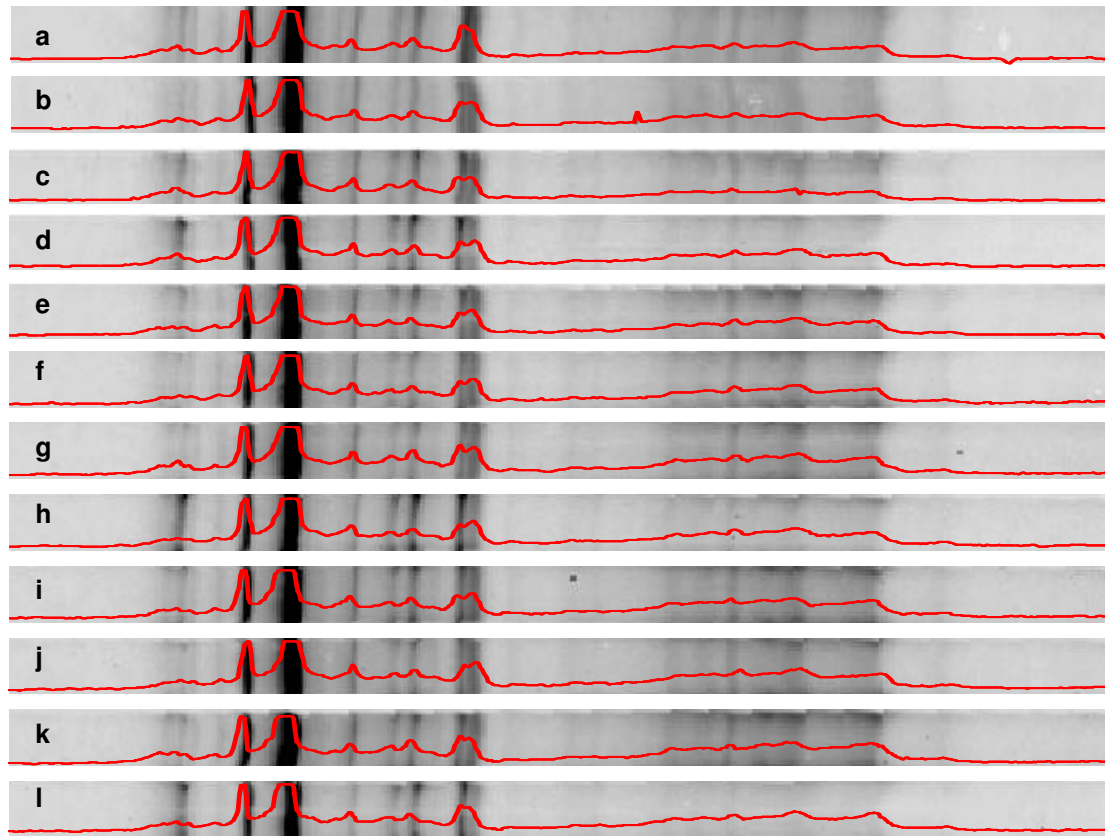
*Left: DNA extracted from P. putida F1 samples (unfrozen, frozen, and frozen with granular media at -80°C for 1 month). Right: RNA extracted from Dehalococcoides simulated core samples (unfrozen, and frozen at -80°C for 1 week, 2 weeks, and 2 months).*

**Figure 3. Results of Bacterial rDNA PCR-SSCP of archaeal enrichment culture samples**



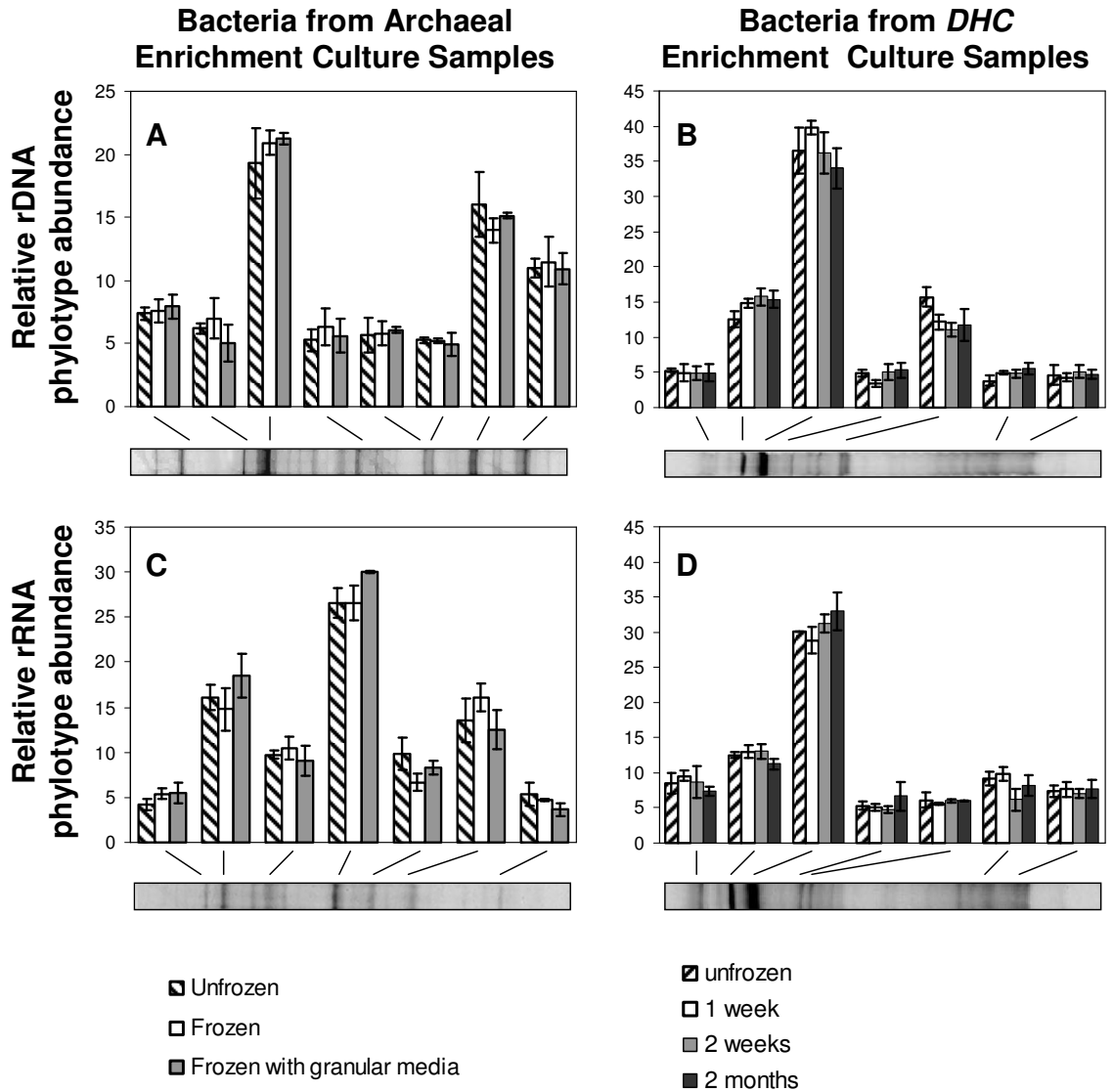
*Shown are gel fingerprints produced by PCR-SSCP of bacterial 16S rDNA from archaeal enrichment culture samples overlaid by the associated densitometric profiles produced using GelCompar software. Unfrozen: a, b & c; frozen: d, e, & f; frozen with granular media: g, h, & i.*

**Figure 4. Results of Bacterial rDNA PCR-SSCP of *DHC* enrichment culture samples**



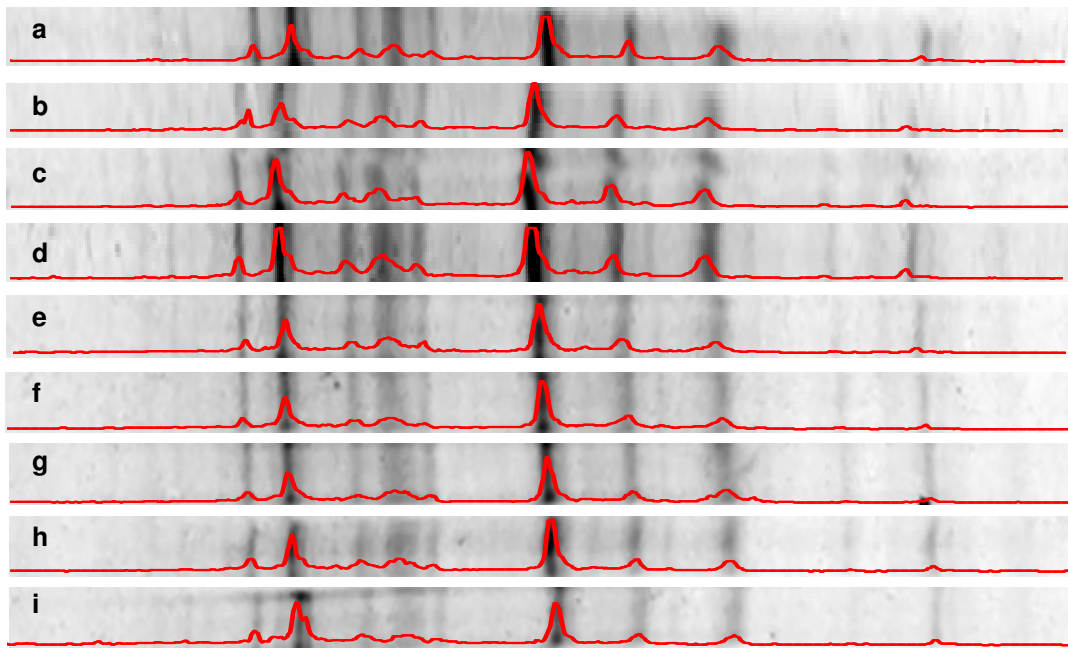
*Shown are gel fingerprints produced by PCR-SSCP of bacterial 16S rDNA from DHC enrichment culture samples overlaid by the associated densitometric profiles produced using GelCompar software. Unfrozen: a, b & c; stored at -80°C for 1 week: d, e, & f; 2 weeks: g, h, & i; and 2 months: j, k, & l.*

**Figure 5. Relative abundance of bacterial phylotypes determined by PCR-SSCP of 16S rDNA (a and b) and rRNA (c and d).**



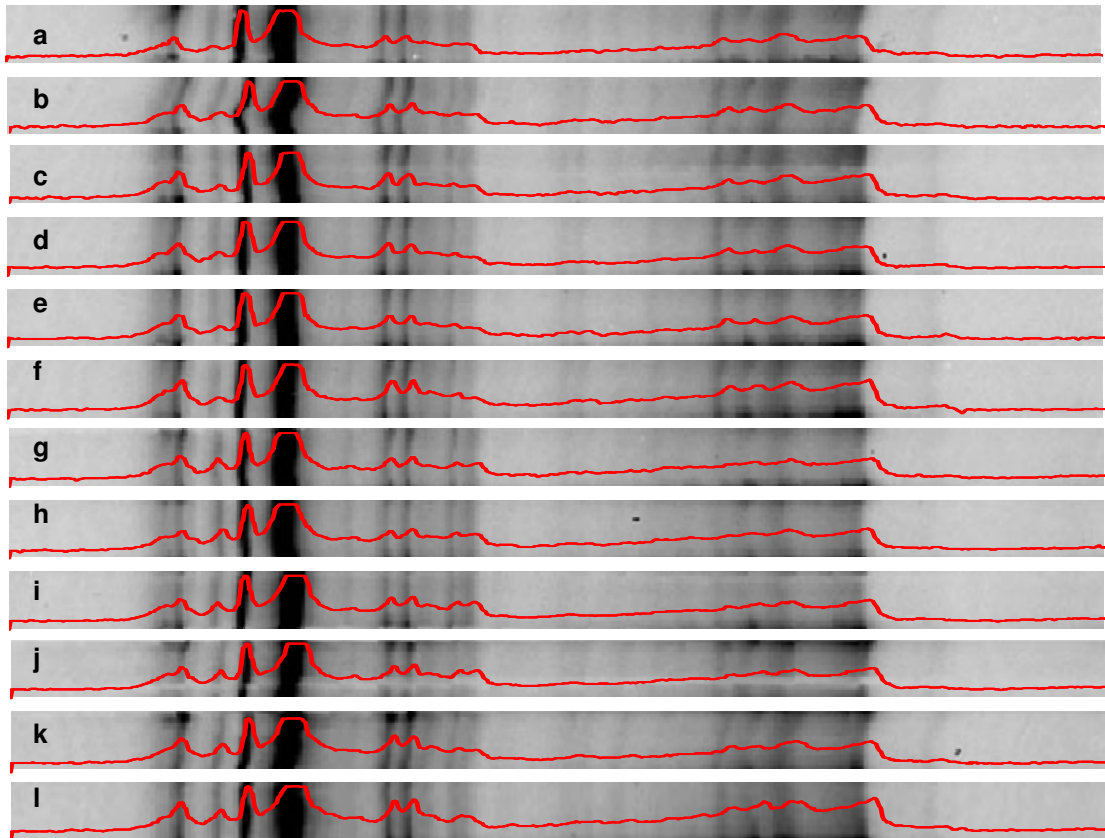
*Data shown for peaks (representing individual bands and phylotypes) that comprised >5% of the total peak area for rDNA (a and b) and rRNA (c and d) archaeal enrichment culture samples (a and c) and DHC enrichment culture samples (b and d). Also shown are corresponding positions within representative gel fingerprints.*

**Figure 6. Results of Bacterial rRNA PCR-SSCP of archaeal enrichment culture samples**



*Shown are gel fingerprints produced by PCR-SSCP of bacterial 16S rRNA from archaeal enrichment culture samples overlaid by the associated densitometric profiles produced using GelCompar software. Unfrozen: a, b & c; frozen: d, e, & f; frozen with granular media: g, h, & i).*

**Figure 7. Results of Bacterial rRNA PCR-SSCP of DHC enrichment culture samples**



*Shown are gel fingerprints produced by PCR-SSCP of bacterial 16S rRNA from DHC enrichment culture samples overlaid by the associated densitometric profiles produced using GelCompar software. Unfrozen: a, b & c; stored at -80°C for 1 week: d, e, & f; 2 weeks: g, h, & i; and 2 months: j, k, & l.*

## **4. Mesocosm scale evaluation of cryogenic preservation and storage, and high-resolution cryogenic core sampling for the molecular characterization of microorganisms in sediment**

### **4.1. Abstract**

Sediment samples collected across a toluene plume in a model aquifer were used to evaluate the effects of cryogenic preservation and storage on microbial community composition, as well as the recovery and quantification of functional genes. Freezing was shown to not affect the relative abundance of 16S rDNA or rRNA phylotypes as determined by the community profiling technique PCR-single-strand conformation polymorphism (PCR-SSCP). Similarly, quantitative PCR (qPCR) analysis revealed that cryogenic preservation did not adversely affect the recovery, quantification, or amplification efficiency of functional genes associated with toluene biodegradation. Additionally, the efficacy of cryogenic core sampling for molecular biological analysis was assessed by collecting a frozen sediment core from the model aquifer. Results from the cryogenically-collected core agreed favorably with those obtained from co-localized unfrozen sediment samples. It is thus concluded that cryogenic core sampling is a viable technique for the accurate characterization of subsurface microbial communities.

## 4.2. Introduction

In Chapter 3, bench scale simulated sediment samples were used to demonstrate the efficacy of freezing to preserve the molecular characteristics of microorganisms in sediments. In this chapter, that work is expanded to include sediment samples from a large scale model aquifer, which represents a more environmentally relevant system. As discussed in Chapter 3, as much as 99% of bacterial populations, including those that degrade a variety of contaminants, are attached to solid-phase materials in both laboratory-scale column experiments, and in the field (12-16). It is not, however, simply a matter of numerical dominance. Numerous studies have shown that sediment and pore water harbor distinct microbial populations which differ in community structure, as well as activity (17,18,65). Sediment has even been shown to support more exclusive phylotypes than the associated groundwater, indicating that the sediment-attached community is not merely a subset of the suspended community, as was once thought (66).

The implications of this are that sediment samples are necessary in order to accurately assess subsurface microbial communities. Collection of core samples, therefore, an optimal sampling approach, particularly with respect to monitoring subsurface biodegradation, which relies on accurate assessments of *in-situ* microbial populations. Traditional subsurface coring, however, can result in incomplete sample recovery and the redistribution of pore fluids during sample collection, which may obscure biogeochemical interfaces relevant to ongoing remediation activities. Additionally, the preservation of DNA and RNA within intact sediment cores presents its own set of challenges. Whereas water samples can be filtered on site and stored in extraction buffer or preservation media (e.g., with RNAlater®, etc.) to prevent the

degradation of nucleic acids, it is difficult to separate cells from soil in the field, and disturbing or destroying the core would obscure biogeochemical interfaces. Consequently, the preservation of biomolecules such as DNA and RNA within intact core samples is an important issue.

A potential solution to both biomolecule preservation and pore water redistribution is to freeze the core *in-situ* prior to extraction to the surface. Immobilizing the pore fluids would not only allow for examination of small-scale features, but may also prevent degradation of nucleic acids and minimize sample contamination during extraction and handling. Historically, cryogenic core sampling has been used for a variety of subsurface sample collection activities. For example, cryogenic sampling of stream beds for microbiological and physical characterization has been a practice for at least 30 years (42,43,67,68). Additionally, Durford et al. used a cryogenic approach to determine the distribution of non-aqueous phase liquids (NAPLs) in aquifer materials (69). Although cryogenic sampling has often been used for such physical and chemical analyses, its use by the bioremediation community has been limited. This is at least in part due to a lack of information about the effects of whole-core freezing on biomolecules of interest to bioremediation researchers.

In the work presented here, the effects of cryogenic preservation on the integrity of DNA and RNA in sediment were evaluated using samples taken from across a toluene plume in a model aquifer. PCR-SSCP was used to evaluate the effects of freezing on the relative abundance of bacterial 16S rDNA and rRNA phylotypes. qPCR was used to assess the effects of freezing on the recovery and quantification of functional genes associated with toluene biodegradation. Finally, a cryogenic core sampling technique

was tested in which a sediment core was frozen *in-situ* in the model aquifer, and extracted for molecular biological analysis. Results from the cryogenically-collected core were compared to those from unfrozen sediment samples collected from ports installed through the side of the model aquifer.

### **4.3. Methods**

#### **4.3.1. Model aquifer**

As illustrated in **Figure 1**, the dimensions of the model aquifer are 7.3 m long × 2.4 m high × 0.5 m thick. Groundwater flow in the model was approximately 30 cm/d. A solution of toluene ( $\approx 65$  mg/L) and fluorescein was injected through an upgradient port located at a height of 1.65 m to simulate a contaminant plume, the shape of which can be seen in **Figure 2**.

#### **4.3.2 Sample collection for MBT analysis**

All samples for molecular biological analysis were collected 2.9 m downgradient of the injection port spanning the upper interface of the toluene contaminant plume (**Figures 1a, 3a,b**). Sediment samples for qPCR analysis were collected at 5 cm intervals through the sediment sampling ports, and were subsequently homogenized, and divided into 1 g fractions. 1 fraction from each sample was immediately processed for DNA and served as the unfrozen control. Remaining fractions were frozen by immersion in liquid nitrogen for 10 s, and were stored at  $-80^{\circ}\text{C}$  for 2 weeks until processing. One sediment sample was randomly selected for further analysis by PCR-single strand conformation polymorphism (PCR-SSCP) as described later. Pore water samples ( $\approx 15$  ml) for

chemical analysis were collected in airtight syringes from water sampling ports installed at depths corresponding to the sediment sampling ports.

In addition to the port-collected samples, a sediment core was also cryogenically collected using a Geoprobe core sampler (Geoprobe Systems, Salina, KS) modified to freeze the core *in-situ* prior to extraction to the surface. Briefly, the core was advanced to the proper depth in the model aquifer using a concrete vibrator (**Figure 3c**). Liquid nitrogen coolant was then pumped through coils of copper tubing between the outer pipe casing and the inner core barrel (**Figure 3d**). Once frozen, the aluminum core sleeve containing the frozen sample was removed from the core barrel and transferred to an on-site -20°C freezer (**Figure 3e**) where it was stored for 3 days before being cut (while still in the freezer) into 2.5 cm sections (**Figure 3f**) using a tube cutter. Individual sections were then stored at -80°C until processing for DNA.

### **4.3.3 Nucleic acid extraction and qPCR**

All DNA extractions were performed on 1 g sediment fractions using the FastDNA Spin Kit for Soil (MP Biomedicals, Solon, OH). RNA was extracted from 4 replicate 1 g fractions of the sample selected for PCR-SSCP analysis as described in Smith et al. (50), and pooled. All nucleic acids were stored at -80° until analysis. RNA was treated with Turbo DNA-free (Applied Biosystems, Carlsbad, CA) and was confirmed to be free of DNA contamination by a qPCR without reverse transcriptase. Total RNA was converted to complementary DNA (cDNA) using SuperScript III First-Strand Synthesis Supermix (Invitrogen Corp., Carlsbad, CA). Quantitative PCR of DNA and cDNA was performed in a MyiQ real-time qPCR detection system using iQ SYBR

Green Supermix (BioRad Laboratories Inc., Hercules, CA), and primers (200 nM) targeting genes involved in toluene degradation.

#### **4.3.4 Quantitative PCR**

qPCR was performed in triplicate 25  $\mu$ L reactions in a MyiQ real-time qPCR detection system using iQ SYBR Green Supermix (BioRad Laboratories Inc., Hercules, CA). Primers targeting *bssA* and *tmoA* genes were added at a final concentration of 200 nM. Cycling conditions consisted of 5 min initial denaturation at 95°C followed by 40 cycles of 45 s denaturation at 95°C, 1 min annealing, and 1.5 min extension at 72°C. Annealing temperatures were 61.5 and 60°C for *bssA* and *tmoA*, respectively. qPCR data were analyzed using LinReg PCR (56) and gene copy numbers were determined by comparison to standard curves.

#### **4.3.5 Microbial community analysis**

PCR-single strand conformation polymorphism (PCR-SSCP) was used to examine the effects cryogenic preservation and storage on the relative abundance of bacterial 16S rDNA (5 months storage) and rRNA (10 months storage) phlotypes in the model aquifer sediment. RNA was converted to cDNA as described. DNA and cDNA were PCR-amplified in triplicate independent reactions using universal bacterial 16S rRNA gene primers (FAM-labeled 357F (5' - CCT ACG GGA GGC AGC AG -3') and 519R (5' - ACC GCG GCT GCT GGC AC -3')) (32). Cycling parameters consisted of 4 min initial denaturation at 95°C and 20 touchdown cycles of 30 s denaturation at 95°C, 1 min annealing starting at 66°C, and 1.5 min extension at 72°C. The annealing temperature was decreased 0.5°C with every cycle until a final annealing temperature of

56°C was reached. The touchdown step was followed by 20 cycles of 30 s denaturation at 95°C, 1 min annealing at 56°C, and 1.5 min extension at 72°C, with a final extension of 7 min at 72°C.

After amplification, PCR products were purified using the Wizard SV gel and PCR clean-up system (Promega Corp., Madison, WI). Purified PCR products were combined with SSCP stop solution (Lonza, Basel, Switzerland), denatured at 95°C for 3 minutes, and placed on ice as described in Sliwinski and Goodman (58). Products were run on a 0.75 mm 1×MDE polyacrylamide gel (Lonza, Basel, Switzerland) at 300 V for 25 hours at 17°C. After electrophoresis, the gel was imaged directly on a Typhoon variable mode imager (GE Healthcare Bio-Sciences Corp., Piscataway, NJ).

Gel fingerprint patterns were analyzed using GelCompar II software (Applied Maths, Austin, TX), which was used to detect bands, create densitometric profile curves, and calculate the area under each peak. This information was transformed into a relative area under each peak (relative to the sum of the areas under all peaks), thus making possible the comparison of independent samples. Additionally, similarity matrices of the densitometric curves were calculated based on pair-wise Pearson's correlations.

## **4.4. Results and Discussion**

### **4.4.1 Chemical analysis of pore water**

Results from the chemical analysis of model aquifer pore water are shown in **Figure 4**. These data represent a cross section of the plume at a distance of 2.9 m downstream of the injection port (height = 1.65 m). The toluene plume is characterized by steep gradients of both dissolved oxygen (DO) and nitrate at plume fringes. This

representative profile remained stable over several months of system operation (data not shown).

#### **4.4.2 Cryogenic sample preservation and storage**

The effects of cryogenic preservation and storage were assessed by profiling the depth distribution of *bssA* and *tmoA* genes in fractions of unfrozen, and frozen sediment samples collected from the model aquifer. These genes are known to be biomarkers of anaerobic, and aerobic toluene biodegradation, respectively, and are thus of interest to bioremediation practitioners. The *bssA* genes codes for benzylsuccinate synthase, the key enzyme involved in anaerobic toluene degradation, and has been found in all isolates capable of anaerobic toluene degradation to date (70). The *tmoA* gene codes for toluene-4-monooxygenase, one of several oxygenases involved in toluene degradation under aerobic conditions (71).

The depth distributions of *bssA* and *tmoA* genes from unfrozen, and frozen sediment fractions can be seen in **Figure 5**. Profiles generated from sediment fractions that were frozen and stored at -80°C for two weeks matched those generated from unfrozen fractions both qualitatively, and quantitatively (i.e. both the distribution patterns, and absolute gene abundances were similar). Additionally, no differences could be seen in qPCR amplification efficiency between frozen and unfrozen samples as assessed by LinReg PCR which determines amplification efficiency by monitoring individual-sample reaction kinetics.

The community fingerprinting technique, PCR-SSCP, was used to further evaluate the effects of cryogenic preservation and storage by including DNA and RNA from a broad range of bacterial phyla. Bacterial 16S rDNA and rRNA phylotypes from

unfrozen sediment, and sediment which had been frozen and stored at -80°C were profiled in triplicate. Resulting gel fingerprint patterns and associated densitometric profiles can be seen in **Figures 6 and 7**. DNA and RNA extracted from cryogenically-stored sediment produced densitometric profiles that were highly similar to those from unfrozen sediment. Pearson's correlation coefficients ( $r$ ) calculated for comparisons of unfrozen and frozen samples averaged 0.96 and 0.97 for rDNA and rRNA, respectively, whereas  $r$  values comparing replicates of the same sample averaged 0.97 and 0.98 for rDNA and rRNA, respectively (**Tables 1 & 2**).

The area under each peak in each densitometric profile was converted to a relative peak area by dividing by the area under all peaks in the profile. Peaks (representing unique phylotypes) comprising >5% of the total peak area were plotted in **Figure 8**, which also shows the corresponding peak positions in a representative PCR-SSCP gel lane and densitometric profile. PCR-SSCP profiles of bacterial rDNA and rRNA from unfrozen and frozen sediment were comparable in the relative abundance of the dominant phylotypes, i.e. cryogenic preservation and storage did not disproportionately affect any individual phylotype. The results with rRNA are particularly significant because biodegradation depends upon active bacterial populations, and *in-vivo* rRNA content is often correlated with cellular growth rate (59-61).

#### **4.4.3 Cryogenic core sampling**

*BssA* and *tmoA* genes were profiled in the frozen sediment core recovered from the model aquifer, and the profiles were compared to those generated from unfrozen sediment collected from the sampling ports (**Figure 9**). The depth distribution patterns of these genes in the frozen core sample were similar to those in the unfrozen sediment

samples. Specifically, both *tmoA* and *bssA* gene abundances peaked near the plume interface, with the *tmoA* peak occurring on the oxic side of the interface, and *bssA* on the anoxic side.

Although the overall distribution patterns of *bssA* and *tmoA* genes in the frozen core and the unfrozen sediment were qualitatively similar, absolute gene abundances were consistently about 2 fold higher in the frozen core. Correspondingly, overall DNA recovery from the sediment core was also greater than from port-collected sediment samples (data not shown). Freeze-thaw cycling is a commonly used method of DNA extraction, the mechanism of which is physical disruption of cells by the formation of ice crystals. At first glance, it may seem as if this aided overall DNA recovery in the frozen core thus explaining the results. However, the presence of a freeze-thaw cycle alone is not sufficient to explain the increased yield since the frozen fractions of the port-collected sediment did not produce higher DNA yields (data not shown), or *tmoA* and *bssA* genes abundances (**Figure 5**) than the unfrozen fractions. However, the speed at which freezing occurred in the core versus the 1 g sediment fractions may have resulted in higher yields from the frozen core.

Cellular disruption from ice crystal formation typically occurs at temperatures ranging from -4 to -40°C. Rapid cooling through this critical zone prevents the formation of ice crystals, and thus serves as the basis of many protocols for the preservation of viable cells (72). The small, 1 gram fractions of sediment were frozen within just a few seconds by immersion in liquid nitrogen. By contrast, *in-situ* measurements taken during freezing suggest that temperatures at the center of the core were in the -4 to -40°C range

for about 80 seconds (**Figure 10**). This may have resulted in intracellular ice crystal formation and thus greater DNA yields from aided cell lysis.

#### **4.5. Conclusions**

Sediment samples from a model aquifer were used to evaluate the efficacy of cryogenic preservation, and cryogenic core sampling for molecular biological analysis of microorganisms in sediment. The introduction of toluene to the model aquifer resulted in the formation of a stable anaerobic toluene plume. qPCR was used to profile the depth distribution of genes involved in toluene biodegradation across the upper interface of the plume. Sediment fractions which had been frozen and stored at -80°C for 2 weeks prior to processing produced functional gene profiles matching those generated from unfrozen sediment fractions. Furthermore, microbial community analysis by PCR-SSCP revealed no difference in the relative abundance of bacterial phylotypes between unfrozen and frozen sediment, indicating that freezing did not disproportionately affect any particular phylotype. This was true not only for rDNA phylotypes, but also for rRNA phylotypes. This is important because biodegradation depends upon active bacterial populations, and *in-vivo* rRNA content is often correlated with cellular growth rate (59-61).

Results with sediment from the model aquifer suggest that cryogenic preservation is a viable approach for preserving the molecular signature of microorganisms in sediment. That work was further extended to the evaluation of cryogenic sediment coring, in which a sediment core was frozen *in-situ* in the model aquifer prior extraction to the surface. The development of such a technique would serve the dual purposes of biomolecule preservation, and the preservation of biogeochemical interfaces relevant to bioremediation.

With the cryogenically-collected core, it was possible to profile the abundance of functional genes to within a resolution of 2.5 cm. This represents a significant improvement over the resolution of groundwater sampling, which is, at best, on the order of meters (23). Further, many studies suggest that the poor spatial resolution of groundwater sampling makes it inadequate to capture “hotspots” of biodegradation which often occur in narrow plume interfaces, where overlapping countergradients of electron donors and acceptors exist (23-26,37,38).

The absolute abundance of genes recovered from the frozen core was roughly 2 fold higher than from the port-collected sediment. This is likely due to intracellular ice crystal formation in the core which contributed to cell lysis and therefore increased DNA extraction efficiency. Nonetheless, the vertical distribution patterns of functional genes were similar in the cryogenically-collected core, and in the unfrozen sediment, indicating that cryogenic coring could be used to accurately characterize subsurface microbial populations. In fact, given the susceptibility of biomolecules, particularly RNA, to decay, immediate freezing may be the only viable way to preserve the *in-situ* microbial characteristics of sediment. It also has the additional advantage of being able to capture small-scale features such as biogeochemical interfaces that conventional groundwater sampling cannot adequately resolve.

**Table 1. Pearson's correlation coefficients for bacterial rDNA PCR-SSCP profiles**

	<b>unfrozen 1</b>	<b>unfrozen 2</b>	<b>unfrozen 3</b>	<b>frozen 1</b>	<b>frozen 2</b>	<b>frozen 3</b>
<b>unfrozen 1</b>	<b>1.00</b>					
<b>unfrozen 2</b>	0.99	<b>1.00</b>				
<b>unfrozen 3</b>	0.99	0.99	<b>1.00</b>			
<b>frozen 1</b>	0.98	0.98	0.98	<b>1.00</b>		
<b>frozen 2</b>	0.98	0.98	0.97	0.99	<b>1.00</b>	
<b>frozen 3</b>	0.98	0.97	0.96	0.98	0.99	<b>1.00</b>

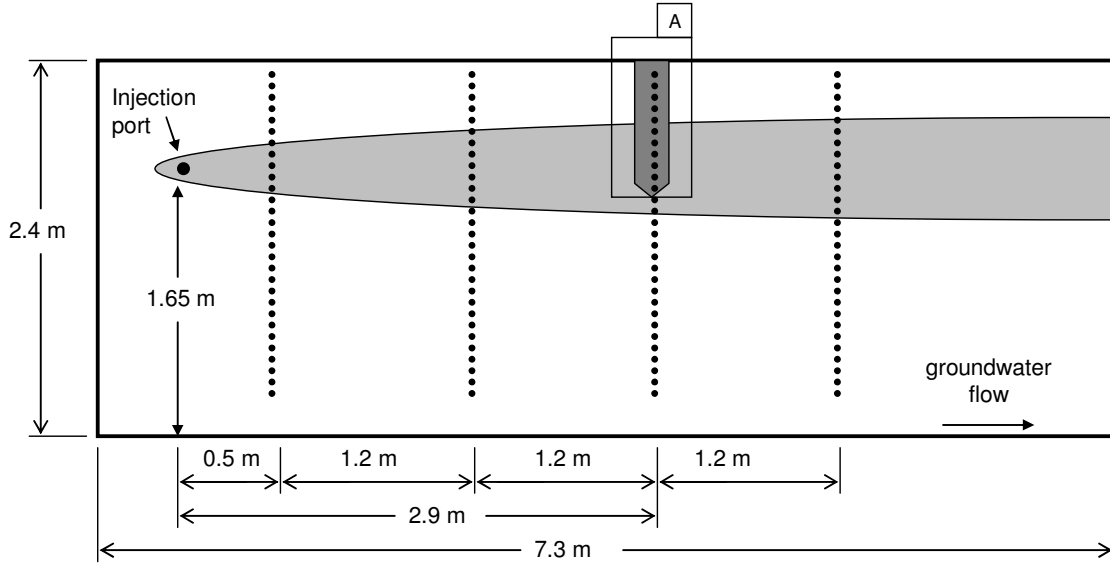
*Matrix of pair-wise Pearson's correlation coefficients of densitometric profiles generated from PCR-SSCP of bacterial 16S rDNA in unfrozen model aquifer sediment, and sediment that had been stored at -80°C for 5 months.*

**Table 2. Pearson's correlation coefficients for bacterial rRNA PCR-SSCP profiles**

	<b>unfrozen 1</b>	<b>unfrozen 2</b>	<b>unfrozen 3</b>	<b>frozen 1</b>	<b>frozen 2</b>	<b>frozen 3</b>
<b>unfrozen 1</b>	<b>1.00</b>					
<b>unfrozen 2</b>	0.99	<b>1.00</b>				
<b>unfrozen 3</b>	0.99	0.99	<b>1.00</b>			
<b>frozen 1</b>	0.98	0.98	0.98	<b>1.00</b>		
<b>frozen 2</b>	0.98	0.98	0.97	0.99	<b>1.00</b>	
<b>frozen 3</b>	0.98	0.97	0.96	0.98	0.99	<b>1.00</b>

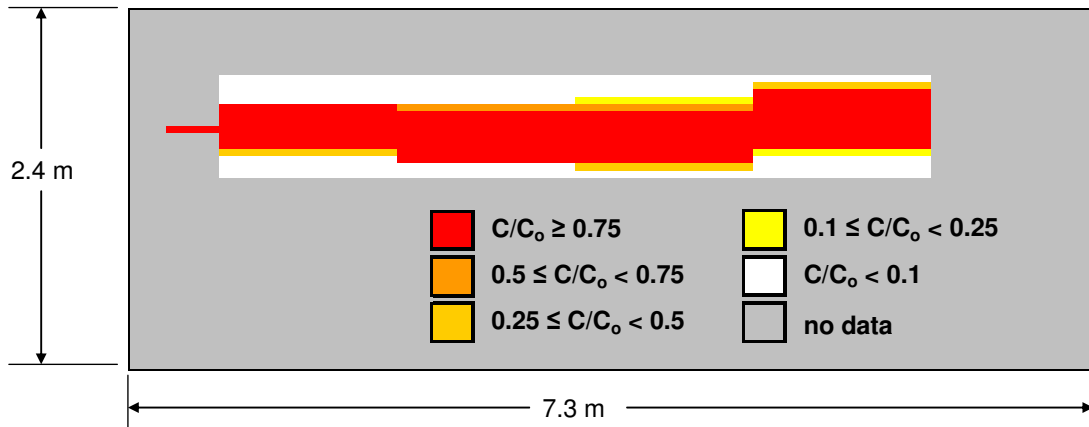
*Matrix of pair-wise Pearson's correlation coefficients of densitometric profiles generated from PCR-SSCP of bacterial 16S rRNA in unfrozen model aquifer sediment, and sediment that had been stored at -80°C for 10 months.*

**Figure 1. Model aquifer**



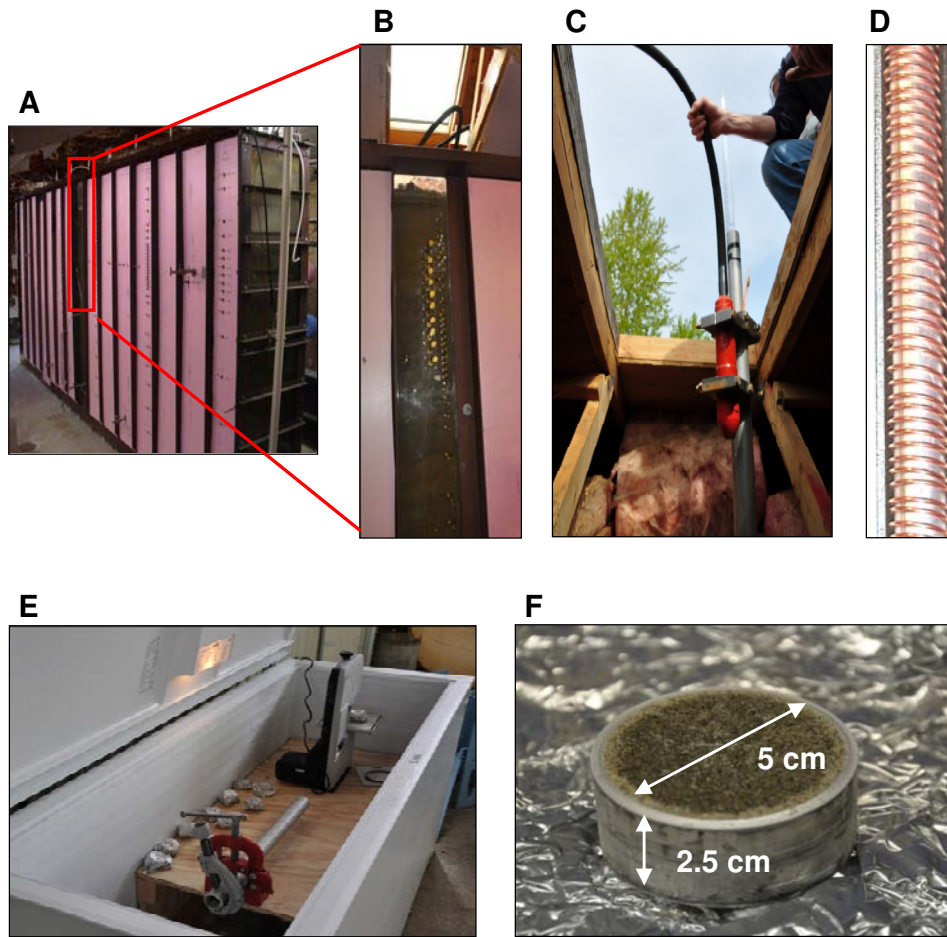
*Side-view schematic of the model aquifer. Its dimensions are 7.3 m long, by 2.4 m tall by 0.5 m thick (not shown). The injection port is located at a height of 1.65 m at the upgradient end of the model. Groundwater flow in the model is from left to right as shown. Four transects of groundwater sampling ports (black circles) are installed at transects 0.5, 1.7, 2.9, and 4.1 m downgradient from the injection port. In addition, sediment sampling ports are installed adjacent to the groundwater sampling ports highlighted by box A in the figure, which also denotes the location of the cryogenically-collected sediment core.*

**Figure 2. Evolution of contaminant plume in the model aquifer**



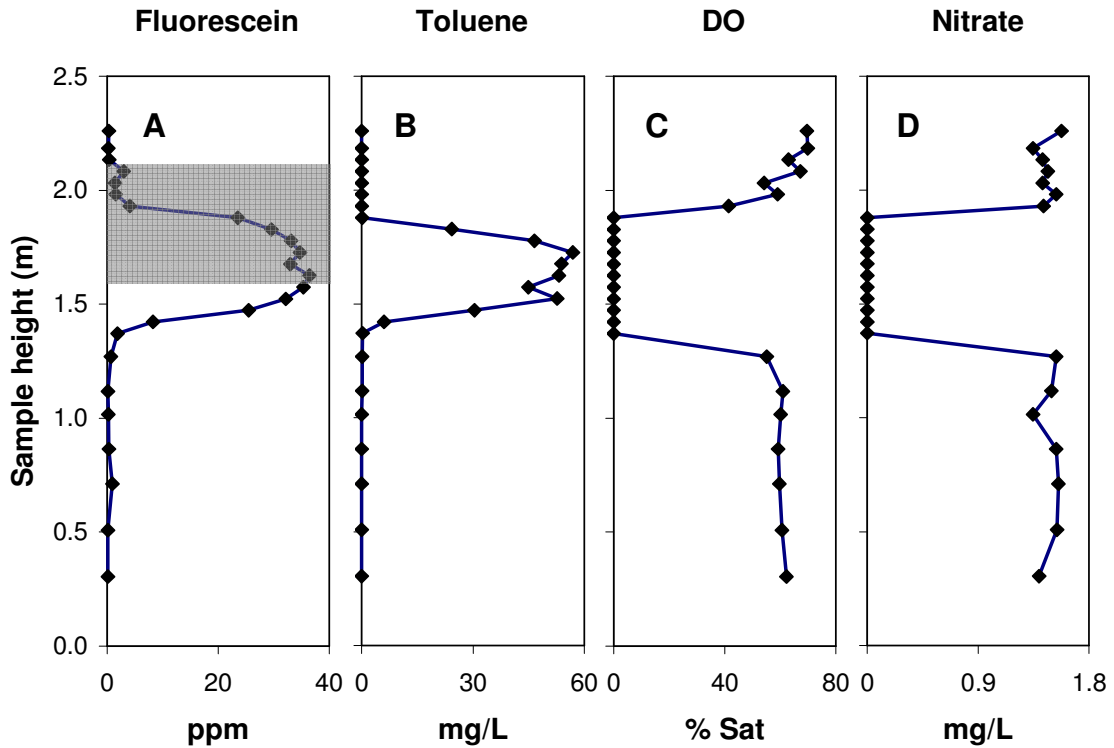
*Schematic illustrating the shape of the contaminant plume based on measured concentrations of the fluorescein tracer ( $C$ ) in pore water collected from the 4 sampling transects and the sampling port located 10 cm downgradient of the injection port. Data shown as values relative to the injection concentration ( $C_0$ ) of fluorescein.*

**Figure 3. Cryogenic core sampling**



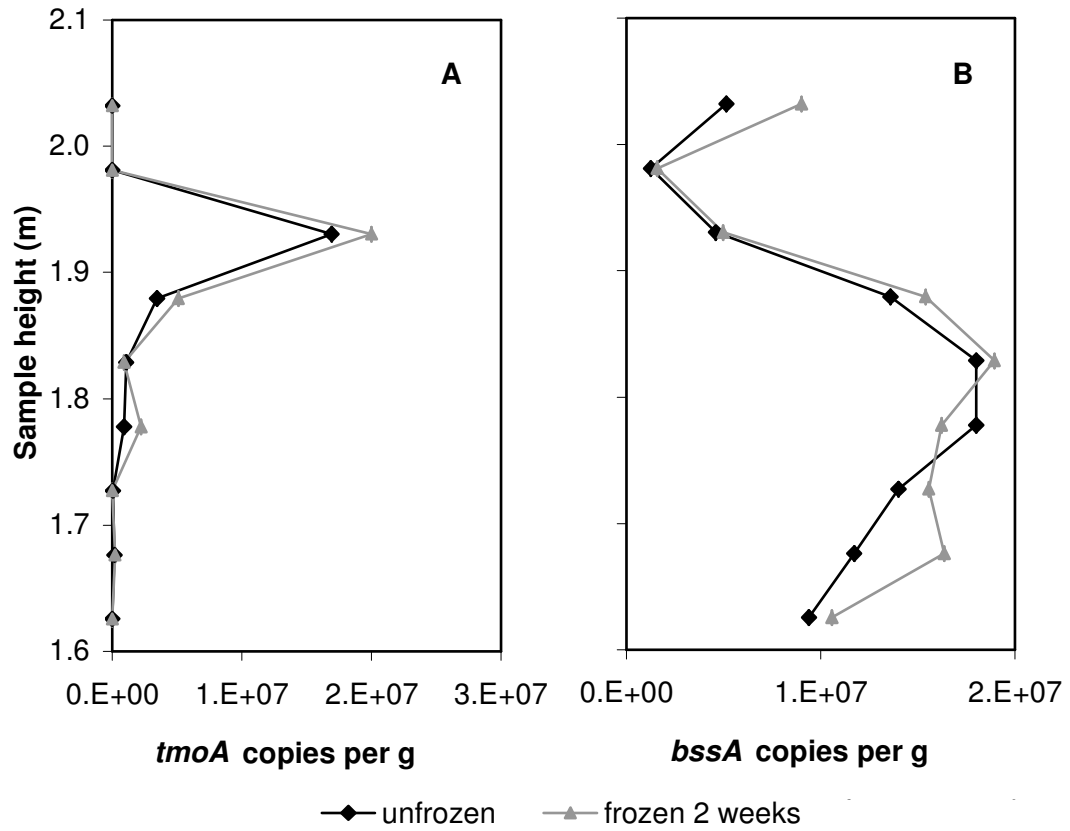
*Illustrated above are the model aquifer (A) and cryogenic core sampling procedures. Panel B shows the sampling location 2.9 m downgradient of injection port with detail of the sediment and water sampling ports. The core was advanced into place using a concrete vibrator (C). Panel D is a cut-away section of the core sampler showing the copper cooling coils. The aluminum core containing the sample was removed and stored in a chest freezer at  $-20^{\circ}\text{C}$  (E) until it was cut into 2.5 cm sections (F) using a tube cutter.*

Figure 4. Depth-resolved model aquifer chemistry



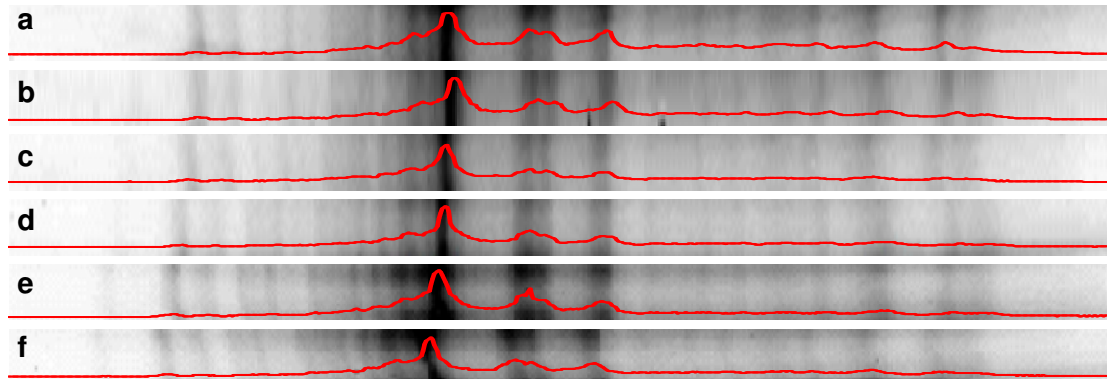
Shown are the depth-resolved profiles of fluorescein (A), toluene (B), dissolved oxygen (DO) (C), and nitrate (D) in pore water collected at 5 cm intervals across the toluene plume in the model aquifer. Injection port located 2.9 m upstream of sampling locations at a height of 1.65 m. Grey box in A illustrates depths over which unfrozen sediment samples, and the frozen core sample were collected for molecular biological analysis.

**Figure 5. Frozen versus unfrozen gene profiles**



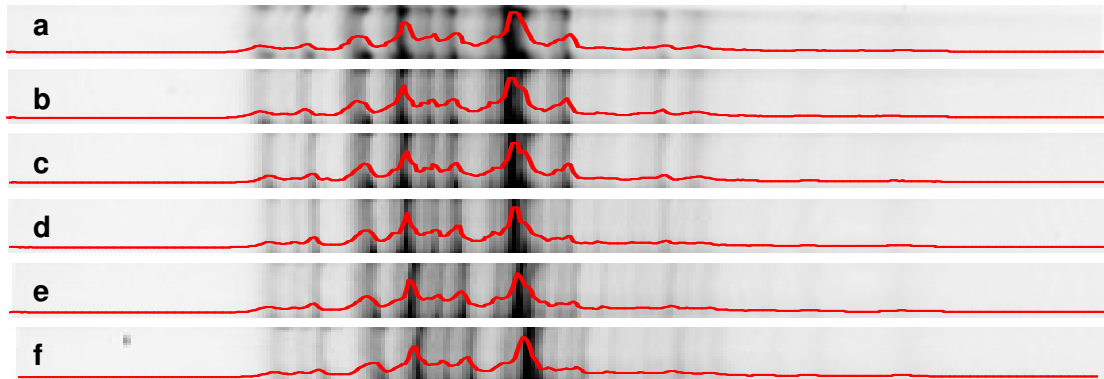
*Depth distribution of tmoA (A) and bssA (B) genes recovered from unfrozen fractions of port-collected sediment (black diamonds), and fractions which were frozen and stored at -80°C for 2 weeks prior to processing (grey triangles).*

**Figure 6. rDNA PCR-SSCP gel images and associated densitometric curves**



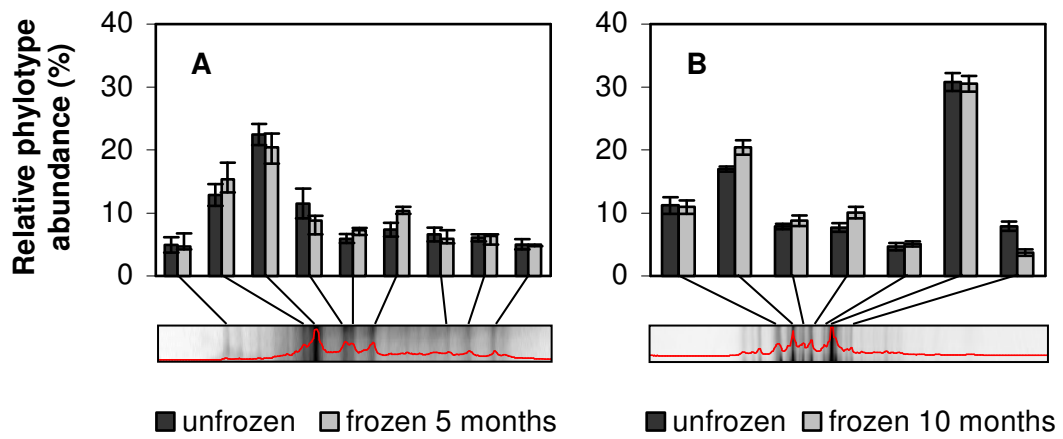
*Shown are gel fingerprints produced by PCR-SSCP of bacterial 16S rDNA from unfrozen (a, b, and c) model aquifer sediment, and sediment that had been stored at -80°C for 5 months (d, e, and f). Overlaid are the associated densitometric profiles produced using GelCompar software.*

**Figure 7. rRNA gel images and associated densitometric curves**



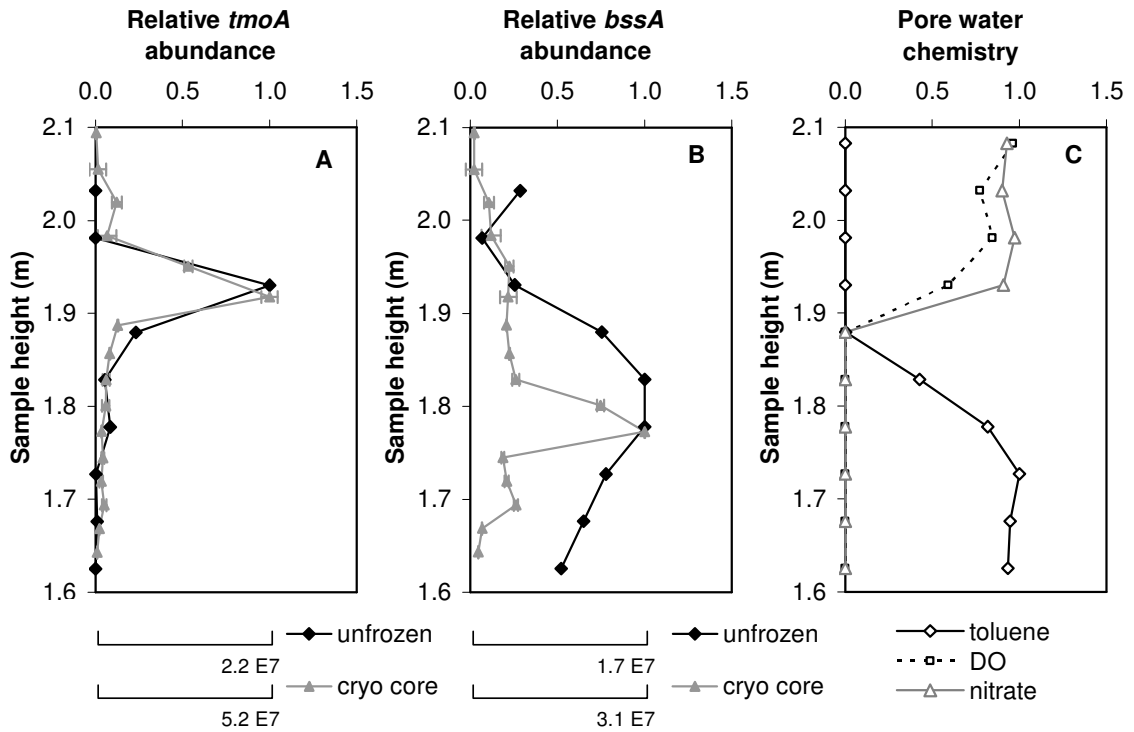
*Shown are gel fingerprints produced by PCR-SSCP of bacterial 16S rRNA from unfrozen (a, b, and c) model aquifer sediment, and sediment that had been stored at -80°C for 10 months (d, e, and f). Overlaid are the associated densitometric profiles produced using GelCompar software.*

**Figure 8. Relative phylotype abundance**



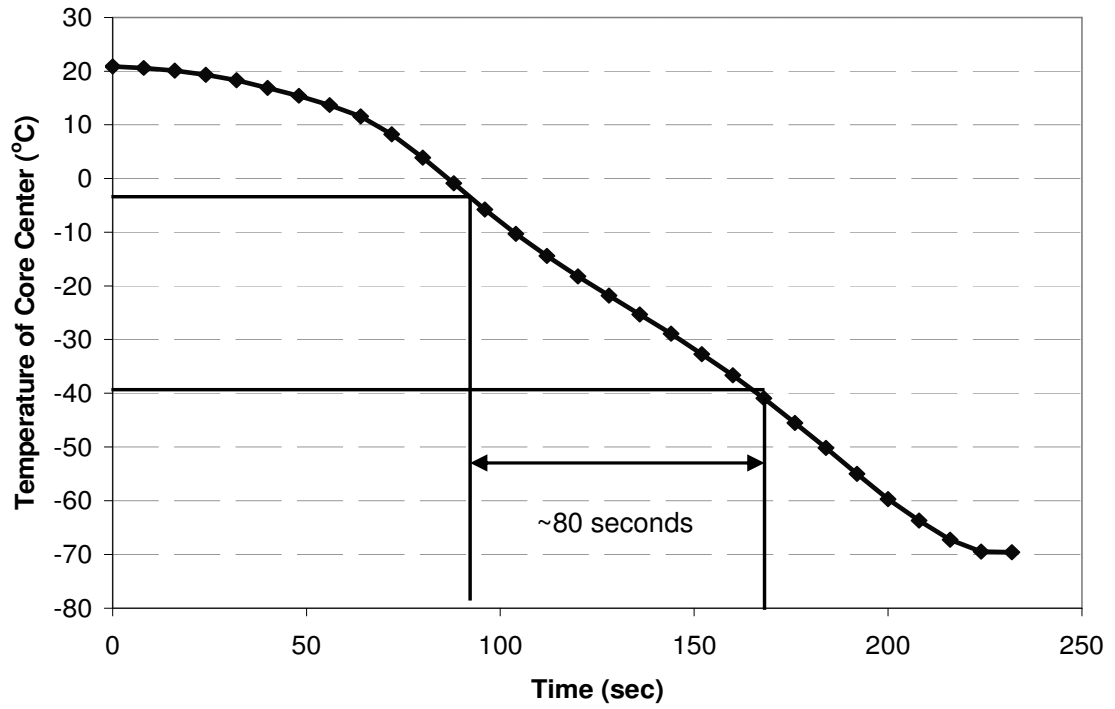
*Relative bacterial 16S rDNA (A) and rRNA (B) phylotype abundance. Data shown for peaks (representing individual phylotypes) that comprised >5% of the total peak area. Error bars represent the standard deviation of 3 replicate profiles from independent reactions.*

**Figure 9. Depth distribution of genes in the port collected sediment and the cryogenically collected core**



*Depth distribution of tmoA (A) and bssA (B) genes recovered from unfrozen port-collected sediment samples (black diamonds) and the cryogenically-collected core (grey triangles). Data plotted as abundance relative to the maximum abundance. Absolute abundance in copies per g can be seen by scale bars at bottom. Error bars, where present, represent the standard deviation of two extractions performed on replicate sediment fractions. Also shown is the pore water chemistry (toluene, dissolved oxygen (DO), and nitrate) associated with these sample (C).*

**Figure 10. Core temperature during cryogenic sampling**



*Plot of temperature at the center of the core as a function of time after liquid nitrogen flow was initiated to freeze the core.*

## **5. Effects of sampling bias revealed by high-resolution molecular biological analysis of paired sediment and water samples from a model aquifer**

### **5.1. Abstract**

Molecular biological tools were used to study microbial communities in paired, high-resolution sediment and water samples taken from a vertical transect across a toluene plume in a model aquifer. PCR-single-strand conformation polymorphism (PCR-SSCP) was used to compare sediment-attached and pore water microbial community structures. Quantitative PCR (qPCR) was used to profile the abundance of functional genes associated with toluene degradation. Sediment and pore water bacterial communities were largely distinct, exclusively so within the toluene plume. Additionally, the vertical distribution pattern of functional genes differed significantly between the water and sediment. Pore water profiles were suggestive of active degradation throughout the plume, whereas sediment-based profiles were in better agreement with electron acceptor availability, and the extent of toluene degradation. Results indicate that bias associated with the selection of a sampling method could lead to inaccurate delineation of zones of active biodegradation, which could, in turn, lead to an overestimation of actual *in-situ* biodegradation activity.

## 5.2. Introduction

The advantages of core sampling over groundwater sampling for molecular biological analysis of contaminated aquifers have been largely based on two factors. First, on a volume per volume basis, the abundance of sediment-attached microorganisms is generally greater than that of the associated pore water, often by several orders of magnitude (18,65). This has led some to suggest that sediment communities are thus more representative of overall subsurface populations. Second, sediment core sampling provides vertical resolution generally not achievable with even the best multi-level groundwater sampling systems (24,23). This is important given recent work demonstrating that degradation processes may be largely confined to the fringes of contaminant plumes where overlapping countergradients of electron donors and acceptors exist. "Plume fringe theory," as it is sometimes called, has been repeatedly demonstrated in both laboratory (25) and field studies (24,23,26).

Additionally, much work exists which expounds differences between sediment-attached, and suspended populations. These differences extend from microbial community composition (18,66), to cellular activities such as the dechlorination of chlorinated hydrocarbons (19), biodegradation of aromatic hydrocarbons (21), and other cellular activities (20,22,12). However, the absence of data from paired high-resolution sediment and groundwater samples has largely limited our ability to determine which strategy is more appropriate for characterizing *in-situ* biodegradation.

In the work presented here, differences between sediment-attached and suspended microbial populations were investigated by high-resolution sampling of both sediment and pore water across a toluene contaminant plume in a well-controlled model aquifer.

Differences between sediment-attached and suspended populations were examined in relation to local groundwater chemistry in an attempt to reconcile profound differences observed between the two compartments.

### **5.3. Methods**

#### **5.3.1. Model Aquifer**

As shown in **Figure 1**, the dimensions of the model aquifer are 7.3 m long  $\times$  2.4 m high  $\times$  0.5 m thick. A solution of toluene (65 mg/L) and fluorescein was continually injected at the up-gradient end through an injection port installed at a height of 1.65 m. Groundwater flow in the model was approximately 30 cm/d.

#### **5.3.2 Sample collection for MBT analysis**

Sampling ports for pore water collection were installed in 4 vertical transects located 0.5, 1.7, 2.9, and 4.1 m downgradient from the injection port (**Figure 1**). Vertical resolution within each transect was 5 cm. Additionally, there was one water sampling port installed 10 cm downgradient of the injection port. Pore water samples for molecular biological analysis (50 ml) were collected from the ports and filtered onto 0.2  $\mu$ m filters for DNA extraction. A sediment core spanning the upper plume interface (see **Figure 1, box A**) was collected cryogenically (see chapter 4) at a downstream distance of 2.9 m corresponding to the third vertical pore water sampling transect. The core was divided into 2.5 cm sections which were subsequently stored at -80°C until processing.

#### **5.3.3. DNA extraction and quantitative PCR**

DNA extractions were performed on filtered water samples, and 1 g fractions of sediment using the FastDNA Spin Kit for Soil (MP Biomedicals, Solon, OH). Independent DNA extractions were performed on duplicate sediment subfractions from

each depth. (Duplicate water samples were not possible without reducing sample resolution.)

Quantitative PCR was performed in a MyiQ real-time qPCR detection system using iQ SYBR Green Supermix (BioRad Laboratories Inc., Hercules, CA). Primers targeting *bssA* and *tmoA* genes were added at a final concentration of 200 nM. Cycling conditions consisted of 5 min initial denaturation at 95°C followed by 40 cycles of 45 s denaturation at 95°C, 1 min annealing, and 1.5 min extension at 72°C. Annealing temperatures were 61.5 and 60°C for *bssA* and *tmoA*, respectively. qPCR data were analyzed using LinReg PCR (56) and gene copy numbers were determined by comparison to standard curves.

#### **5.3.4. Microbial community analysis**

PCR-single strand conformation polymorphism (PCR-SSCP) was used to profile dominant bacterial 16S rDNA phlotypes recovered from the sediment core and associated pore water, and to compare the microbial community structures in the two compartments. DNA was PCR-amplified using universal bacterial 16S rRNA gene primers (FAM-labeled 357F (5' - CCT ACG GGA GGC AGC AG -3') and 519R (5'- ACC GCG GCT GCT GGC AC -3')) (32). Cycling parameters consisted of 4 min initial denaturation at 95°C and 20 touchdown cycles of 30 s denaturation at 95°C, 1 min annealing starting at 66°C, and 1.5 min extension at 72°C. The annealing temperature was decreased 0.5°C with every cycle until a final annealing temperature of 56°C was reached. The touchdown step was followed by 20 cycles of 30 s denaturation at 95°C, 1 min annealing at 56°C, and 1.5 min extension at 72°C, with a final extension of 7 min at 72°C.

After amplification, PCR products were purified using the Wizard SV gel and PCR clean-up system (Promega Corp., Madison, WI). Purified PCR products were combined with SSCP stop solution (Lonza, Basel, Switzerland), denatured at 95°C for 3 minutes, and placed on ice as described in Sliwinski and Goodman (58). Products were run on a 0.75 mm 1×MDE polyacrylamide gel (Lonza, Basel, Switzerland) at 300 V for 25 hours at 17°C. After electrophoresis, the gel was imaged directly on a Typhoon variable mode imager (GE Healthcare Bio-Sciences Corp., Piscataway, NJ). Gel fingerprint patterns were analyzed using GelCompar II software (Applied Maths, Austin, TX), which was used to detect bands, create densitometric profile curves, and perform a cluster analysis based on Pearson's correlations of the densitometric profiles.

## **5.4. Results and discussion**

### **5.4.1 Toluene plume**

The shape of the contaminant plume generated in the model aquifer can be seen in **Figure 2** which is based on measurements of a conservative tracer, fluorescein, in pore water collected from all four sampling transects, as well as from a plume centerline port located 10 cm downgradient of the injection port. Additionally, results from chemical analyses of model aquifer pore water from the transect located 2.9 m downgradient of the injection port are shown in **Figure 3**. The introduction of toluene resulted in the formation of a stable anaerobic toluene plume extending down the length of the model aquifer with minimal toluene degradation (**Figure 3**). The plume was characterized by steep gradients of both dissolved oxygen (DO) and nitrate at the plume fringes (upper fringe at  $\approx 1.9$  m, lower fringe at  $\approx 1.4$  m). This representative profile remained stable over several months of system operation (data not shown).

#### **5.4.2 DNA yields**

DNA yields were consistently greater from sediment than from an equivalent volume of the associated pore water (**Figure 4**). This is consistent with the idea that sediment-attached microorganisms make up the majority of the microbial community in the model aquifer, and is in agreement with observations of microbial populations in the field (14,15).

#### **5.4.3. Microbial community analysis**

PCR-SSCP was used to compare the bacterial community structures in sediment and associated pore water from the model aquifer. Gel fingerprint patterns were converted to densitometric curves (**Figures 5 and 6**) which were used in a cluster analysis based on Pearson's correlation coefficients. As illustrated in **Figure 7**, sediment-attached and pore water bacterial communities grouped largely independently of one another. Furthermore, clustering becomes exclusive when considering only those profiles generated from samples within the toluene plume (sample height <1.9 m). These results are consistent with field studies in which aquifer sediment and pore water microbial communities were shown to be distinct by various other community profiling techniques such as terminal restriction fragment length polymorphism (T-RFPL)(17), and PCR denaturing gradient gel electrophoresis (DGGE )(18).

#### **5.4.4 Depth distribution of functional genes**

*BssA* and *tmoA* genes were selected as biomarkers for anaerobic and aerobic toluene degradation, respectively, and their abundance was profiled in both the sediment core, and associated pore water collected from the vertical transect at 2.9 m. The *bssA*

gene codes for benzylsuccinate synthase, the key enzyme involved in anaerobic toluene degradation, and has been found in all isolates capable of anaerobic toluene degradation to date (70). *TmoA* codes for toluene-4-monooxygenase, one of several oxygenases involved in toluene degradation under aerobic conditions (51).

The depth distribution of *bssA* and *tmoA* genes recovered from the sediment and water samples can be seen in **Figure 8**. Data are shown as abundances relative to the sample with the highest copy number. Absolute copy numbers are shown by the scale bars. The distribution patterns of both genes differ significantly between the sediment and the associated pore water. *BssA* gene abundance in the sediment peaks at 1.77 m and drops with increasing depth into the plume. In contrast, the abundance of *bssA* genes in the pore water continues to rise throughout the plume reaching a maximum near the centerline of the plume at 1.64 m. *TmoA* gene abundance in the pore water is also at its maximum near the center of the plume, but exhibits an additional peak within the plume interface at 1.88 m ( $C/C_{\max} = 0.79$ ). In the sediment, the *tmoA* peak coincides with the oxic/anoxic interface at 1.92 m, and comparatively few *tmoA* copies can be detected near the centerline of the plume.

The disparity between sediment-attached, and pore water gene profiles is problematic with respect to delineating zones of *in-situ* degradation using functional genes as biomarkers. But perhaps more importantly, it underscores the need for a better understanding of the differences between sediment-attached and free-living populations. Specifically, what are the causes of these differences, and how do they relate to assessments of *in-situ* biodegradation. This is particularly true with regard to selection of

an appropriate sampling strategy, i.e. groundwater, sediment, or some combination of the two, for use with molecular biological analyses.

Based on combined molecular and chemical analyses, it seems the sediment core samples were more appropriate for characterizing biodegradation in the model aquifer. For example, sediment-based gene profiles better reflected solution chemistry than did pore water gene profiles. Pore water *bssA* and *tmoA* gene abundances both peaked nearest to the center of the plume which is both nitrate, and oxygen depleted. The absence of suitable electron acceptors thus makes the plume core an unlikely place for the proliferation of microbial populations capable of toluene degradation under either anaerobic denitrifying conditions, or aerobic conditions. In contrast, *bssA* and *tmoA* gene abundance profiles in the sediment both show narrow peaks in or near the plume interface, which is more consistent with electron acceptor availability. *TmoA* gene abundance in the sediment reaches its maximum within the oxic/anoxic interface where countergradients of toluene and oxygen exist. *BssA* gene abundance peaks slightly below this interface. Although not detectable in the chemical analysis, it is possible that trace amounts of nitrate remained in the upper part of the plume, and together with toluene provided an environment conducive to the development of a population capable of anaerobically degrading toluene under denitrifying conditions.

Additionally, sediment-based *bssA* and *tmoA* gene profiles are also more consistent with the extent of toluene degradation which took place. Pore water *bssA* and *tmoA* gene profiles suggest degradation could be occurring throughout the thickness of the plume. However, very little toluene degradation was observed during the experiment, and toluene concentrations 2.9 m downgradient of the injection port remained >80% of

the injection concentration (**Figure 3a**). These results are more consistent with degradation taking place in only a fraction of the plume's volume, i.e. along narrow biogeochemical interfaces at the plume fringes, as would be suggested by *bssA* and *tmoA* gene abundance profiles in the sediment core.

## 5.5. Conclusions

Based on DNA yields from sediment and pore water, the microbial community in the model aquifer appeared to be dominated by sediment-attached populations. It was not, however, simply that sediment-attached populations were more abundant. Analysis by PCR-SSCP revealed that the two compartments fostered microbial communities with structures that clustered largely independently from one another. Furthermore, the clustering became exclusive when taking into account only those samples collected from within the toluene plume.

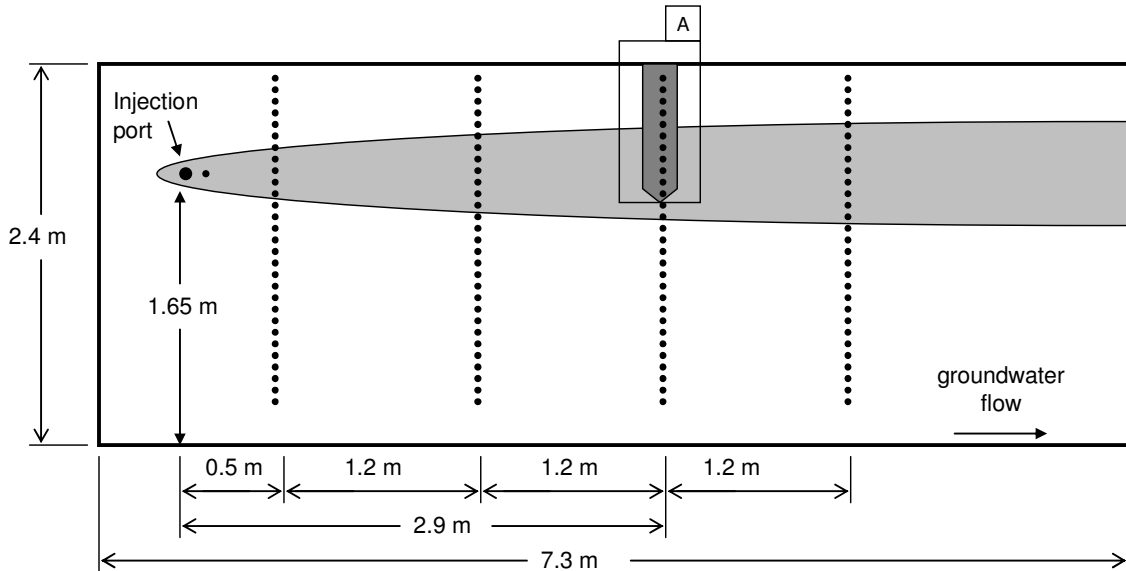
Perhaps of even greater significance are the results profiling the abundance of functional genes associated with toluene biodegradation. The depth distribution of *bssA* and *tmoA* genes differed significantly between sediment and the associated pore water. Though differences in microbial abundance and community structure have long been observed between sediment and groundwater, there do not appear to be any studies showing differences in functional gene abundance patterns between the two compartments. This likely stems from the difficulty associated with acquiring paired, high-resolution sediment and water samples as was possible in the model aquifer.

Peak *bssA* and *tmoA* abundances in the pore water were observed nearest to the centerline of the plume where electron acceptors associated with their respective degradation pathways were depleted. In contrast, sediment *bssA* and *tmoA* profiles

exhibited narrow peaks in, or near the plume interface, and thus were in better agreement with electron acceptor availability. Additionally, the limited nature of toluene degradation stands in opposition to pore water gene profiles in which toluene degrading organisms are present throughout the thickness of the plume and could presumably be degrading toluene. Plume fringe theory, however, would contend that degradation is confined narrowly to the plume fringes, where overlapping countergradients of electron donors and acceptors exist. This is consistent with both the limited extent of toluene degradation, and the narrow peaks of *bssA* and *tmoA* genes in sediment near the plume interface.

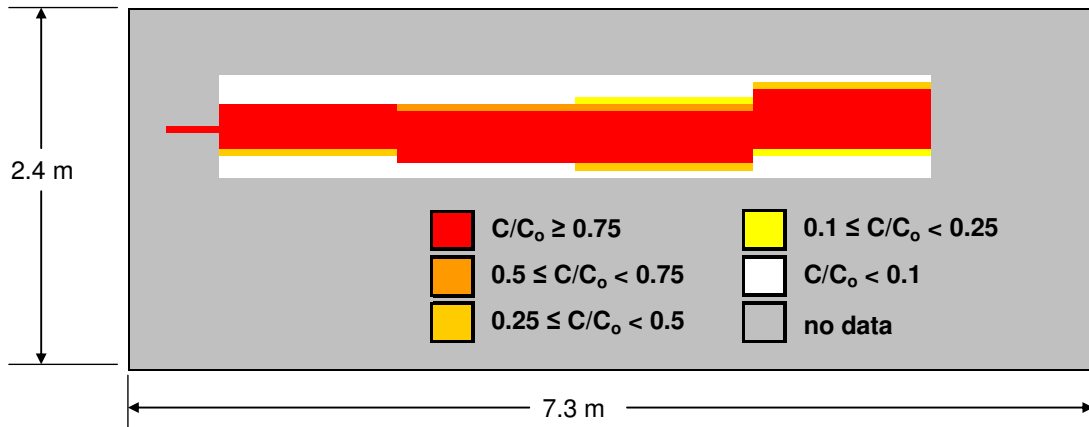
Based on these results, it appears that the sediment core was appropriate for delineating zones of toluene biodegradation in the model aquifer using functional genes as biomarkers. Also implicit in these results is the notion that high functional gene abundance in pore water doesn't necessarily correlate with gene expression, or by extension, contaminant degradation. The relatively high abundance of *tmoA* and *bssA* genes in anoxic, nitrate-deplete pore water despite limited toluene degradation would suggest that these genes, although present, were not highly expressed. It is conceivable that organisms harboring these genes originated upgradient where chemical conditions favored their growth and activity (e.g. prior to the depletion of electron acceptors in the case of the model aquifer). This idea is explored in more detail in Chapter 6.

**Figure 1. Model aquifer**



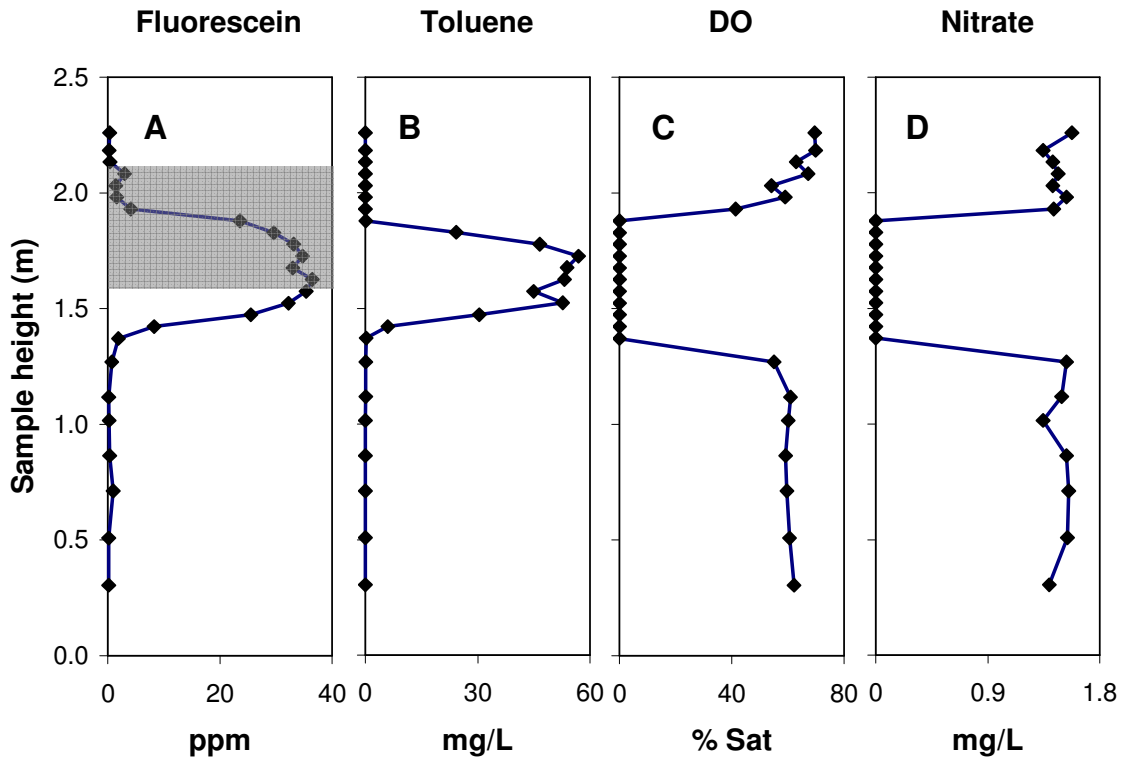
*Side-view schematic of the model aquifer. Its dimensions are 7.3 m long, by 2.4 m tall by 0.5 m thick (not shown). The injection port is located at a height of 1.65 m at the upgradient end of the model. Groundwater flow in the model is from left to right as shown. Four transects of groundwater sampling ports (black circles) are installed at transects 0.5, 1.7, 2.9, and 4.1 m downgradient from the injection port. There is one additional groundwater sampling port 10 cm downgradient of the injection port. The sediment core was taken across the upper plume interface 2.9 m downgradient from the injection port and corresponding to the third groundwater sampling transect. Box (A) is used to highlight the samples, both water and sediment, used for molecular biological analysis.*

**Figure 2. Shape of plume developed in the model aquifer**



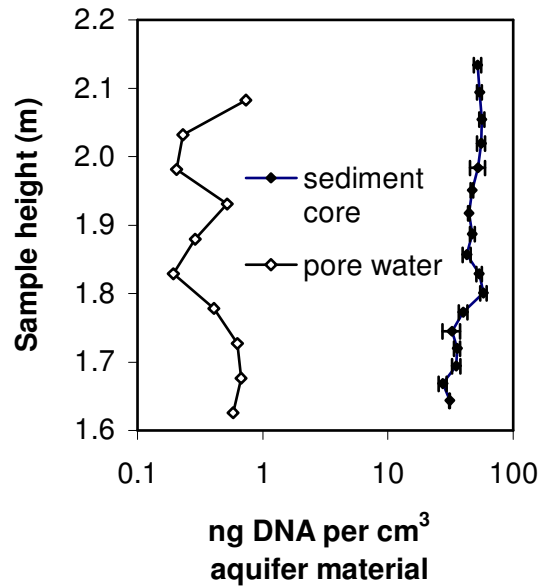
*Schematic illustrating the shape of the contaminant plume based on measured concentrations of the fluorescein tracer ( $C$ ) in pore water collected from the 4 sampling transects and the sampling port located 10 cm downgradient of the injection port. Data shown as values relative to the injection concentration ( $C_0$ ) of fluorescein.*

**Figure 3. Depth-resolved chemical analysis of pore water**



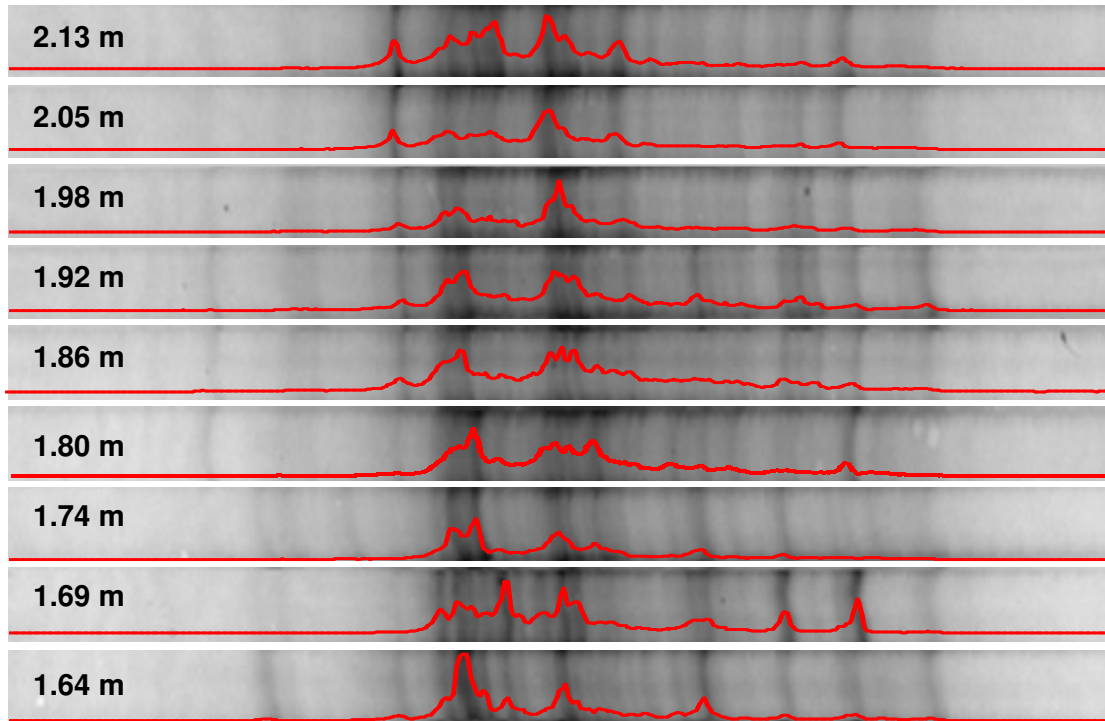
*Shown are the depth-resolved profiles of fluorescein, (A), toluene (B), dissolved oxygen (DO) (C), and nitrate (D) in pore water collected at 5 cm intervals across the toluene plume in the model aquifer 2.9 m downgradient of the injection port (injection port height = 1.65 m). Grey box in A illustrates depths over which water and sediment were also collected for molecular biological analysis.*

**Figure 4. DNA yields**



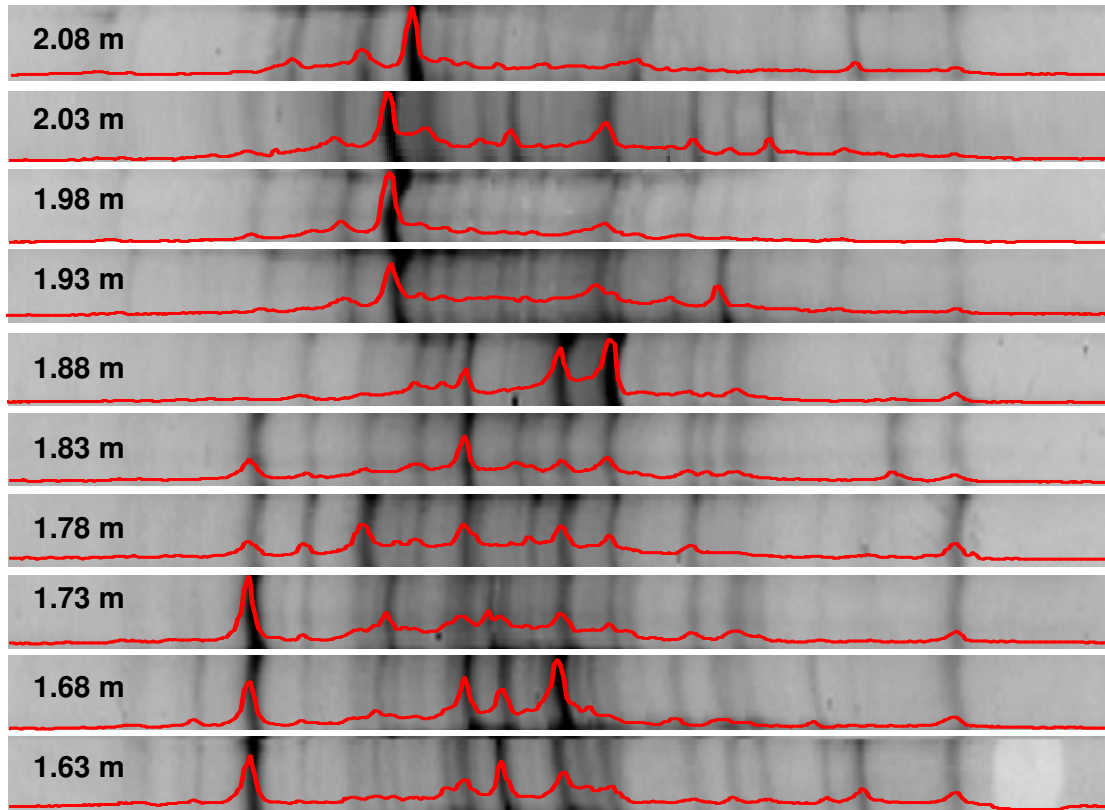
*DNA yields from equivalent volumes of model aquifer sediment (closed diamonds) and pore water (open diamonds). Error bars represent the standard deviation of two replicate sediment extractions. No replicate extractions were performed on water samples.*

**Figure 5. Sediment PCR-SSCP gel fingerprints and densitometric profiles**



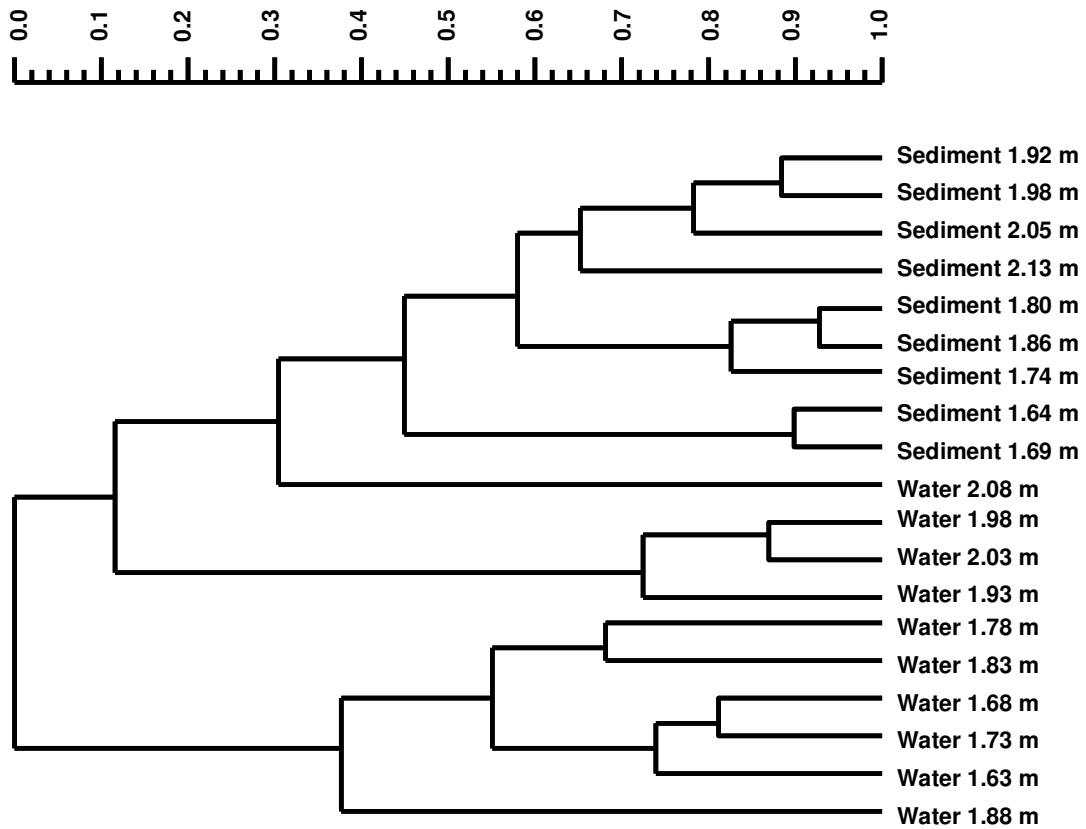
*Shown are gel fingerprints produced by PCR-SSCP of bacterial 16S rDNA from fractions of the cryogenically-collected sediment core. Overlaid are the associated densitometric profiles produced using GelCompar software.*

**Figure 6. Pore water PCR-SSCP gel fingerprints and densitometric profiles**



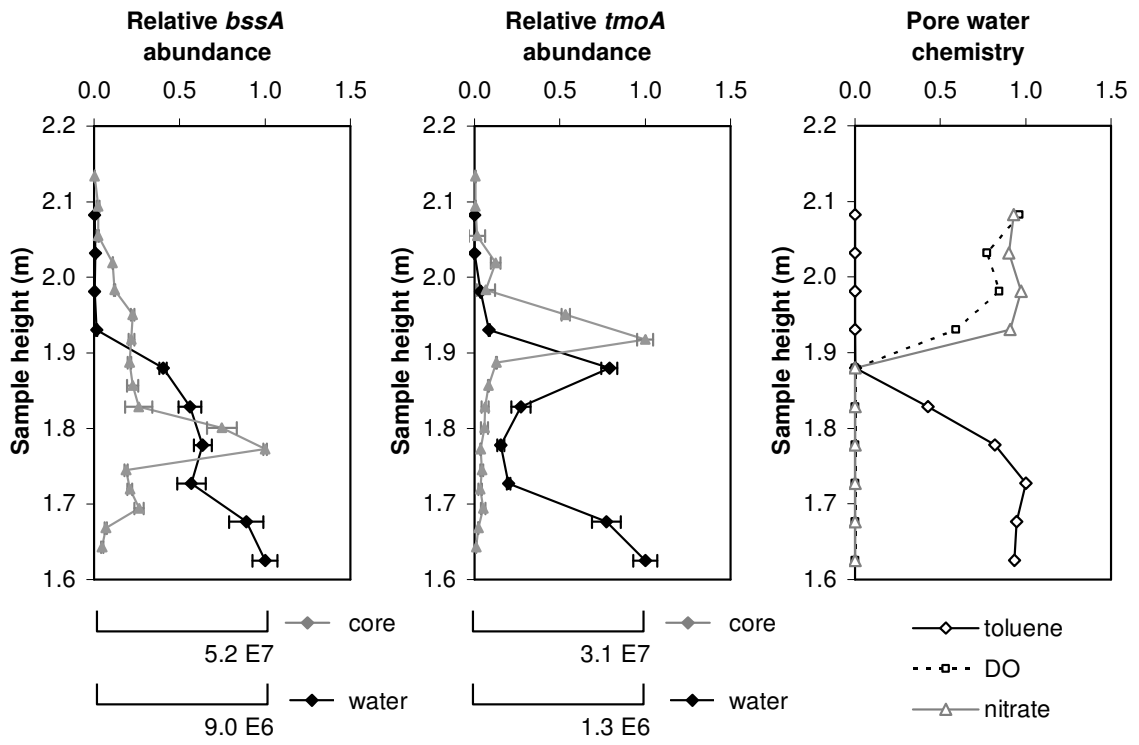
*Shown are gel fingerprints produced by PCR-SSCP of bacterial 16S rDNA from pore water samples collected from the model aquifer. Overlaid are the associated densitometric profiles produced using GelCompar software.*

**Figure 7. Pearson-based cluster analysis**



*Cluster analysis based on Pearson's pair-wise correlation coefficients of densitometric curves generated from PCR-SSCP of bacterial 16S rDNA in model aquifer sediment and pore water.*

**Figure 8. Depth distribution of *bssA* and *tmoA* genes in the model aquifer**



Depth distributions of *bssA* (A) and *tmoA* (B) genes recovered from the sediment core and pore water from the model aquifer 2.9 m downgradient of the injection port. Data presented as relative abundances. Absolute copy numbers are shown by the scale bars. Error bars represent standard deviations (of 2 replicate extractions for the core, and 2 replicate PCR reactions for the water). Also shown are data from chemical analysis of the pore water (C).

## **6. Microbial transport hinders use of functional gene abundance in pore water to characterize zones of active biodegradation**

### **6.1. Abstract**

Quantitative PCR (qPCR) was used to profile the abundance of genes associated with toluene degradation across a contaminant plume in a model aquifer. Profiles generated from sediment samples were in better agreement with electron acceptor availability, and the extent of toluene degradation than were profiles generated from pore water samples. Experiments using nitrate to stimulate anaerobic toluene biodegradation revealed that *bssA* genes, although present, were not highly expressed in groundwater lacking nitrate and toluene. Results were consistent with the hypothesis that organisms, and their genes, detected in groundwater may be artifacts of microbial transport from upstream where chemical conditions favored their growth.

The transcription of *bssA* genes from denitrifying toluene degraders was induced by toluene, but only in the presence of nitrate. Transcript abundance dropped rapidly following the removal of either toluene or nitrate. The loss of *bssA* transcripts pursuant to the removal of toluene could be described by an exponential decay function with a rate constant of  $0.44 \text{ hr}^{-1}$  and a half life of 1.6 hrs. Interestingly, *bssA* transcripts never disappeared completely, but rather appeared to be basally transcribed at a consistent level even in the absence of toluene and nitrate. A significant implication of these results is that *bssA* transcripts alone may not be suitable for use as biomarkers of metabolic activity. Instead, an integrated approach combining functional gene abundance and gene transcript analysis is recommended.

## 6.2. Introduction

The adoption of molecular biological tools (MBTs) has significantly improved our ability to characterize subsurface microbial populations and accurately assess the effectiveness of bioremediation (74). MBTs provide information on microbial community structure, metabolic potential, and metabolic activity with respect to the degradation of contaminants (3). Such information, in conjunction with hydrogeochemical data, are critical to all phases of bioremediation, from design, to implementation and monitoring. The detection of functional genes is useful in that it suggests the presence of microorganisms capable of contaminant degradation by the pathway and enzyme the gene encodes. Since the number of functional genes is related to the abundance of contaminant-degrading organisms, they are frequently used to delineate zones of active biodegradation in aquifers (3,1). However, the presence of functional genes provides information only on genetic potential, and not *in-situ* metabolic activity (6,1).

As discussed in Chapter 5, the gene, *bssA*, encoding the key enzyme of anaerobic toluene degradation was detected in pore water throughout the toluene plume in the model aquifer despite the absence of significant toluene degradation. This has significant implications for the use of functional genes recovered from groundwater as biomarkers of contaminant degradation. In this instance, pore water *bssA* genes would make a poor choice for use as a biomarker to delineate zones of active toluene biodegradation. Results may suggest that *bssA* genes, although present, were not highly expressed (i.e. relatively little mRNA production), and that their abundance may be explained by microbial transport from upstream where chemical conditions favored their growth.

Understandably, this complicates the use of aqueous functional genes as biomarkers for degradation, and, by extension, for reasonably predicting *in-situ* biodegradation rates.

This chapter describes experiments using a combination of qPCR and reverse transcriptase qPCR to further examine the hypothesis that *bssA* genes detected in nitrate-limited model aquifer pore water were present, but not highly expressed, and may be artifacts of microbial transport. Nitrate was added to the toluene plume to stimulate anaerobic toluene degradation under denitrifying conditions and facilitate description of *bssA* gene abundance and expression across interfaces (i.e. nitrate/no nitrate, toluene/no toluene). A lifetime experiment was conducted to determine the rate at which *bssA* gene transcripts disappear following the removal of toluene. Finally, *bssA* gene abundance and expression were monitored in the model aquifer following the termination of biostimulation in order to understand how quickly the system responds to the depletion of electron acceptors (i.e. nitrate). Together, these data suggest a strategy for using molecular tools to delineate zones of active biodegradation.

## **6.3. Methods**

### **6.3.1. Model aquifer**

As shown in **Figure 1**, the dimensions of the model aquifer are 7.3 m long  $\times$  2.4 m high  $\times$  0.5 m thick. Initially, a solution of toluene (65 mg/L) and fluorescein was introduced at the up-gradient end of the model through an injection port installed at a height of 1.65 m. Studies performed under these conditions are described in detail in Chapter 5, and will be referred to as phase 1 of the experiment in the model aquifer. Phase 2 involved the addition of 80 mg/L nitrate to the injection solution to stimulate toluene biodegradation under denitrifying conditions. In phase 3, the nitrate

concentration was reduced to 52 mg/L, while in phase 4, biostimulation with additional nitrate ceased. Groundwater flow in all phases of the experiment was approximately 30 cm/d.

### **6.3.2. Sample collection for MBT analysis**

Sampling ports for pore water collection were installed in 4 vertical transects located 0.5, 1.7, 2.9, and 4.1 m downgradient from the injection port. Vertical resolution within each transect was 5 cm. Additionally, there were 8 water sampling ports along the centerline of the plume between the injection port, and the transect at 2.9 m. Pore water samples (25-100 ml) were collected from the ports and filtered onto 0.2 µm filters for DNA and RNA extraction. A sediment core spanning the upper plume interface (see **Figure 1, box A**) was collected cryogenically (see chapter 4) at a downstream distance of 2.9 m corresponding to the third vertical pore water sampling transect. The core was divided into 2.5 cm sections which were subsequently stored at -80°C until processing.

### **6.3.3. Nucleic acid extraction and quantitative PCR**

DNA extractions were performed on filtered water samples, and 1 g fractions of sediment using the FastDNA Spin Kit for Soil (MP Biomedicals, Solon, OH). Independent DNA extractions were performed on duplicate sediment subfractions from each depth. (Duplicate water samples were not possible without reducing sample resolution.) RNA was extracted from filters as described by Smith et al. (50). A similar procedure was used for sediment with the exception that 4 independent extractions were performed on replicate 1 g subfractions, and the RNA was pooled during elution. RNA was treated with Turbo DNA-free (Applied Biosystems, Carlsbad, CA) and was confirmed to be free of DNA contamination by a RT-minus qPCR. Total RNA was

converted to complementary DNA (cDNA) using SuperScript III and random primers (Invitogen Corp., Carlsbad, CA) at a concentration of 300 ng per 20 ul reaction.

Quantitative PCR was performed in a MyiQ real-time qPCR detection system using iQ SYBR Green Supermix (BioRad Laboratories Inc., Hercules, CA). Primers targeting *bssA* and *tmoA* genes were added at a final concentration of 200 nM. Cycling conditions consisted of 5 min initial denaturation at 95°C followed by 40 cycles of 45 s denaturation at 95°C, 1 min annealing, and 1.5 min extension at 72°C. Annealing temperatures were 61.5 and 60°C for *bssA* and *tmoA*, respectively. qPCR data were analyzed using LinReg PCR (56) and gene copy numbers were determined by comparison to standard curves.

#### **6.3.4. Lifetime of *bssA* transcripts following removal of toluene**

To assess the lifetime of *bssA* gene transcripts following the depletion of toluene, 800 ml of pore water was collected from the plume centerline port located 0.5 m downgradient from the injection port. Toluene in the sample was removed via sparging with helium gas, which was also used to keep the sample anaerobic. Subsamples (100 ml) for RNA analysis were collected at the beginning of the experiment ( $t = 0$ ), and at 2, 4, 8, 12, 20, and 30 hours. Additionally, 15 ml samples were collected periodically in gas-tight syringes for analysis of toluene and nitrate concentrations. Samples for DNA analysis (25 ml) were also collected at the beginning, and end of the experiment.

### **6.4. Results and Discussion**

#### **6.4.1 Phase 1**

As discussed in Chapter 4, the introduction of toluene to the model aquifer resulted the in the formation of a stable, anaerobic toluene plume with steep gradients of

both oxygen and nitrate at the plume fringes (**Figures 2 a, b, & c**). Functional genes associated with aerobic and anaerobic toluene degradation (*tmoA* and *bssA*, respectively) were profiled in sediment and water samples collected from a vertical transect 2.9 m downgradient of the injection port (**Figure 3**). The vertical distribution patterns of these genes differed significantly between the water and the sediment, with the sediment-based profiles agreeing better with plume fringe theory, measured electron acceptor availability, and the limited extent of toluene degradation. Specifically, the highest abundances of both *tmoA* and *bssA* genes in pore water samples were nearest the plume's center, where electron acceptors associated with their respective degradation pathways were completely depleted. In contrast, highest abundances of *tmoA* and *bssA* genes in the sediment were largely confined to narrow peaks near the plume interface, where electron acceptor availability would be more favorable.

Implicit in these results is the notion that high gene abundances in the pore water samples do not correlate with high gene expression, or by extension, biodegradation activity. The high abundance of *tmoA* and *bssA* genes in anoxic, nitrate-deplete pore water despite the limited extent of toluene degradation would suggest that these genes, although present, were not highly expressed. It is likely that organisms (and their genes) detected in the pore water samples originated upgradient where chemical conditions favored their growth and activity (e.g. prior to the depletion of electron acceptors in the case of the model aquifer).

#### **6.4.2. Phase 2**

In order to examine the relationship between electron acceptor availability and functional gene abundance and expression in the model aquifer, nitrate was added to the

injection solution (80 mg/L) to stimulate anaerobic toluene biodegradation. This resulted in removal of >97% of the toluene within 0.5 m of the injection port, with no toluene detectable at any downgradient location (data not shown). Additionally, nitrate within the plume was undetectable beyond 10 cm of the injection port. This is illustrated in **Figures 2 d & f** which depict the profiles of toluene and nitrate at the transect 2.9 m downgradient from the injection port during phase 2 of the experiment.

Biostimulation with 80 mg/L nitrate had a significant effect on the depth distribution of *bssA* and *tmoA* genes recovered from pore water within the vertical transect at 2.9 m. The abundance of *tmoA* genes from all pore water samples dropped significantly, and notably, the peak observed within the plume interface during phase 1 of the experiment disappeared (see inset in **Figure 3b**). This result is consistent with the disappearance of the toluene/oxygen interface within the transect, as well as with the hypothesis that anaerobic toluene degradation outcompeted aerobic toluene degradation after the addition of nitrate. Concomitantly, the number of *bssA* genes recovered from pore water within this transect increased by as much as 21 fold (see inset in **Figure 3a**).

### **6.4.3. Phase 3**

The increase in abundance of pore water *bssA*-containing organisms at 2.9 m in the absence of nitrate and toluene supports the idea that these organisms originated upgradient, where biostimulation with nitrate had the largest effect. However, the lack of detectable nitrate or toluene within the vertical transect precludes any direct assessments of the relationship between cellular activity (i.e. gene expression), and chemical conditions. To remedy this, phase 3 of the model aquifer experiment involved reducing the injection concentration of nitrate to 52 mg/l, and sampling along a horizontal transect

within the center of the plume in order to capture toluene and nitrate interfaces at the leading edge of the toluene plume.

As shown in **Figure 4a**, toluene and nitrate within the plume decreased to 4 and 0% of their influent concentrations, respectively, over 2.9 m during phase 3 of the model aquifer experiment. Over this distance, the abundance of *bssA* genes initially increased and remained fairly constant throughout the plume, while the abundance of *bssA* transcripts peaked 0.5 m downgradient, and proceeded to drop off sharply (**Figure 4b**). In fact, the ratio of *bssA* gene transcripts to gene copies (**Figure 4c**) peaked 0.5 m downgradient where toluene and nitrate were present at 40 and 24% of their influent concentrations, respectively, and then rapidly decreased over 300 fold by 2.9 m. This confirms the hypothesis that *bssA* genes are present, but not highly expressed in groundwater downstream of where toluene was degraded under denitrifying conditions. It also supports the idea that organisms (and their genes) detected in groundwater may be present as a result of transport from upstream where conditions favored their growth and activity.

In light of this result, it is important to understand how quickly *bssA* gene expression decreases in response to changing environmental conditions such as the depletion of toluene and nitrate. The ratio of *bssA* gene transcripts to gene copies dropped over 90% from 0.5 to 0.9 m. Given a groundwater flow of 30 cm/d, this distance represents 32 hours of travel time. However, at this sampling resolution it is not possible to decouple gene expression and solution chemistry because toluene is still present, though being degraded, throughout this time period.

#### 6.4.4. Lifetime of *bssA* transcripts following removal of toluene

In order to assess the speed at which gene expression decreases following the disappearance of toluene, an 800 ml sample of pore water was collected from the plume centerline port at 0.5 m, in which relative *bssA* activity (i.e. the *bssA* transcript to copy number ratio) was its greatest. Toluene was removed from the sample via sparging with helium gas, and *bssA* gene expression was monitored over the next 30 hours. The concentration of toluene in the sample fell to 3 and 1% of its initial value within 1 and 2 hours respectively, and no toluene was detected beyond 2 hours (**Figure 5**). As a result, the abundance of *bssA* transcripts dropped 92% in the same period of time before reaching a stable level. The drop in *bssA* transcripts in the first 8 hours following the removal of toluene can be described by an exponential decay function with a rate constant of 0.44 per hour and a half life of 1.6 hours (**Figure 6**).

This may seem like a long time, particularly in comparison to *E. coli* which has reported mRNA half lives on the order of minutes (75). However, such a comparison may not be valid. No transcriptional inhibitor was used in the *bssA* lifetime experiment, therefore the 1.6 hour “half life” represents not simply the decay rate of existing transcripts, but rather an accumulation of mRNA, which could include transcription of new mRNA during the time period monitored. Additionally, since it took more than 2 hours to completely sparge toluene from the system, 1.6 hours is likely a gross overestimation of the *bssA* half life when the term is used in its conventional sense. Nonetheless, half lives determined in this fashion are useful because they demonstrate the applicability of functional gene expression for assessing the physiological state of organisms in biodegradation projects, which typically span time periods of months to

years. Furthermore, the *bssA* half life reported here is comparable to those determined in similar fashion for other functional genes of interest for bioremediation. For example, in the absence of inducers, *tceA* and *vcrA* dehalogenase gene transcripts from *Dehalococcoides* species decay exponentially with reported half lives of 6.1 and 4.8 hours (39).

#### **6.4.5. Phase 4**

As demonstrated by results from phases 1, 2 and 3 of the model aquifer experiment, toluene appears to induce the expression of *bssA* genes (and concomitant toluene degradation), but only in the presence of nitrate. Conversely, the removal of toluene alone from the sample in the lifetime experiment resulted in a rapid decrease in *bssA* gene expression, confirming that toluene in the presence of nitrate, and not the nitrate alone, that is the inducer. In phase 4 of the model aquifer experiment, biostimulation with nitrate was terminated, and *bssA* genes and gene transcripts at two locations along the plume (0.5 and 2.9 m) were monitored in conjunction with pore water chemistry.

Toluene degradation ceased rapidly following the termination of biostimulation (**Figure 7**). Within 3 weeks, the toluene plume had evolved down the length of the model aquifer, resuming its pre-biostimulation state. Changes in groundwater chemistry were accompanied by equally rapid changes in the abundance and expression of *bssA* genes. On the third day, a spike was observed in the abundance of *bssA* genes recovered at 0.5 m (**Figure 8a**). This was likely due to re-entrainment of attached cells following the reduction in pore water ionic strength caused by the removal of nitrate. Re-entrainment upon decreases in ionic strength results from expansion of the electrical

double layer surrounding particles and sediment surfaces. As a result, the effective distance of electrostatic repulsion increases, causing the release of particles reversibly-held in secondary energy minima (76). This phenomenon has been well documented for both biological (77) and non biological colloids (78) in saturated porous media. The fact that a similar, but delayed pulse of *bssA* genes was not evident at 2.9 m is not necessarily surprising. The combined actions of dispersion and additional attachment-detachments acting over the intervening distance could likely spread the peak, making it difficult to detect.

High numbers of *bssA* transcripts ( $> 10^7$  copies per ml) were detected in pore water at 0.5 m for two days following the termination of biostimulation (**Figure 8b**). Between days 2 and 3, their abundance dropped 2 orders of magnitude, and continued to fall more slowly thereafter, reaching a steady level of about  $10^4$  transcripts per ml. The ratios of *bssA* transcripts to *bssA* gene copies at 0.5 m also dropped sharply from day 2 to day 3, from  $\approx 0.3$  to 0.001. The initial drop in overall transcripts numbers and ratios coincided with the complete disappearance of nitrate at 0.5 m ( $C/C_o = 0.17$  and 0.0 at days 2 and 3, respectively), and with downgradient movement of the leading edge of the toluene plume (**Figure 7**).

It is important to note that *bssA* transcripts never completely disappeared in the pore water at 0.5 m, rather they reached a steady level of roughly  $10^4$  transcripts per ml. In fact, roughly  $10^4$  *bssA* transcripts per ml could be detected in all samples lacking both toluene and nitrate, including those from phases 3 of the model aquifer experiment, and the *bssA* lifetime experiment. This seems to suggest that *bssA* transcription continues at some basal level, even in the absence inducers. The significance of this is that functional

gene transcripts in and of themselves may not be suitable biomarkers for *in-situ* microbial activity. However, the data do suggest that an integrated approach combining functional gene and gene transcript analysis may prove useful. In the case of the model aquifer, for example, *bssA* transcript to gene abundance ratios on the order of  $10^{-1}$  were associated with active toluene degradation, while ratios of  $10^{-3}$  or less were observed elsewhere. A ratio of greater than  $10^{-2}$ , therefore, may be a reasonable biomarker for toluene biodegradation in this system.

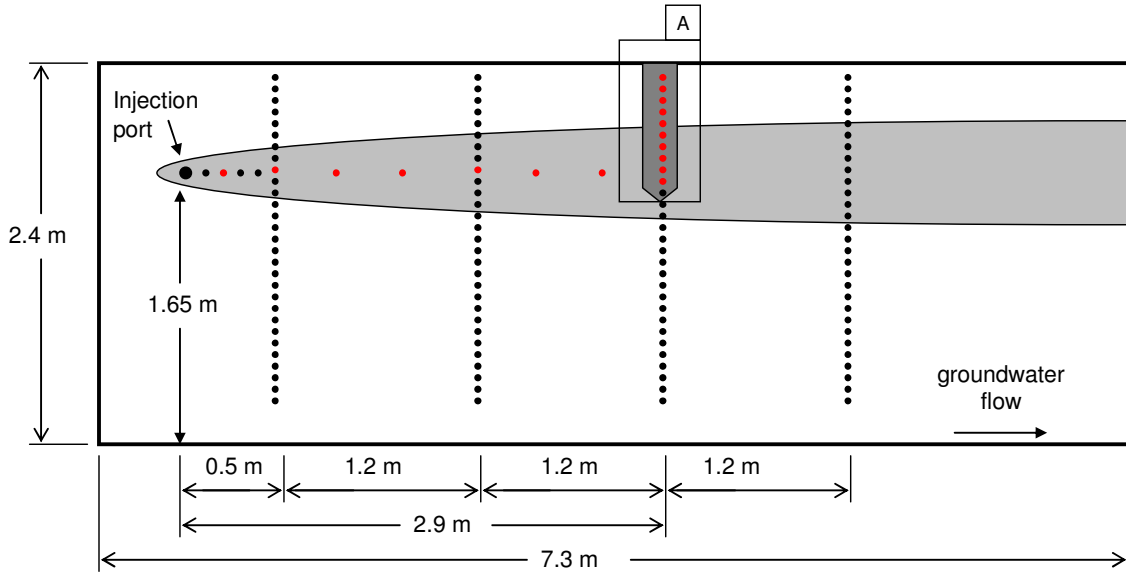
## 6.5. Conclusions

Prior to biostimulation, paired, high resolution sediment and water samples from a model aquifer showed significant differences in the depth distribution of genes associated with toluene biodegradation. Gene abundance profiles generated from sediment samples were in better agreement with plume fringe theory, electron acceptor availability, and the limited extent of toluene degradation. It was theorized that organisms (and their genes) detected in the pore water samples may have originated upgradient where chemical conditions favored their growth and activity. Experiments were conducted in which nitrate was added to the toluene plume to stimulate toluene biodegradation under denitrifying conditions. Results confirmed that high gene abundance downstream in the plume was not correlated with gene expression or degradation activity, thereby making it likely that microbial transport played a role in shaping the profiles of functional genes in the pore water.

Induction of *bssA* gene expression by toluene was shown to occur only in the presence of nitrate, and to fall sharply following the removal of either toluene, or nitrate. Results from a lifetime experiment indicated that the disappearance of *bssA* transcripts

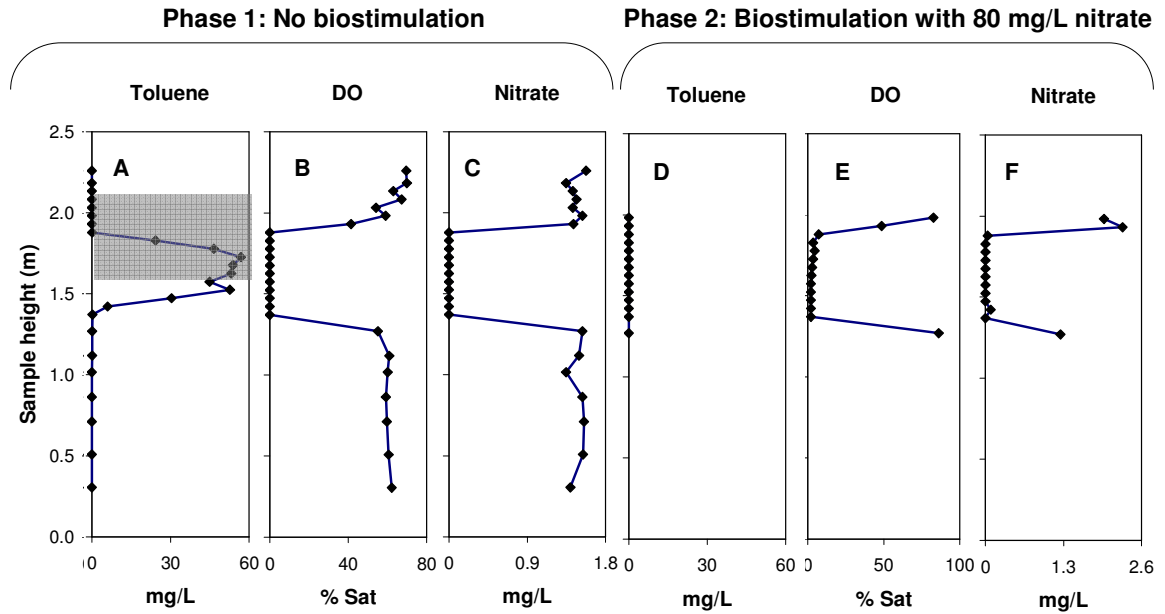
following the removal of toluene could be described by an exponential decay function with a half life of 1.6 hours. This supports the use of *bssA* transcripts for assessing the physiological state of organisms capable of toluene biodegradation. However, results also indicate that *bssA* may be continually transcribed at some basal level even in the absence of toluene and nitrate, thus complicating their exclusive use as a biomarker for active biodegradation. Instead, it is proposed that an integrated approach combining functional gene and gene transcript analysis may be more appropriate. In the case of the model aquifer, it appeared that *bssA* transcript to gene copy ratios greater than  $10^{-2}$  were indicative of active zones of toluene degradation. Such “activity thresholds” would have to be determined experimentally for different systems, but should provide the best measure of *in-situ* metabolic activity, and therefore significantly improve assessments and predictions of biodegradation.

**Figure 1. Model aquifer**



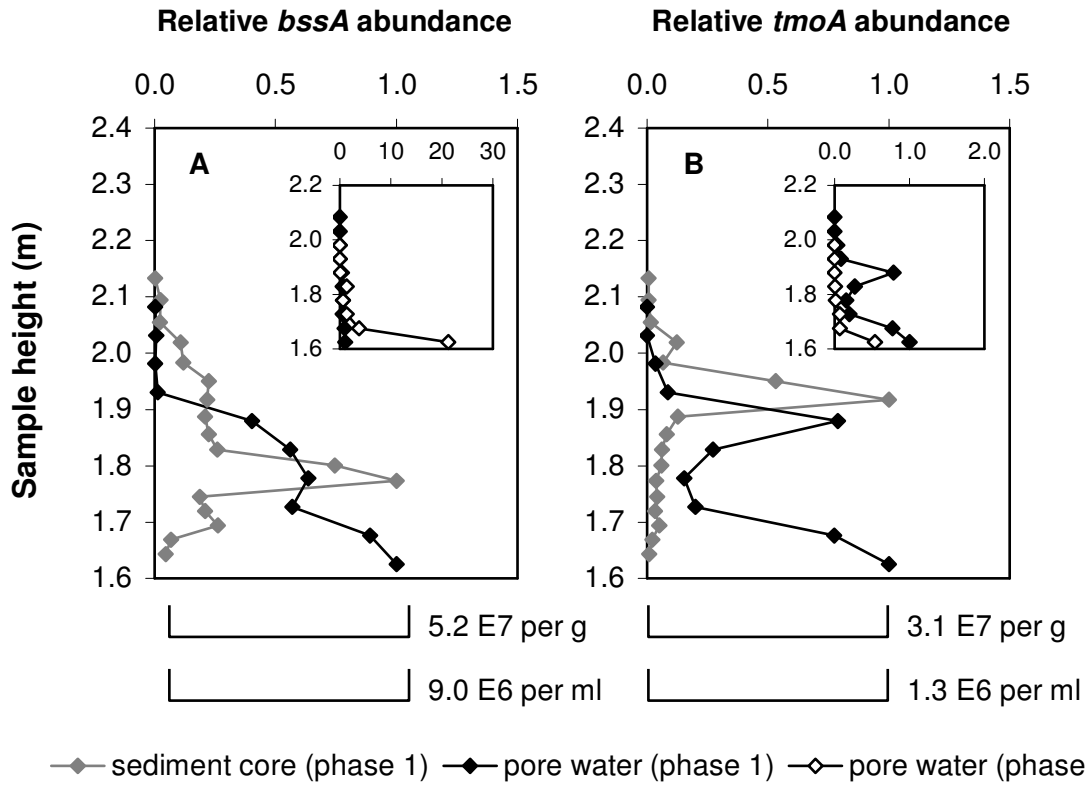
*Side-view schematic of the model aquifer. Its dimensions are 7.3 m long, by 2.4 m tall by 0.5 m thick (not shown). The injection port is located at a height of 1.65 m at the upgradient end of the model. Groundwater flow in the model is from left to right as shown. Four vertical transects of groundwater sampling ports (black circles) are installed at 0.5, 1.7, 2.9, and 4.1 m downgradient from the injection port. There are 8 additional groundwater sampling ports installed along the centerline of the plume between the injection port, and 2.9 m. Box (A) is used show the location of the sediment core. Locations of samples used for molecular biological analyses are shown in red.*

**Figure 2. Chemical pore water analysis in vertical transect**



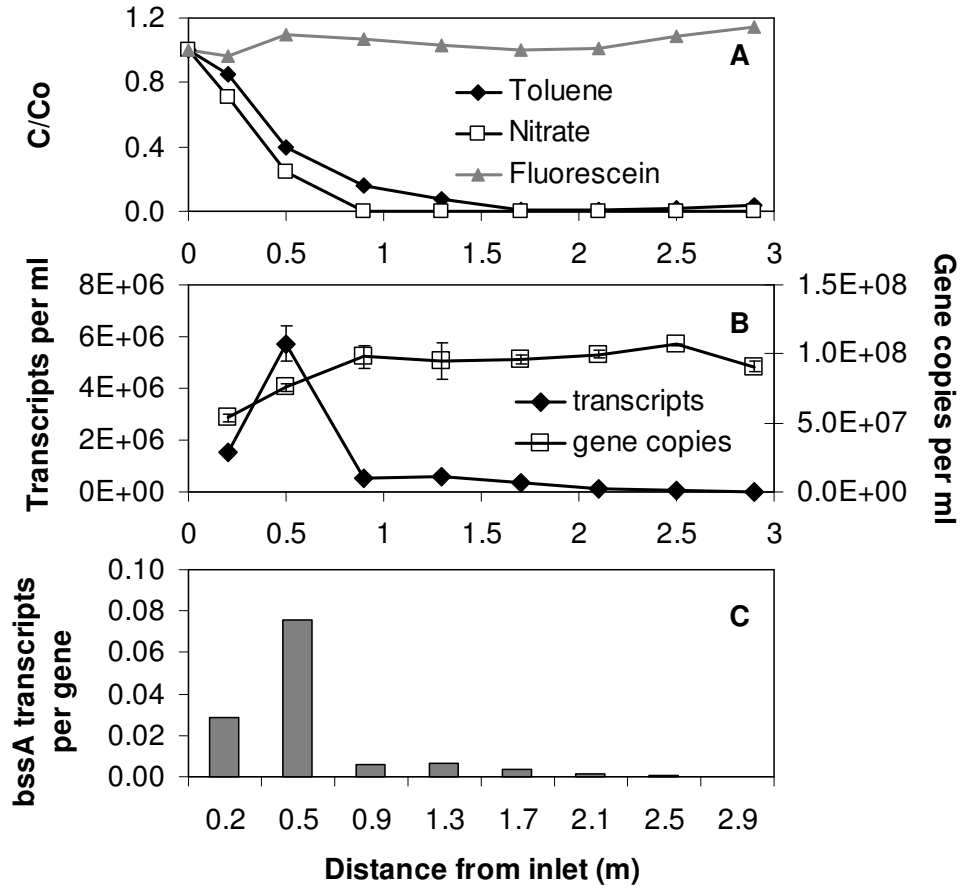
*Shown are the depth-resolved profiles of toluene, (A & D), dissolved oxygen (DO) (B & E), and nitrate (C & F) in pore water collected at 5 cm intervals across the toluene plume in the model aquifer 2.9 m downgradient of the injection port (injection port height = 1.65 m). Grey box in A illustrates depths over which water and sediment were also collected for molecular biological analysis.*

**Figure 3. Depth distribution of *bssA* and *tmoA* genes in the model aquifer**



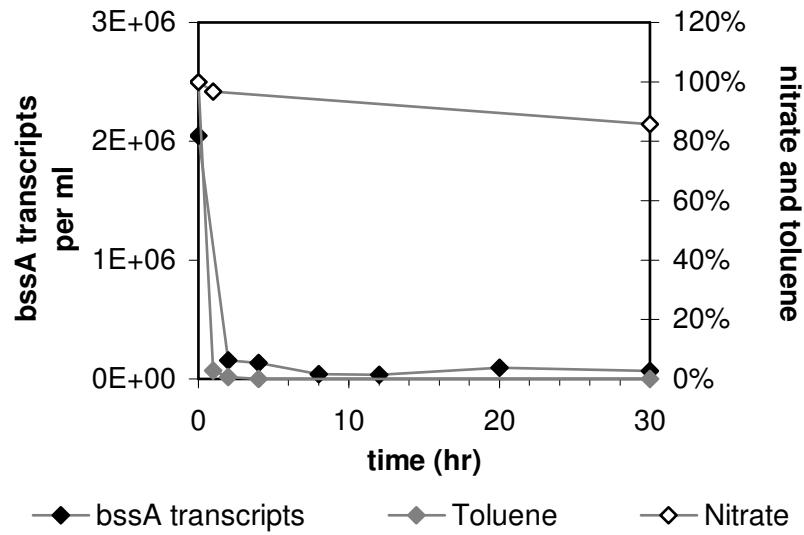
*Depth distributions of *bssA* (A) and *tmoA* (B) genes recovered from sediment and pore water from the model aquifer 2.9 m downgradient of the injection port. Data in the main panels are from phase 1 of the experiment (prior to biostimulation), and are presented as relative abundances. Absolute copy numbers are shown by the scale bars. Inset panels compare gene abundance profiles from before (phase 1) and after (phase 2) biostimulation with 80 mg/L nitrate. Sediment data presented as average of two replicate DNA extractions. Water data represent average of 2 independent qPCR reactions.*

**Figure 4. Water chemistry and *bssA* gene abundance and expression in pore water along centerline of plume**



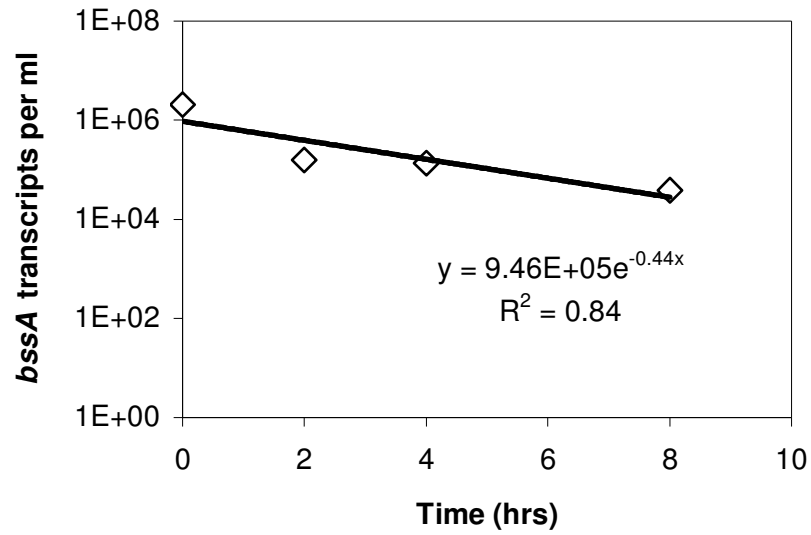
*Relative abundance of toluene, nitrate and fluorescein in pore water collected along the centerline on the plume downgradient of the injection port (A). Also shown are the abundance of *bssA* genes and gene transcripts (B), and ratio of *bssA* transcripts to gene copies (C). Error bars represent standard deviations of 2 independent PCR reactions.*

**Figure 5. Disappearance of *bssA* transcripts following toluene removal**



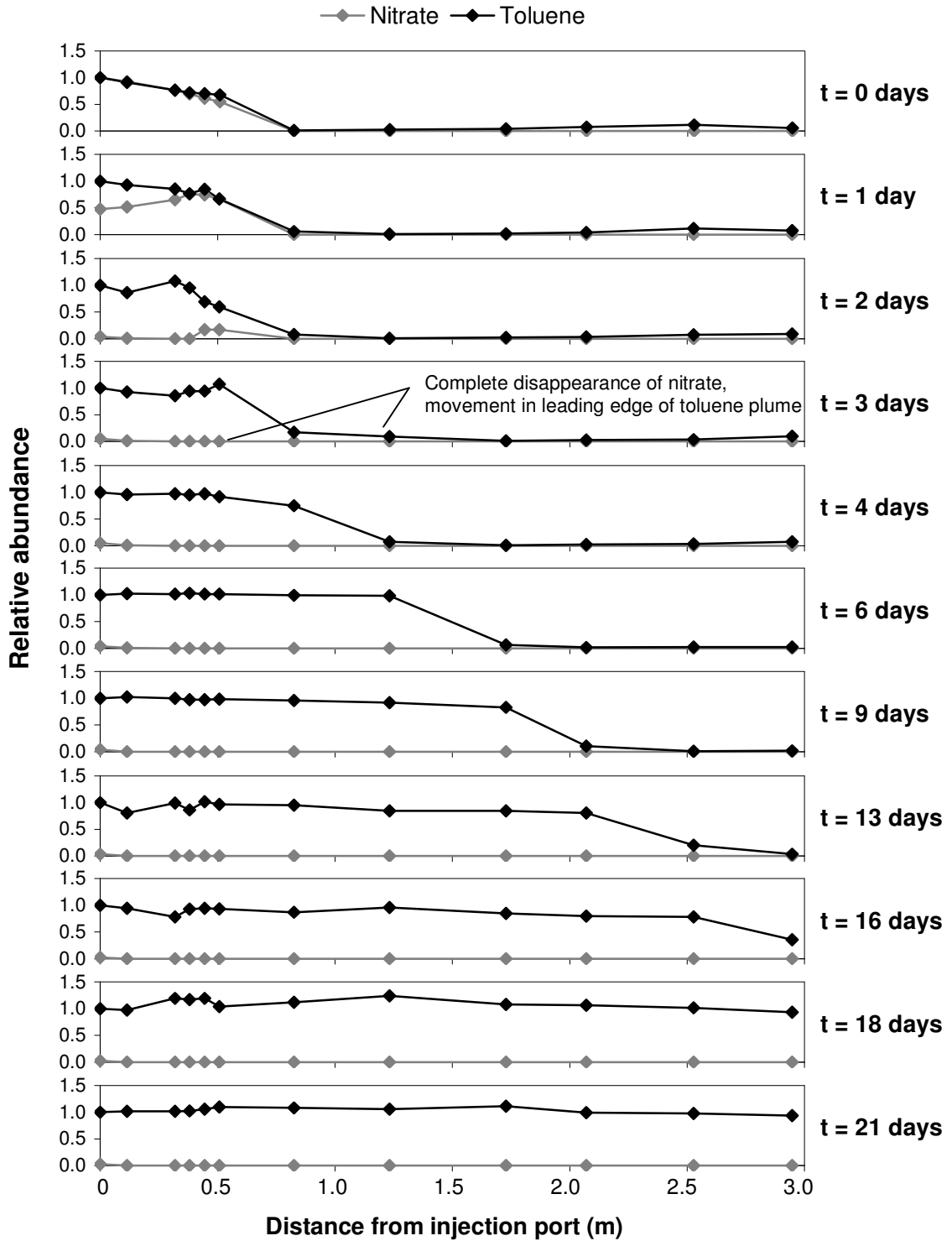
*Abundance of *bssA* transcripts per ml following removal of toluene via sparging with helium gas. Also shown are the abundance of nitrate and toluene relative to their initial concentrations.*

**Figure 6. Decay profile of *bssA* transcripts following stripping of toluene**



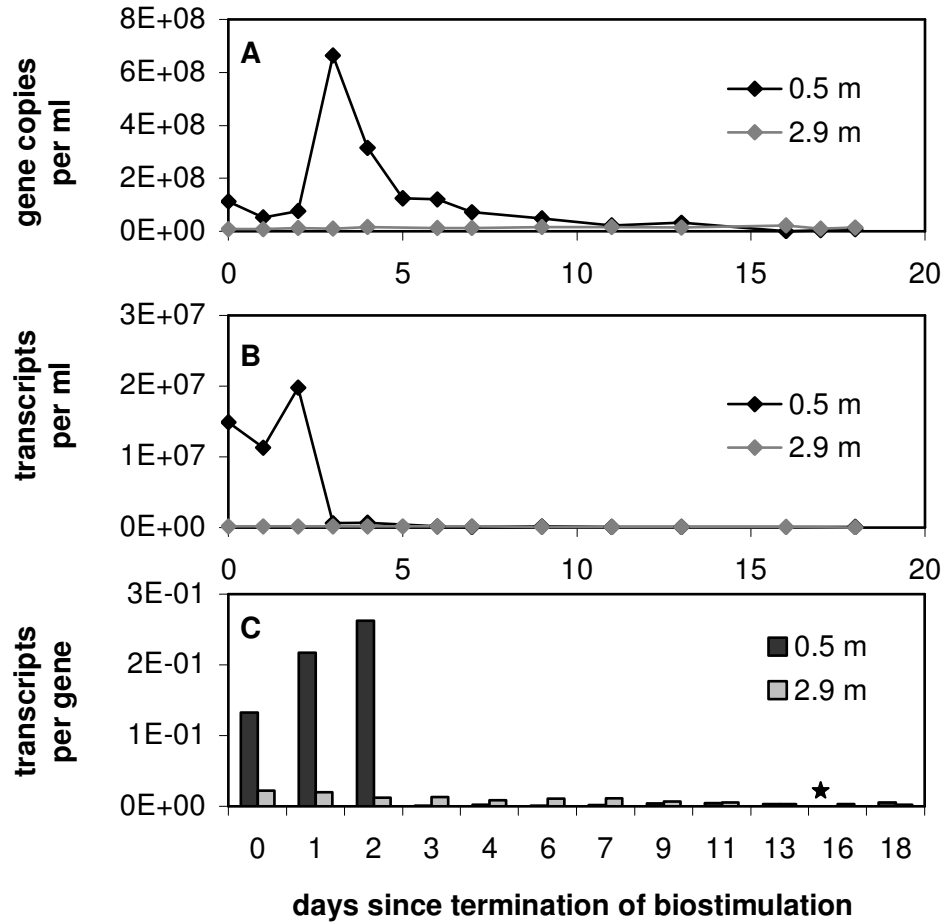
*Decay profile of *bssA* gene transcripts during the first 8 hours of the *bssA* lifetime experiment. Data are fit to an exponential decay function with a rate constant of 0.44 hr per hour, and a half life of 1.6 hours.*

**Figure 7. Evolution of toluene plume following termination of biostimulation**



*Evolution of toluene and nitrate in the model aquifer following the termination of biostimulation with nitrate. Toluene data presented relative to injection concentration. Nitrate data presented relative to injection concentration prior to termination.*

**Figure 8. Response of *bssA* following termination of biostimulation**



*Abundance of *bssA* genes (A) and gene transcripts (B) in pore water along the plume centerline collected at 0.5 and 2.9 m downgradient of the injection port. Also shown are ratios of *bssA* transcripts to *bssA* copy numbers (C). The star in panel C indicates that a ratio is not available at 16 days, 0.5 m due to a lack of available transcript data.*

## 7. Summary

Experiments with laboratory-generated samples, and samples from a model aquifer indicated that freezing and cryogenic storage are a viable way to preserve the *in-situ* molecular characteristics of microorganisms in sediment. Neither freezing, nor storage at -80°C affected the quality of DNA or RNA as evidenced by qPCR and RT-qPCR of genes and gene transcripts from a variety of different organisms including *Dehalococcoides*, which are known to reductively dechlorinate TCE. Especially noteworthy are the qPCR results which demonstrated that short-lived mRNA molecules were not degraded upon freezing, or storage. Additionally, the relative abundance of dominant bacterial 16S rDNA phylotypes was unaffected by freezing and storage of sediment at -80 °C. Significantly, this was also true of rRNA phylotypes. This is important because biodegradation depends upon active bacterial populations, and *in-vivo* rRNA content is often correlated with cellular growth rate.

Not only is freezing a viable approach for preserving sediment samples for molecular biological analysis, but it also provides a unique way with which to sample sediment for MBT analysis. A cryogenic core sampling technique was tested in the model aquifer. Using liquid nitrogen, a sediment core was frozen *in-situ*, and then extracted to the surface. Results from the cryogenically-collected core agreed favorably with those from co-localized unfrozen sediment. Cryogenic core sampling serves the dual purposes of biomolecule preservation, and the preservation of interfaces relevant to biodegradation. This is particularly important given that biodegradation in the subsurface is often confined to narrow biogeochemical interfaces where overlapping countergradients of electron donors and acceptors exist. With the cryogenically-collected

core, it was possible to profile the abundance of functional genes associated with toluene biodegradation to within a resolution of 2.5 cm. This represents a significant improvement over the resolution of groundwater sampling, which is, at best, on the order of meters.

In the model aquifer, the depth distribution of functional genes for toluene degradation differed significantly between the sediment, and the associated pore water. It has long been shown that sediment-attached and suspended microbial communities differ. However, the lack of paired high-resolution sediment and water samples has largely precluded any interpretation of these data as they relate to specific degradation processes. In the model aquifer, sediment-based functional gene profiles were in better agreement with the geochemistry of the associated pore water, and the limited extent of toluene degradation. In addition, the sediment-based profiles were also in agreement with plume fringe theory, whereas the pore water-based profiles suggested that biodegradation could be occurring throughout the plume despite an absence of suitable electron acceptors.

Based on these results, it appears that core samples were more appropriate for characterizing zones of active toluene biodegradation in the model aquifer than was the groundwater. Also implicit in these results is the notion that high functional gene abundance in pore water doesn't necessarily correlate with gene expression, or by extension, contaminant degradation. It is conceivable that organisms harboring these genes originated upgradient where chemical conditions favored their growth and activity (e.g. prior to the depletion of electron acceptors).

This idea is supported by the gene abundance and expression data gathered while nitrate was added to the plume to stimulate toluene degradation under denitrifying

conditions. Results confirmed that high gene abundance was not necessarily correlated with gene expression or degradation activity, thereby making it likely that microbial transport played a roll in shaping the profiles of functional genes in the pore water.

Results showed that the transcription of the functional gene for anaerobic toluene degradation (*bssA*) was induced by toluene, but only in the presence of nitrate. Additionally, *bssA* transcript abundance fell sharply following the removal of either toluene or nitrate. Results from a lifetime experiment indicated that the disappearance of *bssA* transcripts following the removal of toluene could be described by an exponential decay function with a half life of 1.6 hours. This would seem to support the use of *bssA* transcripts for assessing the physiological state of toluene-degrading organisms.

However, results also suggest that *bssA* genes are transcribed at some basal level, even in the absence of toluene and nitrate. This complicates their use as a biomarker for active toluene degradation. Instead, it is proposed that an integrated approach combining functional gene and gene transcript analysis may be more appropriate. In the case of the model aquifer, it appeared that *bssA* transcript to gene ratios greater than  $10^{-2}$  were indicative of active zones of toluene degradation. Such “activity thresholds” would have to be determined experimentally for different systems, but could possibly provide the best measure of *in-situ* metabolic activity, and therefore significantly improve assessments and predictions of biodegradation.

## 8. References

- (1) Bombach, P.; Richnow, H. H.; Kästner, M.; Fischer, A. Current approaches for the assessment of *in-situ* biodegradation. *Appl. Microbiol. Biotechnol.* **2010**, *86*, 839-852.
- (2) Foght, J. Anaerobic biodegradation of aromatic hydrocarbons: Pathways and prospects. *J. Mol. Microbiol. Biotechnol.* **2008**, *15*, 93-120.
- (3) Andreoni, V.; Gianfreda, L. Bioremediation and monitoring of aromatic-polluted habitats. *Appl. Microbiol. Biotechnol.* **2007**, *76*, 287-308.
- (4) Smets, B. F.; Pritchard, P. H. Elucidating the microbial component of natural attenuation. *Curr. Opin. Biotechnol.* **2003**, *14*, 283-288.
- (5) Wiedemeier, T. H.; Rifai, H. S.; Wilson, J. T.; Newell, C. *Natural attenuation of fuels and chlorinated solvents in the subsurface*; Wiley, **1999**.
- (6) Lovley, D. R. Cleaning up with genomics: applying molecular biology to bioremediation. *Nat. Rev. Microbiol.* **2003**, *1*, 35-44.
- (7) Beller, H. R.; Ding, W.-H.; Reinhard, M. Byproducts of anaerobic alkylbenzene metabolism useful as indicators of *in-situ* bioremediation. *Environ. Sci. Technol.* **1995**, *29*, 2864-2870.
- (8) Elshahed, M. S.; Gieg, L. M.; McInerney, M. J.; Suflita, J. M. Signature metabolites attesting to the *in-situ* attenuation of alkylbenzenes in anaerobic environments. *Environ. Sci. Technol.* **2001**, *35*, 682-689.
- (9) Reusser, D. E.; Istok, J. D.; Beller, H. R.; Field, J. A. *In-situ* transformation of deuterated toluene and xylene to benzylsuccinic acid analogues in BTEX-contaminated aquifers. *Environ. Sci. Technol.* **2002**, *36*, 4127-4134.

- (10) Dempster, H. S.; Sherwood Lollar, B.; Feenstra, S. Tracing organic contaminants in groundwater: A new methodology using compound-specific isotopic analysis. *Environ. Sci. Technol.* **1997**, *31*, 3193-3197.
- (11) Brad, T.; Van Breukelen, B. M.; Braster, M.; Van Straalen, N. M.; RÅling, W. F. M. Spatial heterogeneity in sediment-associated bacterial and eukaryotic communities in a landfill leachate-contaminated aquifer. *FEMS Microbiol. Ecol.* **2008**, *65*, 534-543.
- (12) Lehman, R. M.; Roberto, F. F.; Earley, D.; Bruhn, D. F.; Brink, S. E.; O'Connell, S. P.; Delwiche, M. E.; Colwell, F. S. Attached and unattached bacterial communities in a 120-meter corehole in an acidic, crystalline rock aquifer. *Appl. Environ. Microbiol.* **2001**, *67*, 2095-2106.
- (13) Harvey, R. W.; Smith, R. L.; George, L. Effect of organic contamination upon microbial distributions and heterotrophic uptake in a Cape Cod, Mass., aquifer. *Appl. Environ. Microbiol.* **1984**, *48*, 1197-1202.
- (14) Hazen, T. C.; Jiménez, L.; López de Victoria, G.; Fliermans, C. B. Comparison of bacteria from deep subsurface sediment and adjacent groundwater. *Microb. Ecol.* **1991**, *22*, 293-304.
- (15) Alfreider, A.; Krössbacher, M.; Psenner, R. Groundwater samples do not reflect bacterial densities and activity in subsurface systems. *Wat. Res.* **1997**, *31*, 832-840.
- (16) Griebler, C.; Mindl, B.; Slezak, D.; Greiger-Kaiser, M. Distribution patterns of attached and suspended bacteria in pristine and contaminated shallow aquifers

- studied with an *in-situ* sediment exposure microcosm. *Aq. Microbiol. Ecol.* **2002**, 28, 117-129.
- (17) Flynn, T. M.; Sanford, R. A.; Bethke, C. M. Attached and suspended microbial communities in a pristine confined aquifer. *Wat. Resour. Res.* **2008**, 44, w07425.
- (18) Iribar, A.; Sánchez-Pérez, J. M.; Lyautey, E.; Garabétian, F. Differentiated free-living and sediment-attached bacterial community structure inside and outside denitrification hotspots in the river-groundwater interface. *Hydrobiologia.* **2007**, 598, 109-121.
- (19) Doong, R.-a; Chen, T.-f; Wu, Y.-w Anaerobic dechlorination of carbon tetrachloride by free-living and attached bacteria under various electron-donor conditions. *Appl. Microbiol. Biotechnol.* **1997**, 47, 317-323.
- (20) Haglund, A.-L.; Törnblom, E.; Boström, B.; Tranvik, L. Large differences in the fraction of active bacteria in plankton, sediments, and biofilm. *Microb. Ecol.* **2002**, 43, 232-241.
- (21) Holm, P. E.; Nielsen, P. H.; Albrechtsen, H. J.; Christensen, T. H. Importance of unattached bacteria and bacteria attached to sediment in determining potentials for degradation of xenobiotic organic contaminants in an aerobic aquifer. *Appl. Environ. Microbiol.* **1992**, 58, 3020-3026.
- (22) Lehman, R. M.; O'Connell, S. P. Comparison of extracellular enzyme activities and community composition of attached and free-living bacteria in porous medium columns. *Appl. Environ. Microbiol.* **2002**, 68, 1569-1575.
- (23) Winderl, C.; Anneser, B.; Griebler, C.; Meckenstock, R. U.; Lueders, T. Depth-resolved quantification of anaerobic toluene degraders and aquifer microbial

- community patterns in distinct redox zones of a tar oil contaminant plume. *Appl. Environ. Microbiol.* **2008**, *74*, 792-801.
- (24) Wilson, R. D.; Thornton, S. F.; Mackay, D. M. Challenges in Monitoring the natural attenuation of spatially variable plumes. *Biodeg.* **2004**, *15*, 359-369.
- (25) Bauer, R. D.; Maloszewski, P.; Zhang, Y.; Meckenstock, R. U.; Griebler, C. Mixing-controlled biodegradation in a toluene plume--results from two-dimensional laboratory experiments. *J. Contam. Hydrol.* **2008**, *96*, 150-168.
- (26) Tuxen, N.; Albrechtsen, H.-J.; Bjerg, P. L. Identification of a reactive degradation zone at a landfill leachate plume fringe using high resolution sampling and incubation techniques. *J. Contam. Hydrol.* **2006**, *85*, 179-194.
- (27) Burland, S. M.; Edwards, E. A. Anaerobic benzene biodegradation linked to nitrate reduction. *Appl. Environ. Microbiol.* **1999**, *65*, 529-533.
- (28) Mesarch, M. B.; Nakatsu, C. H.; Nies, L. Development of catechol 2,3-dioxygenase-specific primers for monitoring bioremediation by competitive quantitative PCR. *Appl. Environ. Microbiol.* **2000**, *66*, 678-683.
- (29) US EPA FY 2010 Annual report on the underground storage tank program; **2010**.
- (30) Leuthner, B.; Leutwein, C.; Schulz, H.; Hörth, P.; Haehnel, W.; Schiltz, E.; Schägger, H.; Heider, J. Biochemical and genetic characterization of benzylsuccinate synthase from *Thauera aromatica*: a new glycyl radical enzyme catalyzing the first step in anaerobic toluene metabolism. *Mol. Microbiol.* **1998**, *28*, 615-628.
- (31) Altschul, S. F.; Gish, W.; Miller, W.; Myers, E. W.; Lipman, D. J. Basic local alignment search tool. *J. Mol. Biol.* **1990**, *215*, 403-410.

- (32) Lane, D. J. *Nucleic acid techniques in bacterial systematics*; Stackebrandt, E.; Goodfellow, M., Eds.: Chichester, United Kingdom, **1991**.
- (33) Yanisch-Perron, C.; Vieira, J.; Messing, J. Improved M13 phage cloning vectors and host strains: nucleotide sequences of the M13mp18 and pUC19 vectors. *Gene*. **1985**, *33*, 103-119.
- (34) Sy, A.; Giraud, E.; Jourand, P.; Garcia, N.; Willems, A.; de Lajudie, P.; Prin, Y.; Neyra, M.; Gillis, M.; Boivin-Masson, C.; Dreyfus, B. Methylophilic *Methylobacterium* bacteria nodulate and fix nitrogen in symbiosis with legumes. *J. Bacteriol.* **2001**, *183*, 214-220.
- (35) Baker, G. C.; Smith, J. J.; Cowan, D. A. Review and re-analysis of domain-specific 16S primers. *J. Microbiol. Meth.* **2003**, *55*, 541-555.
- (36) Watanabe, K. Microorganisms relevant to bioremediation. *Curr. Opin. Biotechnol.* **2001**, *12*, 237-241.
- (37) Rees, H. C.; Oswald, S. E.; Banwart, S. A.; Pickup, R. W.; Lerner, D. N. Biodegradation processes in a laboratory-scale groundwater contaminant plume assessed by fluorescence imaging and microbial analysis. *Appl. Environ. Microbiol.* **2007**, *73*, 3865-3876.
- (38) Mayer, K. U.; Benner, S. G.; Frind, E. O.; Thornton, S. F.; Lerner, D. N. Reactive transport modeling of processes controlling the distribution and natural attenuation of phenolic compounds in a deep sandstone aquifer. *J. Contam. Hydrol.* **2001**, *53*, 341-368.

- (39) Lee, P. K. H.; Johnson, D. R.; Holmes, V. F.; He, J.; Alvarez-Cohen, L. Reductive dehalogenase gene expression as a biomarker for physiological activity of *Dehalococcoides* spp. *Appl. Environ. Microbiol.* **2006**, *72*, 6161-6168.
- (40) Everest, F. H.; McLemore, C. E.; Ward, J. F. An improved tri-tube cryogenic gravel sampler. Res. Note: PNW-RN-350; U.S. Department of Agriculture, Forest Service, Pacific Northwest Forest and Range Experiment Station, **1980**; p. 8.
- (41) Moser, D. P.; Fredrickson, J. K.; Geist, D. R.; Arntzen, E. V.; Peacock, A. D.; Li, S.-M. W.; Spadoni, T.; McKinley, J. P. Biogeochemical processes and microbial characteristics across groundwater-surface water boundaries of the Hanford Reach of the Columbia River. *Environ. Sci. Technol.* **2003**, *37*, 5127-5134.
- (42) Petts, G. E.; Coats, J. S.; Hughes, N. Freeze-sampling method of collecting drainage sediments for gold exploration. *T. I. Min. Metall. B* **1991**, *100*, B28-32.
- (43) Petts, G. E.; Thoms, M. C.; Brittan, K.; Atkin, B. A freeze-coring technique applied to pollution by fine sediments in gravel-bed rivers. *Sci. Total Environ.* **1989**, *84*, 259-272.
- (44) Timken, M. D.; Swango, K. L.; Orrego, C.; Chong, M. D.; Buoncristiani, M. R. Quantitation of DNA for forensic DNA typing by qPCR. A report to the U.S. Dpt. of Justice. **2005**.
- (45) Chung, D. T.; Drábek, J.; Opel, K. L.; Butler, J. M.; McCord, B. R. A Study on the effects of degradation and template concentration on the amplification efficiency of the STR miniplex primer sets. *J. Forensic Sci.* **2004**, *49*, 1-8.
- (46) Piyamongkol, W.; Bermudez, M. G.; Harper, J. C.; Wells, D. Detailed investigation of factors influencing amplification efficiency and allele drop-out in

- single cell PCR: implications for pre-implantation genetic diagnosis. *Mol. Hum. Reprod.* **2003**, *9*, 411-420.
- (47) Sambrook, J.; Russell, D. W. *Molecular cloning: A laboratory manual*; 3rd ed.; CSHL Press: Cold Spring Harbor, NY, **2001**.
- (48) Simon, H. M.; Jahn, C. E.; Bergerud, L. T.; Sliwinski, M. K.; Weimer, P. J.; Willis, D. K.; Goodman, R. M. Cultivation of mesophilic soil crenarchaeotes in enrichment cultures from plant roots. *Appl. Environ. Microbiol.* **2005**, *71*, 4751-4760.
- (49) Yu, S.; Dolan, M. E.; Semprini, L. Kinetics and inhibition of reductive dechlorination of chlorinated ethylenes by two different mixed cultures. *Environ. Sci. Technol.* **2005**, *39*, 195-205.
- (50) Smith, M. W.; Herfort, L.; Tyrol, K.; Suci, D.; Campbell, V.; Crump, B. C.; Peterson, T. D.; Zuber, P.; Baptista, A. M.; Simon, H. M. Seasonal changes in bacterial and archaeal gene expression patterns across salinity gradients in the Columbia River coastal margin. *PLoS ONE*. **2010**, *5*, e13312.
- (51) Hendrickx, B.; Junca, H.; Vosahlova, J.; Lindner, A.; Rügge, I.; Bucheli-Witschel, M.; Faber, F.; Egli, T.; Mau, M.; Schlömann, M.; Brennerova, M.; Brenner, V.; Pieper, D. H.; Top, E. M.; Dejonghe, W.; Bastiaens, L.; Springael, D. Alternative primer sets for PCR detection of genotypes involved in bacterial aerobic BTEX degradation: distribution of the genes in BTEX degrading isolates and in subsurface soils of a BTEX contaminated industrial site. *J Microbiol. Meth.* **2006**, *64*, 250-265.

- (52) Kabir, S.; Rajendran, N.; Urushigawa, Y.; Itoh, K. Interference of contaminating DNA in the quantification of a toluene-induced *tod* gene in *Pseudomonas putida*. *J. Biosci. Bioeng.* **2003**, *96*, 250-256.
- (53) Johnsen, K.; Enger, O.; Jacobsen, C. S.; Thirup, L.; Torsvik, V. Quantitative selective PCR of 16S ribosomal DNA correlates well with selective agar plating in describing population dynamics of indigenous *Pseudomonas* spp. in soil hot spots. *Appl. Environ. Microbiol.* **1999**, *65*, 1786-1788.
- (54) Kanno, J.; Aisaki, K.-ichi; Igarashi, K.; Nakatsu, N.; Ono, A.; Kodama, Y.; Nagao, T. "Per cell" normalization method for mRNA measurement by quantitative PCR and microarrays. *BMC Genomics.* **2006**, *7*, 64.
- (55) Peirson, S. N.; Butler, J. N.; Foster, R. G. Experimental validation of novel and conventional approaches to quantitative real-time PCR data analysis. *Nucl. Acids Res.* **2003**, *31*, e73.
- (56) Ruijter, J. M.; Ramakers, C.; Hoogaars, W. M. H.; Karlen, Y.; Bakker, O.; van den Hoff, M. J. B.; Moorman, A. F. M. Amplification efficiency: linking baseline and bias in the analysis of quantitative PCR data. *Nucl. Acids Res.* **2009**, *37*, e45.
- (57) Behrens, S.; Azizian, M. F.; McMurdie, P. J.; Sabalowsky, A.; Dolan, M. E.; Semprini, L.; Spormann, A. M. Monitoring abundance and expression of "Dehalococcoides" species chloroethene-reductive dehalogenases in a tetrachloroethene-dechlorinating flow column. *Appl. Environ. Microbiol.* **2008**, *74*, 5695-5703.
- (58) Sliwinski, M. K.; Goodman, R. M. Spatial heterogeneity of crenarchaeal assemblages within mesophilic soil ecosystems as revealed by PCR-single-

- stranded conformation polymorphism profiling. *Appl. Environ. Microbiol.* **2004**, *70*, 1811-1820.
- (59) Lamond, A. I. The control of stable RNA synthesis in bacteria. *Trends Biochem. Sci.* **1985**, *10*, 271-274.
- (60) Binder, B. J.; Liu, Y. C. Growth rate regulation of rRNA content of a marine *Synechococcus* (*Cyanobacterium*) strain. *Appl. Environ. Microbiol.* **1998**, *64*, 3346-3351.
- (61) Wagner, R. The regulation of ribosomal RNA synthesis and bacterial cell growth. *Arch. Microbiol.* **1994**, *161*, 100-109.
- (62) Lu, X.; Wilson, J. T.; Kampbell, D. H. Relationship between *Dehalococcoides* DNA in ground water and rates of reductive dechlorination at field scale. *Wat. Res.* **2006**, *40*, 3131-3140.
- (63) Lu, X. Evaluation of the role of *Dehalococcoides* organisms in the natural attenuation of chlorinated ethylenes in ground water; Report to the U.S. EPA, **2006**.
- (64) Burlage, R. S.; Atlas, R.; Stahl, D.; Geesey, G.; Sayler, G. *Techniques in microbial ecology*; Oxford University Press US: New York, **1998**.
- (65) Hazen, T. C.; Jiménez, L.; Victoria, G. L. de; Fliermans, C. B. Comparison of bacteria from deep subsurface sediment and adjacent groundwater. *Microb. Ecol.* **1991**, *22*, 293-304.
- (66) Besemer, K.; Moeseneder, M. M.; Arrieta, J. M.; Herndl, G. J.; Peduzzi, P. Complexity of bacterial communities in a river-floodplain system (Danube, Austria). *Appl. Environ. Microbiol.* **2005**, *71*, 609-620.

- (67) Everest, F. H.; McLemore, C. E.; Ward, J. F. An improved tri-tube cryogenic gravel sampler. Research Note, PNW-350, Pacific Northwest Forest and Range Experiment Station, USDA Forest Service. **1980**.
- (68) Moser, D. P.; Fredrickson, J. K.; Geist, D. R.; Arntzen, E. V.; Peacock, A. D.; Li, S.-M. W.; Spadoni, T.; McKinley, J. P. Biogeochemical processes and microbial characteristics across groundwater–surface water boundaries of the Hanford Reach of the Columbia River. *Environ. Sci. Technol.* **2003**, *37*, 5127-5134.
- (69) Durnford, D.; Brookman, J.; Billica, J.; Milligan, J. LNAPL Distribution in a cohesionless soil: A field investigation and cryogenic sampler. *Ground Water Monit. R.* **1991**, *11*, 115-122.
- (70) Winderl, C.; Schaefer, S.; Lueders, T. Detection of anaerobic toluene and hydrocarbon degraders in contaminated aquifers using benzylsuccinate synthase (*bssA*) genes as a functional marker. *Environ. Microbiol.* **2007**, *9*, 1035-1046.
- (71) Hendrickx, B.; Dejonghe, W.; Faber, F.; Boënnne, W.; Bastiaens, L.; Verstraete, W.; Top, E. M.; Springael, D. PCR-DGGE method to assess the diversity of BTEX mono-oxygenase genes at contaminated sites. *FEMS Microbiol. Ecol.* **2006**, *55*, 262-273.
- (72) Greiff, D.; Blumenthal, H.; Chiga, M.; Pinkerton, H. The effects on biological materials of freezing and drying by vacuum sublimation. *J. Exp. Med.* **1954**, *100*, 89-101.
- (73) Baldwin, B. R.; Nakatsu, C. H.; Nies, L. Detection and enumeration of aromatic oxygenase genes by multiplex and real-time PCR. *Appl. Environ. Microbiol.* **2003**, *69*, 3350-3358.

- (74) Selinger, D. W.; Saxena, R. M.; Cheung, K. J.; Church, G. M.; Rosenow, C. Global RNA half-life analysis in *Escherichia coli* reveals positional patterns of transcript degradation. *Genome Res.* **2003**, *13*, 216-223.
- (75) Tong, M.; Li, X.; Brow, C. N.; Johnson, W. P. Detachment-influenced transport of an adhesion-deficient bacterial strain within water-reactive porous media. *Environ. Sci. Technol.* **2005**, *39*, 3888.
- (76) Lee, C.-G.; Park, S.-J.; Han, Y.-U.; Park, J.-A.; Kim, S.-B. Bacterial attachment and detachment in aluminum-coated quartz sand in response to ionic strength change. *Water Environ. Res.* **2010**, *82*, 499-505.
- (77) Tong, M.; Johnson, W. P. Colloid population heterogeneity drives hyperexponential deviation from classic filtration theory. *Environ. Sci. Technol.* **2007**, *41*, 493-499.